PRESSURE GARMENT MODELLING AND DEVELOPMENT

by

Mohamed Najib bin Salleh

A Doctoral Thesis
Submitted in partial fulfilment of the requirement for the award of
Doctor of Philosophy of Loughborough University

July 2009

ABSTRACT

A pressure garment is a medical garment that is used to prevent or reduce the formation of scars after a burn injury. It works by replacing the role played by skin to apply pressure upon the body to ensure that the injured skin is replaced to its original state without scarring. Currently, there are some problems associated with the process of designing and making pressure garments, such as fitting problems, customer satisfaction and delivery time. This research aims to develop a pressure garment that can apply an accurate pressure to a wounded area. In order to achieve the target aim, a system that can design pressure garments for the treatment of burn injuries has been developed. The process included the using of a 3D digital image of human body, obtained from a 3D body scanner, to design a 3D pressure garment model. The model is developed by considering several important parameters, such as pressure to be exerted, fabric properties and radius of curvature. Using the model the 3D pressure garment model is flattened to obtain its 2D pattern. A real pressure garment was constructed based on the 2D pattern. The garment produced from the developed pattern was able to exert a specific pressure when being applied to a cylindrical item. The method developed was extended to more comprehensive pressure garment pattern development for real body parts and then subsequently was experimentally verified. This research has also proposed a non contact pressure simulation method to predict the pressure distribution exerted by the pressure garment. The results from the prediction model compared well to the experimental data obtained from pressure measurements of a finished garment. The pressure distribution model provides an alternative to the actual pressure measurements. This research has also suggested a method to design and construct customized padding with the correct shape to exert a specific pressure on the target area. The developed method can locate areas with a low level of pressure and design a padding to provide extra pressure to the area. The constructed padding along with its pressure garment, have been shown to exert the intended specific pressure to the area.

Keywords: *Pressure garment, 3D pressure garment model, 2D pressure garment pattern, 3D pressure distribution model, padding.*

ACKNOWLEDGEMENTS

First, I would like to say Alhamdullillah, and thanks to Allah for giving me courage and guidance to write this thesis.

I also wish to thanks my sponsor, Malaysian Government and Universiti Utara Malaysia, for their support and understanding during my stay in the UK.

I would like to express my deepest gratitude to both of my supervisors, Professor Memis Acar and Professor Neil Burns, whose help, suggestions and encouragement helped me in all the time of research and writing of this thesis.

Last but not least, I wish to thanks all my colleagues at the Mechatronics Research Centre whose made the research process enjoyable. Thanks guys.

Dedicated ;

to my parents,

Salleh bin Saad and Samsiah bt Mohamad,

To my wife,

Aniza bt Hassan,

And to my little angel,

Najlah Afrina bt Mohamed Najib

NOMENCLATURE

P	Pressure	N/m^2
T	Tension of fabric	N/m
Re	Reduction factor	
ρ	Radius of curvature	m
C_1	Pressure garment circumference	m
C_0	Body model circumference	m
E	Modulus of elasticity or Young's modulus	N/m
κ	Curvature	1/m
G_j	Centroid coordinate of layer j	
C_j	Circumference for the layer *j*	m
θ	Angle from the centroid to pressure garment point	degree
m	Slope tangent	
F	Force	N
A	Area of contact	m^2
l	Length	m
h	Height	m
d	Distance between points	m
δ	Distance difference between data and circle point	m
d_{ave}	Average distance between points	m

LIST OF FIGURES

LIST OF TABLES

Chapter 1 Introduction

Pressure garments are tight fitting, elastic garments which apply pressure to a specific area of the human body with burn injuries for scar treatment. The process of designing and making pressure garments has problems such as correct fitting, delivery and customer satisfaction. This research aims to develop a pressure garment that can apply an accurate pressure to a wounded area. Hence, the objectives of this research are therefore:

i. To develop a 3D pressure garment design from data obtained by a body scanner.
ii. To generate a pressure garment pattern from the 3D design obtained from the body scanner.
iii. To develop a pressure model to simulate the pressure that will be exerted by the pressure garment.
iv. To verify the pressure model experimentally.
v. To develop padding for a low-pressure area and verify experimentally.

This chapter is divided into six main sections. The first section introduces the pressure garment and its mechanism to heal burn injury. The second section describes the current pressure garment manufacturing process. The third section focuses on problems faced by the current manufacturing method. The fourth section describes the suggestion proposed by this research to overcome the problem. The fifth section of the introduction explains the research significance. The last section is about the overview of this thesis.

1.1 Introduction to pressure garments

Burn Survivor Resource Centre (http://www.burnsurvivor.com/) reports that there are around 2.4 million injuries related to burns reported each year in the United States. From this number, approximately one million will suffer substantial or permanent disabilities resulting from their injury. Children, aged from newborn to two-years-old, are most frequently admitted for emergency burn care in a hospital. Burns are also one of the most expensive catastrophic injuries to treat. For example, a burn of 30% of the total body area can cost as much as $200,000 in initial hospitalization costs and for physicians' fees. For extensive burns, there are additional significant costs including the costs for repeat admission for reconstruction and for rehabilitation. There are several treatments for burn injuries, such as surgical procedures, skin substitutes and the use of a pressure garment.

There are two major types of surgical procedures that can help to conceal scarring and replace lost tissue for severe burn victims: dermabrasion and skin grafts. Dermabrasion is a surgical procedure to improve or minimize the appearance of scars, restore function and correct disfigurement resulting from an injury. A skin graft is a surgical procedure in which a piece of skin from one area of the patient's body is transplanted to another area of the body. For many severely burned patients, skin grafts using their own healthy skin may not possible because they have very little healthy skin or they are not strong enough for surgery.

Another alternative way of covering burn wounds is to use artificial skin. The artificial skin is made by living human cells and is dressed onto the wounded area. The artificial skin is only a temporary fix; the patient would still need skin grafts. However, the use of artificial skin means a thinner skin graft, which allows the donor site and the patient to heal faster with less surgery. In addition to the artificial skin, cultured skin is also used. A small piece of skin will be taken from the patient and it will be grown under special tissue culture conditions.

An alternative treatment for burn injuries is the use of a pressure garments. The exact mechanisms of how a pressure garment heals the injuries are not fully understood (Macintyre and Baird, 2005). However, it is believed that the use of a pressure garment can reduce the degree of scarring (Bombaro *et al.*, 2003) because normal undamaged skin is made up of connective issues in the dermis that forms a three-dimensional mesh of collagen fibres aligned parallel to the skin's surface. The skin applies pressure against its underlying layers. Under normal circumstances, the pressure that the skin puts upon the body ensures that injured skin is replaced to its original state without scarring.

When burns destroy the skin and the papillary dermis, normal pressure by these layers no longer exists. Without this pressure, hypertrophic scars will form irregularly causing possible deformities such as contractures, itchiness and pain (Macintyre and Baird, 2006). It will affect a patient's life because the scars are painful and cause a poor appearance that makes the patient feel self-conscious as well as causing other problems. Pressure garments prevent and control the formation of hypertrophic scars by applying counter pressure to the wounded area. Pressure garments aid in reducing the effects of hypertrophic scarring thereby reducing scarring and deformities.

For an effective and faster healing process, it is important that burn patients begin wearing pressure garments while the scar is active and immature. Scar tissue is highly responsive in the early stages so an early application of pressure garments is imperative. Pressure garments should be worn at least 23 hours a day, removing them for bathing and cleaning of the garments only. Most patients will need to wear pressure garments for 12 to 18 months.

The continuous wearing of pressure garments prevents the thickening, buckling, and nodular formations seen in hypertrophic scars. A soft pliable elastic scar develops which allows for normal joint movement. The external pressure applied by the garments decreases inflammatory response and the amount of blood in the scar, reduces itching and prevents collagen from being synthesized. Additionally, pressure garments provide protection against injury.

1.2 Pressure garment manufacture

Currently, pressure garments are manufactured by a cut and sew method (Ng and Hui, 1999). According to Macintyre and Baird (2006) and Ng-Yip (1993), there are two kinds of pressure garment:

i. Ready-made pressure garments - the customer can buy such ready made pressure garment instantly.

ii. Custom-made pressure garments - these are made upon request and thus can be tailored to the customer's needs.

The former pressure garments are better in terms of cost and delivery. However, they normally do not fit patients well because they have been made without any reference to a patient's wound area.

For the latter, since the custom-made pressure garment has been constructed by considering the patient's needs, it usually fits the patient better than the former. The fit of the pressure garment determines the pressure applied on the skin, thus it is the key factor in the treatment (Van den Kerckhove *et al.*, 2005).

The custom-made pressure garment can be constructed using two methods:

(i) from fully-fashioned panels of weft-knitted elastic fabric and

(ii) from lengths of warp-knitted elastic fabric.

The former is made usually by commercial manufacturers while the latter is made either by occupational therapists (OTs) or commercial manufacturers (Macintyre and Baird, 2006).

For the production of a pressure garment made from fully-fashioned panels of weft-knitted elastic fabric, first, the patient's measurements is taken and transmitted to the manufacturer. The manufacturer processes the measurement data using a CAD system and transforms them into knitting instructions. A weft-knitting machine then knits the fabric to develop the pressure garment. The garment is then sent to the hospital for a customer trial. The major advantage of this method is that, since the garment is not cut, it results in fewer seams and would be more attractive. However, this method involves a large investment in a CAD machine and a knitting machine since manual knitting would lead to a slower production of the pressure garment. For this reason, only commercial manufacturers make these pressure garments.

The method of producing pressure garments from warp-knitted elastic fabric is similar to the above mentioned process (refer Figure 1.1). First, a patient's wounded area is measured accurately. A reduction factor, the ratio between the pressure garment's dimensions and the actual measurement, usually expressed in percentage terms, is used to ensure that pressure is applied to the wounded area. Then, patterns are developed based on the reduced measurement, and cut. After that, the parts are sewn together and other features like zips are added to complete the garment. For the commercial pressure garment manufacturers, patients need to fill in a detailed measurement form in order to enable the companies to develop the pressure garment accurately. The pressure garment once complete, is then be sent back to the hospital where it is fitted on the patient. If the pressure garment does not fit well, the product is normally sent back to the company with details of improvement required.

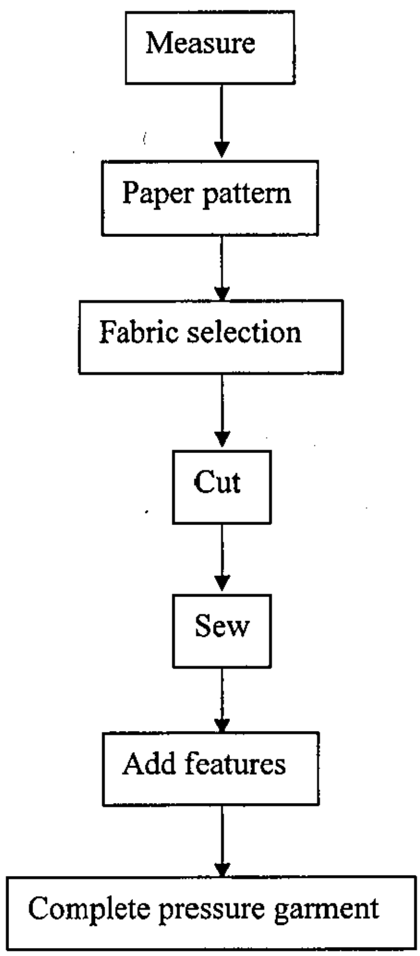

Figure 1.1 Pressure garment manufacturing process

The major advantages of a pressure garment made by occupational therapist (OTs) are that the delivery time is shorter and, because the garment maker is meeting face-to-face with the customer, hence the patient's fitting problems and special requirements can be resolved quickly. The cost of the pressure garment made through this process is also cheaper than those made by commercial makers. However, due to the lack of availability of staff who are trained in pressure garment construction, and that there are alternatives from external suppliers, hospitals tend to use pressure garments made by commercial manufacturers (Macintyre and Baird, 2005).Pressure garments made by commercial companies are manually more attractive and comfortable because their manufacturing and design staff are well trained, experienced and they use more advanced technology to develop the pressure garment (Macintyre and Baird, 2005, Ng-Yip, 1993).

1.3 Background to the Problem

The conventional manufacturing process for a pressure garment has some problems. These problems can be divided into three major categories: fitting problems, customer satisfaction and delivery time.

1.3.1 Fitting problems

'Fit' is defined as "the right size or shape for someone or something". Fitting is important in a pressure garment, as it determines the optimum pressure for effective treatment. Even though there is no agreement between researchers as to the exact pressure that needs to be applied by a pressure garment, most believe that pressures exceeding the capillary pressure (usually quoted as 25 mmHg) are required (Macintyre and Baird, 2006). However, regardless who the pressure garment manufacturer is, whether occupational therapist or commercial, both face the fitting problem (Macintyre and Baird, 2006).

For the occupational therapists, they lack training in pressure garment construction and they also have limited choice of fabric (Macintyre and Baird, 2006, Ng-Yip, 1993). It is possible to achieve different levels of pressure using similar fabrics, but the occupational therapists need to adjust the pattern size and fitting of the pressure garment (Ng-Yip, 1993). However, Macintyre and Baird (2005) and Macintyre (2007) noted that most of the occupational therapists would use a single reduction factor for all types of fabric to create their pressure garment.

Researchers have shown that different fabrics apply different pressures (Ng and Hui, 1999, Macintyre *et al.*, 2004, Ng, 1994, Ghosh *et al.*, 2008). By applying the same reduction factor to all fabrics, it is feared that the pressure that is generated by the pressure garment will not meet the actual pressure requirement. As a result, the pressure garment needs some adjustment to fix this problem. Macintyre and Baird (2005) stated that 40% of occupational therapists in the NHS said they need to adjust their pressure garment to achieve a good fit.

For commercial manufacturers, their pressure garments are also faced with the 'fit' problem because the garment is developed based only on the information given by the customer. Even though the information is detailed, without any real visualisation of the wounded area, it is hard to create an accurate pressure garment. Williams *et al.* (1998) show that the success rates for the initial fit for pressure garments made by two companies in Australia were only 84% and 63% respectively. To ensure that the problems do not occur, the companies usually ask their client to give the most detailed information possible, for example, the circumstances of the affected part, its length and also the required zip position. However, the procedure is time-consuming and needs much effort, and sometimes it does not solve the problem since body measurement is considered to be difficult for ordinary people (Istook and Hwang, 2001, Simmons and Istook, 2003).

The 'fitting problem' will recur as pressure garments must be worn for long durations of between 4 months and 3 years (Williams *et al.*, 1998). During this period, a pressure garment usually will lose its tension due to time (Ng, 1994) so the pressure garment must be constructed again to effectively treat the wounded area. Also, in case of weight gain or loss, the garment must be re-ordered, since over-tight covers may interfere with blood circulation and a loose cover will not heal the wound.

Another fitting problem is low-pressure areas. There are some areas along the body which have a concave or flat shape, which prevent pressure from being delivered by the pressure garment.

1.3.2 Customer satisfaction

Commercial manufacturers also face the need to ensure customer satisfaction. Pressure garments made by them are developed without any involvement from the client except in measured data collection and fitting process. Figure 1.2 shows the involvement of customer in pressure garment making process. William et al. (1998) in their research showed that customer satisfaction for pressure garment made by one company in Australia was only 60%. Thus, it is important to involve the customer in the design stage of the pressure garment.

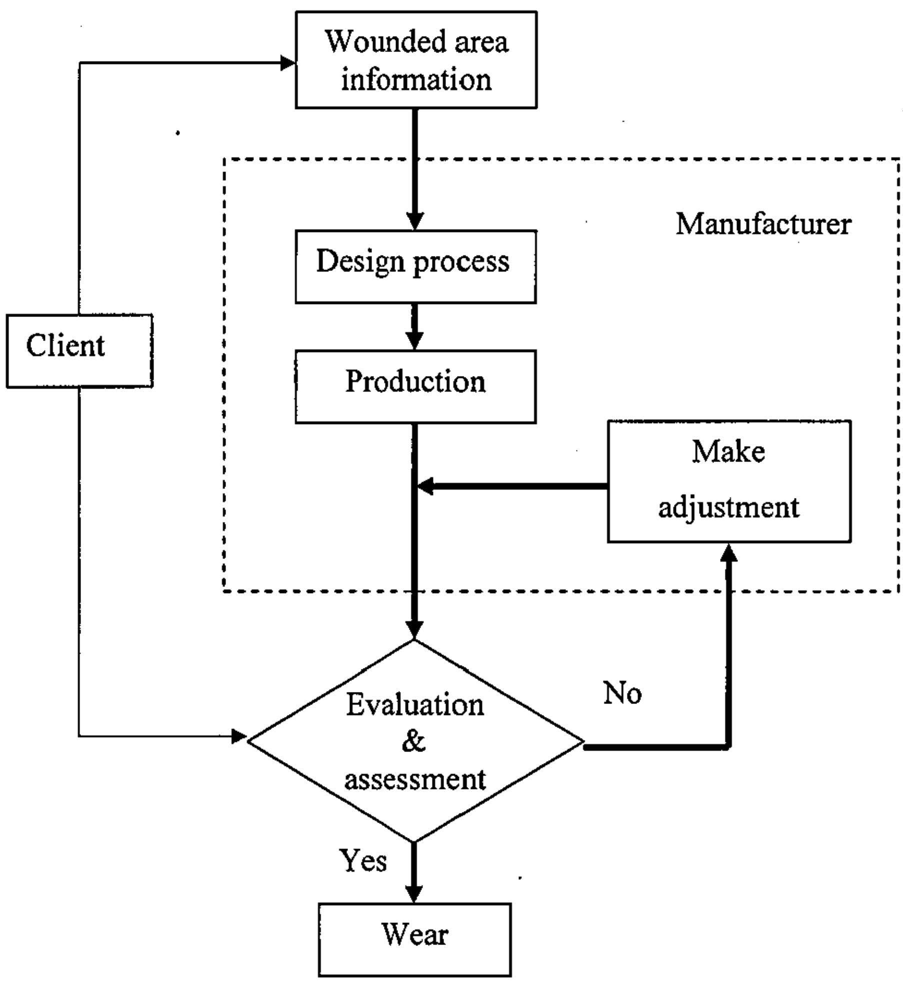

Figure 1.2 **Customer involvement in current pressure garment making process**

1.3.3 Delivery time

Commercial manufacturers also face problems with delivery times (Macintyre and Baird, 2006). Their delivery time is longer than occupational therapists because of the need to fill in the form for sizing and also the time taken to order and deliver the garment. If there is a problem with fitting, then the pressure garment is sent back to the manufacturer for adjustment, and this process thus delays the time taken for the patient to have an effective garment in place.

1.4 Problem statement

It is clear that the main obstacle in developing an effective pressure garment is the 'fit' of the garment. Fitting is extremely important in pressure garment making because it determines how much pressure the pressure garment exerts on the wounded area. The pressure must be right; otherwise the wounded area does not heal without serious scarring problems.

Thus, this research intended to solve the problem by developing a 3D system that can be used specifically to design pressure garments.

A 3D system can provide a more accurate reduction factor according to the type of fabric used. The 3D system can also act as a communication tool between the client and the manufacturer as shown in Figure 1.3. The customer also can play an active role by participate in the designing process. It could enable the manufacturer to obtain more detailed information about the wounded area, for example its exact location and size. The information can be accumulated by using a 3D body model, which can be obtained by using a body scanner. The manufacturer can also design the pressure garment directly using the 3D body part model, show it to the client and get their early evaluation and assessment before manufacture takes place. The system also gives manufacturers some advantages in developing the pressure garment because they can evaluate whether their garment fits accurately on the body part and check whether it exerts the intended pressure. The 3D system benefits the patients as they can evaluate and assess their pressure garment whilst it is in the design stage. By using this process, the client can also give their opinion of the garment.

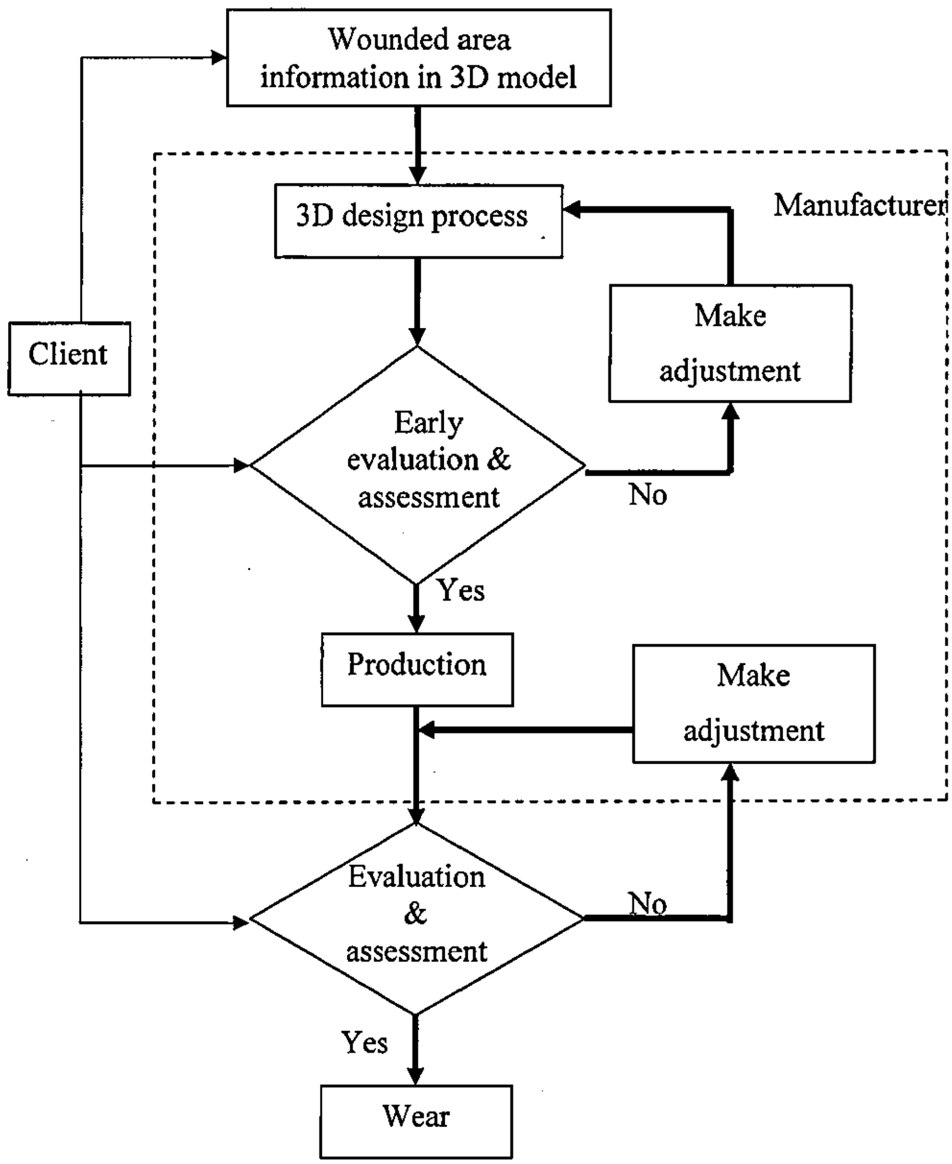

Figure 1.3 **Customer involvement in the new 3D system**

Currently, there are many 3D CAD software packages that can be used to help designers in the garment industry, for example, Gerber, Lectra System and DressingSim. Research is also being conducted to develop more advanced 3D CAD software for use in garment design. However, none of this research is focussed on pressure garment design. The reason why the 3D CAD software is not used for pressure garment development may be the fact that, the ordinary garments and pressure garments do have some differences. Regrettably, these differences make most of the techniques provided by the 3D CAD software unsuitable for the design of pressure garments.

The first difference is in body area coverage. Ordinary garments only cover certain parts of the human body, for example shirts and jackets cover the upper body, and pants cover the lower body. For this reason, most of the developed software can be used to cover certain areas only. Currently, there is no technique developed to design a garment that covers, for example, the finger area, or the head area, because these parts have not been considered as garment parts. Pressure garments can be used to cover any part of the body. Sometimes, for example, they may be used to cover only a fraction of the area of a hand or, sometimes, the whole body area may need covering from head to toe. Thus, in order to develop a pressure garment, it is important to develop a 3D CAD software system that can be used to design a garment for any part of the body.

The next difference is in the allowances. In an ordinary garment, the design must be developed with consideration being given to providing some allowance between human skin and the garment. However, in a pressure garment, there must be close contact between human body and the garment fabric to ensure that the required pressure is applied. Thus, an interference fit is needed in a pressure garment. The effect of the interference is considerable in garment pattern making. Hence, the size of pressure garment patterns must be smaller than the original body part measurement in order to allow the garment to exert pressure on the scarring area. In the ordinary garment CAD system, such a reduction factor is not taken into account as the garment is considered not to apply any pressure on the body.

In an ordinary garment, it is safe to assume that the garment is of a cylindrical shape since there are allowances between the human body and the garment. However, in a pressure garment, the garment needs to closely follow the curvature of the human body, which makes its pattern more difficult to develop, for example, in developing a pattern for a muscular leg. For ordinary trousers, it is safe to assume that the trouserslegs are a cylinder or a truncated cone. However, in developing a pressure garment for a muscular leg, the shape is no longer cylindrical or a truncated cone. It may take a form according to the shape of the leg.

The details of current 3D systems for garment manufacture are explained further in the literature review.

1.5 Research significance

Although there have been many advances in the computerization of ordinary garment manufacture, the same cannot be said for pressure garments. As stated before, pressure garments and ordinary garments are two different entities. It cannot be assumed that the technology that is available for ordinary garment design and manufacture can also be applied to pressure garments. They need different approaches. The literature survey identified a handful of researchers investigating the computerized pressure garment manufacturing process, for example Diaz et al., (2002). They have developed pressure garment using 3D sewing technique based on data that they obtained through body scanner. However, this technique is involved large amount of money for CAD and knitting machines (Macintyre and Baird, 2006). Other pressure garment manufacturers usually used a system that predicts pressure garment pattern based on body measurement. However, the number of measurements is not enough for them to create a 'fit' pressure garment.

Thus, this research is important for the development of computerization in the manufacture of pressure garments. It is hoped that, by developing this technology, the current hurdles that are being faced by pressure garment makers can be eliminated.

1.6 Research overview

The research project is divided into four phases, namely:

i- The literature review

ii- The development of 3D pressure garment model and pattern generation iii- The development of pressure distribution model

iv- Padding development

v- Experiment for validation.

The dissertation consists of seven chapters organized as follows:

Chapter 1 introduces the pressure garment, its current manufacturing process and problems and set the objectives of this research.

Chapter 2 presents a literature survey on pressure garment manufacturing, state of the art on the 3D garment development, pattern generation and pressure measurements.

Chapter 3 suggests a method to develop the pressure garment model from a body scanner and explain the technique to generate the pattern from the model. The chapter also describes an experiment to validate the method.

Chapter 4 proposes a method to predict pressure exerted by the pressure garment on the body. Experiment to measure the pressure exerted and analysis of results are presented and discussed.

Chapter 5 offers a new method to develop and construct padding for concave or flat parts of the body to provide a uniform pressure distribution. For validation, experiments were conducted and its results are analysed and discussed.

Chapter 6 provides discussion of the research presented. The novelty of each developed method and their limitations are also discussed. The benefits of the proposed methods are outlined.

Chapter 7 provides the conclusion of the research work and further improvement areas for future work are identified.

Chapter 2 Literature review

This chapter is organised in seven sections. The first section reviews the research literature concerning the manufacture of pressure garments. The next three sections are about the current technology used in garment design, including the current technology in 3D body visualisation, an overview of research being conducted on creating 3D garment models and pattern generation. A further section reviews the pressure measurement technology. Section six examines the current pressure garment properties. The last section offers a summary.

2.1 Manufacture of pressure garment

Currently, based on a review of the journals, there is no specific research publication in the public domain on computerized pressure garment design except for one patent by Dias *et al.* (2002). Their patent is to developed pressure garment by using 3D sewing technique and there is no reference in any academic journal to the patent. The other literature on pressure garments is related to medical treatment. There are limited sources on pressure garments design and manufacture. Most of these researches discuss how to construct pressure garments that can exert a certain pressure on a wounded area. Since there is a certain range of pressure that needs to be exerted on the wounded area, a number of researchers have attempted to find a way to design pressure garments that can apply the required pressure on the area.

Most of the researchers use the Laplace Law to predict the pressure. This law indicates that pressure depends on the wall tension and its radius of curvature. Macintyre *et al.* (2004) have conducted experiments to develop a connection between circumference, reduction factor and tension, and pressure. In summary, they concluded that pressure is directly proportional to tension and reduction and inversely proportional to circumference or radius. Their findings accord with the Laplace Law.

Ng and Hui (2001) used the Laplace Law to calculate the reduction factor for a pressure garment so that it can apply their intended pressure. They combined Laplace's Law and Hooke's Law to develop a mathematical model by considering the rigidity of the fabric, the compression factor, radius and pressure. Based on the result, they created a pressure garment and applied it. The results are encouraging. It shows that the mean pressure exerted by the pressure garment on the wounded area is almost equal to the intended one.

On the other hand, Thomas (2003) has derived a formula based on the Laplace Law to calculate the pressure exerted by a bandage on the human body. In his formula, he adds two other parameters, width of fabric and number of layers of bandage. Unfortunately, he did not do any experimental studies to validate his equations.

Macintyre *et al.* (2003, 2007) also use this law to estimate the pressure exerted by a pressure garment. They stated that the Laplace Law can be used to predict pressure on an area of large circumference, but, where the circumference is small, it tends to overestimate pressure. They did not give any reason why this happened.

Yildiz (2006) used the formula developed by Thomas (2003) to predict the circumferences that will exert a pressure of 20mmHg on a wounded area. The pressure garment that they constructed using the formula exerted a pressure slightly different from the 20 mmHg that they intended to apply to the wounded area.

Maklewska *et al.* (2006) used a method similar to that of Ng and Hui to determine the size of pressure garment. First, they conducted stress-strain experiments on fabric. Then they searched for a general equation to represent the result. By substituting this equation into the Laplace Law, they developed their own formula to determine the size of the pressure garment. However, unlike Ng & Hui who used a linear equation, they used an exponential relation as the equation to represent the result.

Beside research on developing pressure garments, research is also has been conducted to investigate other parameters that influence the pressure induced by the garment, for example, works by Ng (1994), Hui and Ng (2003) and Ng and Hui (1999). Their work is worthy of consideration because they provide a clearer picture of the level of pressure that is exerted by the pressure garment once it is complete. It will enable designers to construct accurate pressure garments for their customers.

Ng (1994) stated that the elasticity of a fabric would decrease over time and also found that washing would also lessen the fabric's elastic properties. Then Hui and Ng (2003) developed a mathematical model to analyze the tension and pressure decay of a single-layer pressure garment.

Ng and Hui (1999) found that fabric pressure would be exerted differently at various locations from the hem edges of the pressure garment. Their findings show that pressure decreases as the location becomes closer to the edge.

All the researchers used the Laplace Law in either developing the pressure garment or estimating the pressure exerted by the garment. However, in the measurement, they used radius obtained by dividing circumference of the body with 2 pi (π). Nevertheless, the Laplace Law mentions that the radius that should be measured is the radius of curvature and not the radius calculated from the body's circumference.

It is understandable why they need to make this adjustment. When patients/subjects are measured, it is the circumference of the body part that is measured. Moreover, it is hard to measure the radius of curvature for each point in a human body. However, the adjustment affects the pressure exerted by the pressure garment. Macintyre and Baird (2006) reported that one of the problems associated with pressure garments is that their pressure is not evenly applied across the body.

For example, even though both the ellipse and the circle in Figure 2.1 have the same circumferences, the radius of curvature for the ellipse is different from point to point, but for the circle, its radius of curvature is the same at each point. If we put a pressure garment on both shapes, the pressure exerted by the garment on the circle will be uniform at each point because of the constant radius of curvature. However, for the ellipse, the pressure at the parts where the radius of curvature is large is lower than the pressure where the radius of curvature is small.

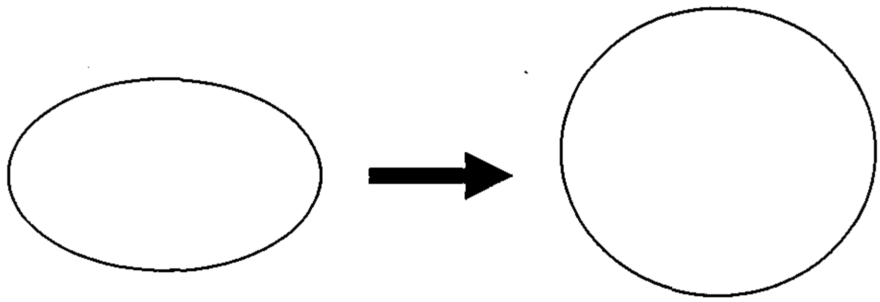

Figure 2.1 Ellipse and circle

Gaied *et al.* (2006) have proved that the variation of pressure is directly caused by the radius of curvature. Figure 2.2 reproduced from their paper, shows that the pressure increases if the angular position is moved to a place where the radius of curvature is small (the cross section of the shape is shown at top right corner of the figure). As shown in Figure 2.2, the pressure at angle $\frac{\pi}{4}$ is greater than at angle $\frac{\pi}{2}$ because at the former angle the curve is sharper than at the latter, which leads to a decrease in the radius of curvature.

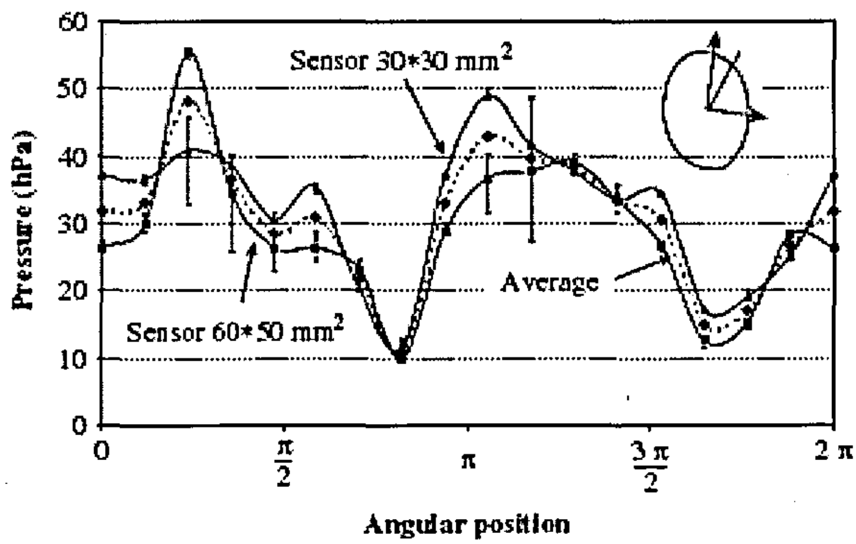

Figure 2.2 Different pressures at different locations on the body (Gaied *et al*, 2006)

In conclusion, it can be assumed that it is impossible to create a pressure garment that can evenly distribute pressure, as the radius of curvature varies from point to point depending on their location on the body. The tension of the fabric can be evenly distributed along the fabric, but the pressure that the fabric exerts on each point still depends on the radius of curvature at each point. However, it is important to keep the pressure within the permitted range, neither too low nor too high. In doing this, a new method to construct a pressure garment must be developed. The method must not only be able to create the pressure garment, moreover, it must show how much pressure the garment will exert at each location.

2.2 Body form data

Size and shape measurements for the human body are an important source of information and affect design decisions (Deason, 1997). Thus, since ancient times, humans have shown a great interest in the study of their body. Hippocrates and Da Vinci are among the famous people for whom the human body has proved fascinating. The study of the human body as a 3D object began in 1973 by Lovesey (as cited in Jones and Rioux, (1997)).

The applications of the 3D body model are limitless, especially in medical fields, human system engineering, comparative morphology, virtual reality and communications (Jones and Rioux, 1997).

Even though there are many techniques to gather body information, the literature in this section focuses on the surface model and surface measurement only. The other anthropometric internal data that can be produced by using MRI (Baulain, 1997, Robb, 2000), CAT scans (Zamenhof *et al.*, 1996, Robb, 2000) or X-rays (Durkin *et al.*, 2002) are excluded. Research on body form data can be divided into two purposes: for measurement (to get the size) or for visualisation (to get the shape).

2.2.1 Body measurement

Body measurement is the first process that must be encountered before any custom-made pressure garment can be designed. The current practice of obtaining the measurement is by traditional methods using tools like a measuring tape. However, this method is considered to be time consuming and usually not accurate (Istook and Hwang, 2001, Simmons and Istook, 2003, Pargas *et al.*, 1997). For a custom-made pressure garment, accuracy is extremely important since it determines the pressure that it applies.

Much research is being conducted to overcome this problem in the apparel industry. The most popular solution is by using non-contact measurement (Simmons and Istook, 2003). Non-contact measurement is a method where body parts are measured without any physical contact with the tools (Hobden, 1998). The development of the 3D body scanner has made non-contact body measurement become a reality due to its capacity to capture a vast amount of information. There are two basic parameters that need to be measured, the circumferences of a body part and the distance between two sections of the body. The main concern is with the methods used to obtain the measurements.

Pargas *et al.* (1997) have developed software to extract body measurements. The body is divided into many horizontal slices. The circumference of a body part can be taken by selecting the slice at the part. The software also allows the user to measure the surface distance between points.

Zhong and Xu (2006) also used a similar concept of measurement to that of Pargas *et al.* (1997). However, instead of dividing the body into slices, they used the proportions of the head length to body height to determine the target parts. For measurement, they divided the body circumferences into two categories, tight contact circumferences and tangential contact circumferences. The former is the contour length of a body part and the latter is the tangential length of a body part. Both need different methods of measurement. Tight contact circumferences can be acquired by sequentially connecting the points of the body part. The other can be obtained by removing all the points that lie between inflexion points and connect all the remaining points to get the tangential contact measurement. They also divided the distance measurement into two categories: linear and curvilinear measurement. The linear distance can be acquired by measuring the length of the direct connection between two given points while the curvilinear distance can be obtained by measuring a part of the circumference between two given points.

Meunier and Yin (2000) used a mathematical model to measure a body that was constructed by using pictures. However, the measurement results were different from the true values.

3D body scanning companies also developed a body measurement system for their products. Simmons and Istook (2003) conducted a survey to compare body measurement techniques between the scanners. In the research, they tried to identify the scanner that could provide the largest number of measures from a pre-identified list, and also had the capability of producing a more specific application for apparel. This research was conducted before 2003, so the result may no longer be accurate. Among the companies that then had the technology to extract body measurements from a 3D body model were $[TC]^2$, Voxelan, Telmat and Cyberware.

The Textile/Clothing Technology Corporation, $[TC]^2$ had developed a software system that could obtain hundreds of automatic measurements from a 3D body model, thus creating custom measurement profiles for automatic measurement. Voxelan also introduced their 3D Measure Workshop software. By just clicking a mouse directly on the 3D body model, measurements could be achieved instantly. The Symcad Optifit system from Telmat and Digisize from Cyberware can also produce body measurements accurately.

For this research, technology to measure body parts from a 3D body model is vital for the development of 3D pressure garment design since it can enable a manufacturer to accumulate data on a wounded area and obtain its measurements from the body model. The information can increase the manufacturer's capabilities of fulfilling the fitting requirements of their customer. It can also avoid inconsistencies and difficulty caused by manual measurement. Thus, in selecting a method, consideration must be given to its capabilities for extracting body measurements at any part of the body, since the wounded area might be small and in an area without a landmark. In order to do this, it is important for the selected method to be able to deliver measurements of any part of the body, fast and accurately.

From the literature reviewed in this section, it is clear that measurement technology has progress significantly, and not limited to 1D measurement only. However, pressure garment manufacturers still did not take advantages of this technology, instead they still depend on manual measurement. The application of body scanning to take body measurement can ease customer burden and reduce time to develop pressure garment. Furthermore, the body scanner also can adds another dimension that manual measurement cannot give; body visualisation.

2.2.2 Body visualisation

Literature on human body visualisation is focussed on a computerized, 3D, human body model. The 3D body model can be developed by various methods. The most popular method employs a body scanner which captures the surface of the subject using optical techniques and transforms it into a computerized model (Istook and Hwang, 2001). Body scanners usually consist of light sources that are projected onto the human body, camera units then capture the image of the projected light on the body, software then transforms the image into a 3D body model and a computer and screen allows this model to be visualized (Daanen and van de Water, 1998).

One of the earliest body scanning techniques was developed in Loughborough University. In this technique, a subject rotates 360 degrees and a slit light is projected in the vertical plane and targeted onto the body. A column of cameras is used to read the image of the projected light and, based on that, the height and location from the centre of rotation can be calculated (Jones *et al.*, 1995).

Rioux (1997) developed a laser-scanning technique called synchronized scanning. It uses a laser source, a double-sided mirror, scanner and a sensor. The technique can be used to capture the shape and colours of the subject. It uses an RGB laser coupled to an optical fibre. First, the laser is targeted on the object. One side of the mirror scans the laser beam and the other side scans the scattered laser spot. An image of the spot is transferred to the sensor. The orientation of the object can be calculated by monitoring the scanner position, while the range of coordinates can be obtained by studying the position on the sensor of the laser spot image.

Linney *et al.* (1997) also used a laser as their light source. In their 3D body scanner, a line beam produced by a low-power InGa laser is projected onto the body surface. The distortion of the line provides a measure of the shape of the surface. The line is viewed by camera from two opposing directions using the mirror arrangement shown in Figure 2.3. The video signal is pre-processed to produce the surface coordinates. In this technique, the subject is rotated 200 degrees on the platform.

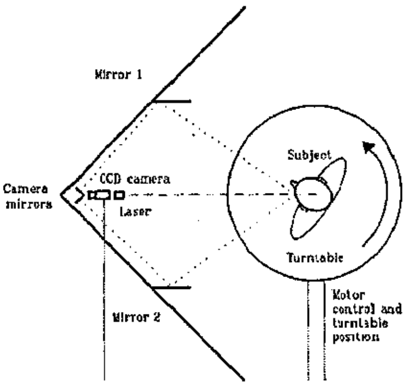

Figure 2.3 3D body scans layout (Linney *et al.*, 1997)

Siebert and Marshall (2000) used a 3D sensing technique known as C3D to develop their body model. C3D is a non-contact optical sensing technology that is based on speckle texture projection photogrammetry. It relies on camera-camera base line triangulation (Figure 2.4) to perform depth sensing. Images that have been captured by both cameras are decoded to produce an explicit depth map. Unlike other body scanners, C3D can capture the whole body instantly, without the need to scan each segment of the body.

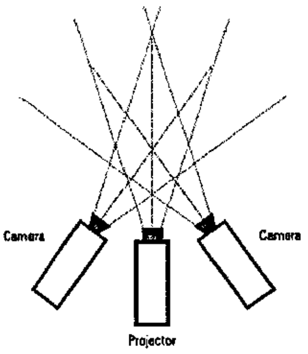

Figure 2.4 Camera-camera base line triangulation

Xu *et al.* (2002) also used a laser as their scanning source. First, they developed a dark booth, which had two linear stages. The stages, which carry a multiple laser line projector and a CCD camera, can move upward and downward to scan the body. It was located to the front and back of the person (refer Figure 2.5). The depth calculation is based on a triangulation algorithm.

Beside researchers, there are companies that are also involved in the development of a 3D body model. Some of researchers on garment design used the companies' technology when developing their 3D body model, like $[TC]^2$ (May-Plumbee *et al.*, 2005), Lectra Systèmes (Rodel *et al.*, 2001) and Cyberware (Sul and Kang, 2004, Kim and Kang, 2002). All of the companies use a 3D body scanner to construct a 3D human body. Istook and Hwang (2001) and Daanen and van de Water (1998) have studied some of the companies that offer the technology. Istook and Hwang (2001) divided the companies into three main groups: the light-based systems companies, laser-based systems companies and the other systems companies.

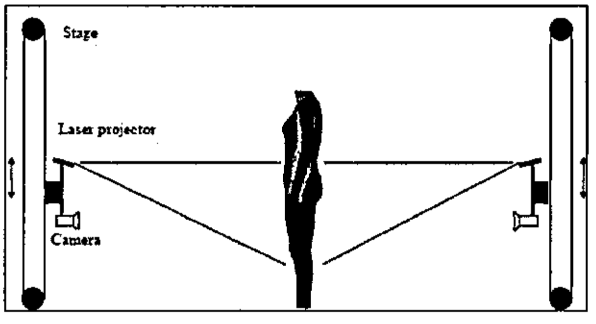

Figure 2.5 Layout of the laser 3D body scanner

Even though frequently used in the clothing industry, 3D body scanning has some limitations. The most obvious limitation is that there is too much data to be stored (Stylios *et al.*, 2001). Thus, it makes quick communication impossible. Moreover, the cost of a 3D body scanner is high, which makes it less competitive (Cho *et al.*, 2005). To overcome this problem, several researchers have introduced new techniques to develop the 3D body model. Instead of body scanning, a 2D, image-based picture has been used to construct their 3D body model.

Meunier and Yin (2000) for example, used front and side pictures of a body and processed them to develop a 3D body model. However, their research focussed on body measurement, thus they did not explain how they developed the body from the pictures.

Hilton *et al.*, (2000) also developed a 3D body model based on 2D images. First, a set of four orthogonal (front, both sides and back) views of a person is captured. Then the image model is separated from its background by using the chroma key technique to obtain its silhouette. After that, an algorithm was used to extract feature points. Then, any point inside the generic model silhouette and a point on the same part inside the captured image silhouette is mapped. By combining the mapping information, a 3D human body can be obtained. Wang *et al.* (2003) also used the same technique with Hilton *et al.* (2000). However, their technique was much faster because they used an improved Chan-Vese algorithm to extract a silhouette of a human model from a photo. However, the body model produced by using this method cannot accurately represent the body because of shape approximation errors (Wang *et al.*, 2003, Hilton *et al.*, 2000). To overcome this problem, more orthogonal images are needed so that more silhouettes can be obtained.

In addition to using body scanning and photographs, some researchers have developed an interactive body model (Cordier *et al.*, 2003, Cho *et al.*, 2006, Cho *et al.*, 2005, Stylios *et al.*, 2001). In this method, a preliminary shape of the 3D body model is created. By adding measurements of the customer's body size, the initial 3D body model can be altered into a new shape according to the body size. The initial model can be developed using ordinary techniques. For example, Stylios *et al.* (2001) developed the model using an algorithm that can captured pictures that show the back view, front view and side view of a person and transform them into an initial 3D body model. Cordier *et al.* (2003) constructed generic models to represent their initial body model. Cho *et al.* (2005) used a mannequin and scanned it to develop their body model.

The method was suitable for online body visualisation since the user only needed to input their body measurement to view the 3D body model. However, the developed model was not an accurate representation of the user's body since it was only an approximation model based on the algorithm used to develop the body (Cho *et al.*, 2005, Cho *et al.*, 2006).

From the literature above, it is clear that researchers are trying to develop a system to construct a 3D body model. A 3D body model is essential for 3D pressure garment design because it enables the manufacturer to study the wounded area further, in order for them to develop a proper pressure garment. For example, by knowing the location, they can produce a pressure garment with suitable features for the client. It also enables the customer to give their opinion or assessment during its design development. In order to do this, a 3D body scanner with capabilities to visualise/show a wounded area is needed.

2.3 3D garment creation methods

Traditionally, designers create garment designs based on their own creativity, subject to current fashion trends and the target market. Their design specification is usually in the form of a paper drawing representing a visualization of the garment. However, one of the weaknesses of this method is its time-consuming nature (McCartney *et al.*, 2000a). Thus, to minimise the time, it is essential for garment manufacturers to adopt a 3D CAD design system to develop their garment. Furthermore, the use of 3D CAD during the garment design process is important for visualisation and for design assessment, fabric suitability and the accuracy of the developed patterns (Hardaker and Fozzard, 1997). It is anticipated that 3D technologies will be the next evolving technology area for the apparel industry (Wang and Yuen, 2005).

This section describes the development of 3D garment design.

Hinds and McCartney (1990) and Hinds *et al.* (1991) initiated a system whereby a 3D garment design can be developed directly on a 3D body model. In this method, a body model resembling a mannequin must be developed first. Then, by using the provided tool-kit, a 3D garment model can be created as a series of connected panels around the body model.

Okabe *et al.* (1992) used two-dimensional paper patterns to create their 3D garment model. In this method, they placed the paper pattern on a 3D body model. Then they applied a physical simulation to wrap the body with the paper patterns, and sewed its lines together to create a 3D garment model.

Magnenat Thalmann from MIRALab in the University of Geneva also used a similar approach with Okabe *et al.* (1992) to develop their 3D garment design (Yang and Magnenat-Thalmann, 1992). In the research, they make another contribution to garment design by providing a simulation and animation of the changing shape of the 3D garment design with a moving body. Magnenat Thalmann has continued the research till now by providing a more powerful animation of the 3D garment (Magnenat-Thalmann and Volino, 2005). However, their work is limited to garment animation only.

Rodel *et al.* (2001) used DesignConcept 3D software to develop their 3D garment design. First, they created 2D pattern pieces and, with the help of the software, seamed the pieces together and draped them over a 3D body model to generate a surface. The design can be created on the surface.

Tarakanov and Adamatzky (2002) and Fontana *et al.* (2005) also used a 2D pattern to develop a 3D garment design. Tarakanov and Adamatzky (2002) used the same method but with a different approach. They applied a hybrid cellular automaton as a parallel computing device to decrease the time required to simulate the 3D garment. For the latter, they constructed a 2D single pattern and then sewed (by using a sewing algorithm) it to other patterns, to create a 3D design. Their objective is to integrate garment design with simulation in order to help designers to evaluate their work more accurately.

Sul and Kang (2004) also used the 2D piece pattern in their earlier work. However, in their next research they introduced a new method of designing a 3D garment (Sul and Kang, 2006). This method is very similar to the use of a 2D piece pattern to develop a 3D design. It mimics a real pattern designers' draping technique. They lay down a simple 3D mesh sheet on a 3D body model and construct a 3D design by using the

NURBS cutting curve and a mesh-cutting algorithm directly on the sheet at the body. The advantage of this method is that they do not need to flatten the 3D design to get the garment pattern because the pattern was generated simultaneously as the mesh sheet was edited.

Kang and Kim (2000b) used the 2D garment patterns that they generated earlier in Kang and Kim (2000a) to develop their 3D garment model. Each pattern is divided into quadrilateral elements using a mesh-generating program. The patterns is then assembled and sewn to create the 3D garment shape. After that, the 3D design is put on a 3D body model for the final drape shape alteration. Their method is different from other 2D-pattern-using methods because, instead of using a predetermined paper pattern, they used a complete 2D garment pattern. Another difference is that they assembled the pattern to create the 3D garment first and then they draped it onto the 3D body model. The other 2D-pattern-using methods cover the body model first and then develop the 3D garment design.

Beside the 2D-pattern-using method, Kang and Kim (2000c) also introduced a new technique to develop the 3D garment design. First, they take an image of a dummy model with meshes on it using a CCD camera. Then, by using stereo calculation, they bring out just the surface with the meshes and assemble the surfaces to form the 3D garment model. Then they put the garment model on a 3D body model. The garment model adjusts to obtain an optimum fit for the body model.

Similar work can be seen in Wang *et al.* (2002a). First, they developed a human model with features on it. Then they created a 3D garment model with features similar to the human model by using 2D free-form strokes. By putting the 3D model on the human model, and by providing some conditions to avoid collision, a new 3D garment design that fits the body model can be achieved. They also present a new technique for made-to-measure garment design. Based on their 2002a research, they developed a technique that can automatically generate a new garment design with the same fashion on different body shapes (Wang *et al.*, 2003). The technique enables designers to produce designs based on client measurements faster, without the need to create a new 3D garment model, as in the previous research. At the same time, Luo and Yuen (2005) provide a new algorithm that can alter a 3D garment design by modifying the garment pattern.

Chiricota (2003) and Chiricota *et al.* (2001) conducted a similar process that is being used in the apparel industry to develop their 3D garment design. First, they gather information on the garment parameters. Then, based on the information, they create geometrical models using a wireframe image. The models will be converted to a masses-springs system, and a physical simulation performed. In Chiricota (2003), a similar process was used to create other garment parts (like pockets, collars etc) and display them on the 3D garment.

Fang and Liao (2005a), Fang and Liao (2005b) used a feature-based mannequin model to develop their 3D apparel. By using information provided by the model, a basic garment surface can be generated over the mannequin. The other parts of the garment, like the collar (Fang, 2003) and sleeve, can be designed by using a mathematical model.

Xu *et al.* (2002) also used the same method as Fang and Liao (2005a). However, unlike them, Xu *et al.*, (2002) used data provided by a body scanner to directly develop their virtual garment by following the shape of the 3D body.

May-Plumbee *et al.* (2005) used a real garment to develop their 3D model. First, using a 3D scanner, they scanned a real garment that hangs on a base stand. Then, they erased all unwanted features from the developed surface, leaving the 3D garment model alone.

As for discussion, in order to develop a 3D pressure garment, it is important to note that a pressure garment is not like an ordinary garment only to be used on a certain body part. It can be used on any part. Thus, the garment must be able to be designed at any place on the body including the leg, head, hand etc. Any method to be used to develop the 3D model should be able to tackle this problem.

The use of the method introduced by May-Plumbee *et al.* (2005) is considered to be inconvenient since it will need a lot of garment data to be stored in a database. For mesh surfaces made by Kang and Kim (2000c), Wang *et al.* (2002a), this was considered to be time consuming as it needed the body part and pressure garment to be sketched with lines.

The method of Fang and Liao (2005a) and Fang and Liao (2005b) is not suitable because it needs human body measurements in order to develop the digital mannequin. As mentioned earlier, the taking of manual measurements will cause uncertainty and hard work. If they were taken by using a body scanner, then it is a waste of time developing two different body models.

The work of Chiricota *et al.* (2001) also is not suitable since the developed 3D garment model is only an approximation based on the given measurements. Moreover it cannot be placed on a 3D body model.

Even though the use of an interactive body surface (Hinds and McCartney, 1990) is possible, this method requires the development of a 3D body model with such capabilities. The method introduced by Sul and Kang (2006) is also possible, but is not yet available in commercial CAD software.

The other methods to develop a 3D pressure garment are by using a 2D paper pattern (Okabe *et al.*, 1992, Yang and Magnenat-Thalmann, 1992, Rodel *et al.*, 2001, Fontana *et al.*, 2005) or using scanning data (Xu *et al.*, 2002).

For this research, method to be employed to create the 3D pressure garment model is by developed it directly on 3D body. The 3D body data was acquired using body scanner. The method is preferred because it can give information on body shape and the information can be used further to create the true size of the pressure garment.

2.4 Garment pattern generation

Pattern making is the process of transforming a fashion design into its constituent flat pattern pieces. It is the starting point of garment manufacturing, which is usually performed by highly skilled pattern makers. With the current developments in technology, automatic pattern generation is seen as a major aim of a 3D CAD system.

This section looks into the development of garment pattern generation. Pattern generation methods can be categorized into two types based on their development techniques. The first category is a pattern developed by using a prediction of human body measurements and the second category is the pattern developed by flattening a 3D garment design.

2.4.1 Pattern development by using predictions of human body measurements

Turner (1994), Kang and Kim (2000a), Eckert and Bez (2000) and Petrak and Rogale (2001) have developed a system to generate a garment pattern automatically based on human body measurements.

Turner (1994) has developed a micro-computer-based system for automatic construction and plotting of made-to-measure bridalware patterns. In this system, the user needs to input their body measurements and the system generates their garment pattern. Eckert and Bez (2000) used a mathematical model of Bezier curves to develop their garment pattern.

Kang and Kim (2000a) formulated a set of pattern-drafting rules using a script language. It generates patterns by compiling corresponding scripts to make modifications to the patterns. Then they also developed a pattern-modification system that can change the geometry and topology of the patterns and generate engineering patterns automatically.

Petrak and Rogale (2001) used AutoCAD to develop a men's shirt pattern. First, they calculate the necessary measurements for the basic points in the pattern. Then they calculate point coordinates to develop the contour of the pattern. The calculation was carried out in Excel. Thus, it is necessary to transform the data into script data files in order to move it into AutoCAD. AutoCAD links all the points to construct the garment pattern.

Chan *et al.* (2005) used a multiple linear regression technique to predict shirt patterns. In this research, they added body parameters to examine the underlying relationship between shirt pattern parameters and body measurements. By doing that, they improved the prediction of the shirt pattern compared with a previous formula produced by a pattern expert.

2.4.2 Pattern development by flattening the 3D garment design

Hinds *et al.* (1991) initiated this method. First, they created quadrilateral meshes on the 3D garment surface using the Newton-Raphson algorithm. Then, by retaining the meshes' lengths and branches, it was mapped in 2D by rolling out each strip of meshes starting from the spine, to develop the pattern design. However, the pattern obtained has many darts since each strip was flattened individually. In McCartney *et al.* (1999), they used triangular meshes to substitute for the quadrilateral meshes. An algorithm that incorporates an energy model was used to flatten the meshes one by one to obtain an initial pattern. If the triangulated surface is a close approximation to a developable surface, the magnitudes of the energy distribution will be very small. However, if the magnitudes are high, they will be eased using an energy relaxation process which alters the positions of the nodes in the pattern. McCartney *et al.* (2005) created triangulation meshes using a front marching algorithm. The developed meshes are more uniform and suitable for the flattening process. In order to reduce offset error in the flattening process, they used a subdivision process to create smaller meshes in areas where problems potentially occur.

Azariadis and Aspragathos (1997) used three steps in order to generate a pattern. In the first step, an analysis was made on a 3D surface to create triangulation and starting locations for the flattening. Then, the surface was unfolded to create the earlier pattern. Sometimes, the pattern was filled with gaps and overlaps as in Hinds *et al.*, (1991). To overcome this problem, they used a geometric approach and generalized inverses to refine the earlier pattern by minimizing the gaps and overlaps on it. However, the final result from this technique was not accurate enough. In Azariadis and Aspragathos (2001), they used an energy model to flatten the surface. With this method, they did not depend on surface parameterization.

Kang and Kim (2000c) used a similar method to that of Hinds *et al.* (1991) by retaining the meshes' lengths to flatten their 3D surfaces. In order to avoid the problem of producing many darts, as in Hinds *et al.* (1991), they divided a 3D garment surface into four areas (front right, front left, back right and back left) with each area split into four panels. Each panel was flattened individually. The developed patterns were assembled together and the edges of the intermediate panels formed darts. However, the pattern is still unsuitable for a typical garment pattern since the number of darts is still considered large. To overcome this problem, Kim and Kang (2002) brought small darts together into a single large dart by allowed some shear in the rows being rolled out. They used triangular instead of quadrilateral meshes in the research.

On the other hand, Wang *et al.* (2002b) used a similar approach to that of McCartney *et al.* (1999) to develop an algorithm to flatten their 3D surface. However, instead of using a strain energy model, they used a spring-mass model based on an energy function. The algorithm enabled them to cut the surface using a gradient method to reduce the error for the resulting developed surface.

2.5 Pressure measurement

Pressure garments are primarily designed to exert pressure on a particular part of the body. Thus, in developing a pressure garment, the pressure exerted by the pressure garment is another consideration that must be taken into account. The pressure will determine the success of the treatment. If the pressure is too low, then it will not heal the scar, and if the pressure is too high, it can cause unpleasant side effects (Macintyre and Baird, 2006).

It is difficult to determine which level of pressure is optimum for scar healing and even researchers differ among themselves on the matter (Macintyre and Baird, 2006). Most researchers agreed that it should be more than the capillary pressure (normally quoted as 25 mmHg). However, this research is not focussed on identifying the effective pressure for the healing process. It concentrates on how to measure the pressure that is being exerted by the pressure garment.

This section reviews the methods used to measure the level of pressure exerted by the pressure garment. This pressure can be measured by direct or indirect means (Giele *et al.*, 1997).

In the first method, measurement is carried out using a sensor cell, which is inserted between the garment and skin, after the garment has been constructed. For example, Ng and Hui (1999), Harries and Pegg (1989), Ng and Hui (2001) and Hui and Ng (2003) used an Oxford pressure monitor to measure the pressure exerted by a pressure garment in use. The sensor cell of the pressure monitor is a small bag made of thin plastic layers. Mann *et al.* (1997) used an I-scan sensor developed by Tekscan, Inc. The sensor uses an ultra-thin (0.007 inch) sensor with multiple sensing locations that sample continuously at 100 times per second, to measure the pressure developed under the pressure garment. They concluded that the system could be used to measure pressure under pressure garments accurately and reliably. Besides this research, there are some other papers (Hunston (2002) and Ferguson-Pell *et al.* (2000)) that also mention the evaluation of a sensor that can be used for measuring the pressure under a pressure garment. Both evaluated sensors were designed by Tekscan, Inc.

However, this external direct measurement has some limitations like distortion of the garment and poor conformity to the skin (Giele *et al.*, 1997). To overcome the problem, Giele *et al.* (1997) developed a new technique to measure directly the sub-dermal cutaneous pressure generated by a pressure garment. First, they inserted a needle that is connected to a low-flow pressure transducer into skin. When the pressure garment is then worn, the pressure that it exerted is measured.

Nevertheless, both methods of direct measurement on the human body are time-consuming and expensive (Fan and Chan, 2005, Chan *et al.*, 2005) because the pressure garment needs to be constructed first and the pressure can only be measured at a limited number of places. To overcome this problem, some researchers have developed indirect methods to estimate the exerted pressure.

Yu *et al.* (2004) developed a mannequin to be used to evaluate the pressure exerted by a pressure garment. Fan and Chan (2005) used the mannequin to measure a girdle's pressure and, by using the information, tried to estimate the pressure on the human body. In the research, they used linear regression to construct their equation for estimation. Even though the research was carried out on a girdle, the method can also be applied to a pressure garment. However, although the method may be suitable for mass produced products, for a tailor-made pressure garment, it is inconvenient for manufacturers to check the clothing pressure for each customer.

Another method is by making predictions based on mechanical models and computer simulations. Zhang *et al.* (2002) developed a mechanical model based on analyzing the contact characteristics between the human body and a garment, to create a simulation of 3D dynamic garment pressure. The model can simulate and predict the dynamic mechanical behaviour of a garment during wear. However, accurate results are difficult to obtain since the models are based on simplified geometrical assumptions (Chan *et al.*, 2005).

Non-contact pressure measurement technique include Pressure Sensitive Paint (PSP), which is based on oxygen quenching of molecular photoluminescence (Reda *et al.*, 1998), or surface-stress-sensitive film which is based on 3D surface deformations (Fonov *et al.*, 2004, Fonov *et al.*, 2005). Both of the techniques are used for measuring the pressure at a surface of a rigid body.

2.6 Fabric properties

Each different type of fabric that is being used in pressure garment making exerts a different level of pressure (Harries and Pegg, 1989, Macintyre *et al.*, 2004). According to Wong *et al.* (2004), garment pressure is affected by body shape, the mechanical properties of the fabric and the style of the garment. However, for a pressure garment, there are three important parameters that will determine the pressure exerted: the fabric properties, the reduction factor and the garment dimensions (Macintyre *et al.*, 2004).

There is little information on the properties of fabrics used in pressure garment making in the literature. According to Macintyre *et al.* (2004) and Thomas (2003), the most important property affecting a fabric's pressure is tension. Fabrics with high tension will exert a high pressure even though they have similar dimensions. In the research, they also found that fabrics with the same properties would also exert a different magnitude of pressure if the dimensions of the fabric are changed. Garments with a larger circumference apply a smaller pressure, and *vice versa*. Considering the reduction factor, an increase in the reduction factor increases the pressure even if both the above-mentioned parameters are constant. Thomas (2003) also conducted similar research in which two more parameters were included in the equation: bandage width and the number of layers applied. However, they did not do any experimental studies to validate their equations.

Ng and Hui (2001) have formulated the relationship between the tensile properties of a fabric, the curvature of a contoured surface and skin-and-garment interfacial pressure into a mathematical expression. Their findings are also in accord with Macintyre *et al.* (2004).

Most of pressure garments are made by weft-knitting and warp-knitting elastic fabric. In a weft knitting machine, yarn feeding and loop formation will occur at each needle in succession across the needle bed during the same knitting cycle (Figure 2.6). However, in warp knitting machine there will be a simultaneous yarn-feeding and loop forming action occurring at every needle in the needle bar during the same knitting cycle (Figure 2.7).

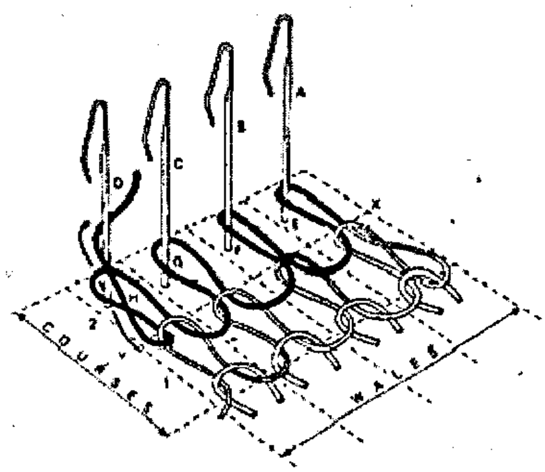

Figure 2.6 Weft knitting (Spencer, 1983)

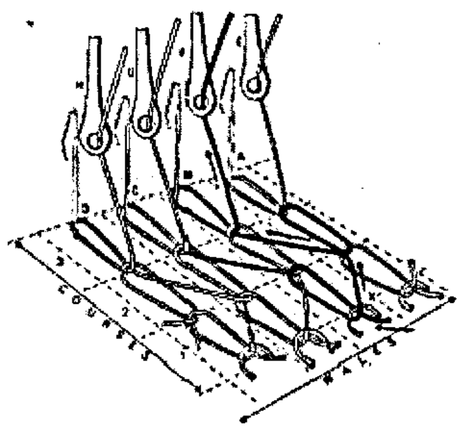

Figure 2.7 Warp-knitting (Spencer, 1983)

This research used a warp-knitted fabric called powernet. It is the most popular fabric structure used in developing pressure garment to UK patients (Macintyre, 2007). The powernet is composed of blends of elastic and synthetic inelastic yarns. The fabric employed elastane as the elastic yarns while the synthetic inelastic components of the fabrics is nylon. The proportions and weight of nylon and elastane in a powernet fabric largely determine its tension delivering potential. The most widely-known structure for the powernet is shown in Figure 2.8. The structure can provide a lengthwise extension of 75-85% and a widthwise extension of 65-75% (Spencer, 1983). The powernet fabric also display a negative Poisson's Ratio if being stretched in courses direction.

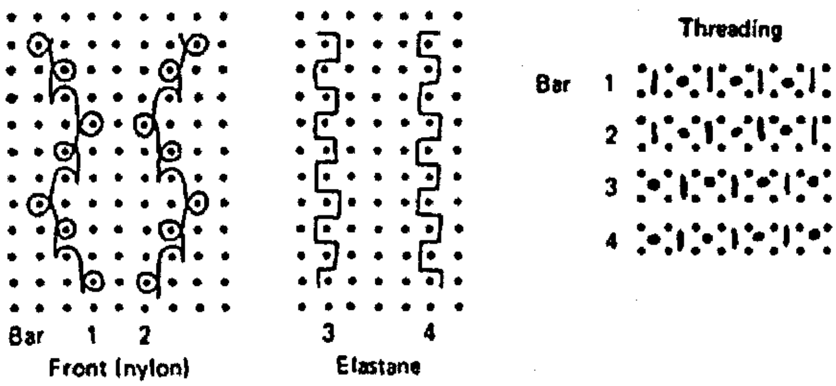

Figure 2.8 Powernet fabrics (Spencer, 1983)

2.7 Discussion

This chapter has reviewed the research into the design of garments and its application in the development of 3D, computer-aided, pressure garment design. In the first section, the current pressure garment production methods have been discussed. This clearly shows that most of the researchers are in search of a method to develop pressure garments that can exert a certain range of pressure. However, their efforts are limited, because of the nature of the human body.

The next sections review the current technology in garment manufacturing. This shows that the advancement of technology in the area makes it possible for the development of a 3D computer-aided pressure garment design. By the development of the 3D computer-aided pressure garment design, it is hoped to transform the current manual design method and provide the customer with improved pressure garment performance.

The literature survey reveals that there are rapid technological progresses in ordinary garment manufacturing area. The introduction of many new technologies, such as body scanning, 3D garment model and pattern generation, has benefits the area to develop further. However, the same cannot be said to the pressure garment manufacturing. The area still used conventional method to construct the garment. The accuracy of the method to provide proper pressure garment is debatable. Current technology that is being researched in ordinary garment manufacturing can be manipulated to be used in developing pressure garment. Thus, it is important to develop a method to integrate the technology so it can be used in pressure garment manufacturing.

The first area that needed new technology is body measurement. Current manual measurement is time consuming and error-prone. New technology is needed to overcome the problem. The next area is to develop mathematical model to create a pressure garment model, especially in calculating its reduction factor. Reduction factor is normally calculated based on circumference. The next area is the development of patterns for pressure garments. Most of pressure garment making companies use predictions of human body measurements to develop the pattern. However, the method is considered as inaccurate as human body is different between each other. Thus, it is important to propose a method that can create pressure garment pattern based on 3D garment model. Another area that needs attention is the pressure measurement. Since the pressure garment can cover wide area of body, it is almost impossible to measure pressure that the garment exerts. To overcome the problem, a model that can predict the pressure is essential.

This research will develop a method to acquire body data from body scanner and develop technique to create pressure garment model and generate its pattern based on the data. A model to predict pressure distribution exerted by the pressure garment also will be developed.

Chapter 3 The 3D pressure garment model and 2D pattern development

This chapter explains how the 3D pressure garment model was developed using 3D body data and then transformed into a 2D pattern, and verify experimentally.

The first process of developing the 3D garment design can be categorized into three main steps; 3D data acquisition, development of the 3D wounded area and development of the 3D pressure garment.

The second process of transformation to the 2D pattern involves two steps: creating a triangulation for the points and flattening the triangulation.

Finally, experiments have been conducted to validate the developed computer program.

3.1 3D data acquisition

A 3D body model is used in this research for both visualisation and measurement. A $[TC]^2$ NX12 3D, horizontal type, body scanner was used to extract the 3D (in x, y, z coordinates) raw data of the subject body.

A body scanner of this type is expensive and may not be practicable to use in each and every burn unit or hospital. However, the technology of body scanning is fast developing and soon there will be affordable, portable scanning units that could be used in burn units.

The scanner used works by projecting a structured light pattern onto a human subject and capturing a series of images. These images are then converted into a large number of data points around the body shape.

Prior to any measurements are taken, the scanner calibration needs to be verified to ensure that its measurements are accurate. A white cylinder is placed in the centre of the scan chamber. The cylinder is scanned and compared to the scanner's internal calibration files.

After being verified, the subject enters the body scanner booth. They stand in the booth in a standard position (refer Figure 3.1). When they are ready, they start the scanning process either by using a remote controller by themselves, or by giving a signal to the researcher to start the scan. As a precaution, the subjects stay in the booth after the scanning process while the data was processed. After a 3D body model is displayed, it is saved into a .wrp file. 3D data coordinates can be obtained by converting this file to a text file (.txt).

The raw data scanned by $(TC)^2$ body scanner, is made up of seven segments: right leg, left leg, torso (including head), right arm, right hand, left arm, left hand. The data of each segment includes two matrixes. One matrix contains the coordinates of the 3D point cloud, another save the coordinate indexes and color values of the triangle patch. In this research, only the coordinates of the 3D point cloud are used. Some of the data is attached in Appendix A.

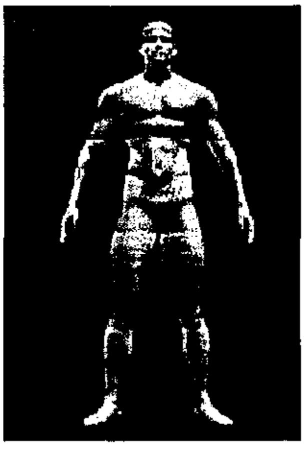

Figure 3.1 Standard standing position

3.2 3D wounded area model development

The text data is exported to Matlab, and the 3D data is transformed again to create a 3D point cloud. A result from the 3D body scanner is shown in Figure 3.2 (a). For this research, effort is made to create a pressure garment for one leg only. A 3D thigh is shown in Figure 3.2(b). The arrangement of the points is such that they start from the front of the body and move clockwise to the other surfaces. Every point is represented by it's coordinate on the x-, y- and z- axes.

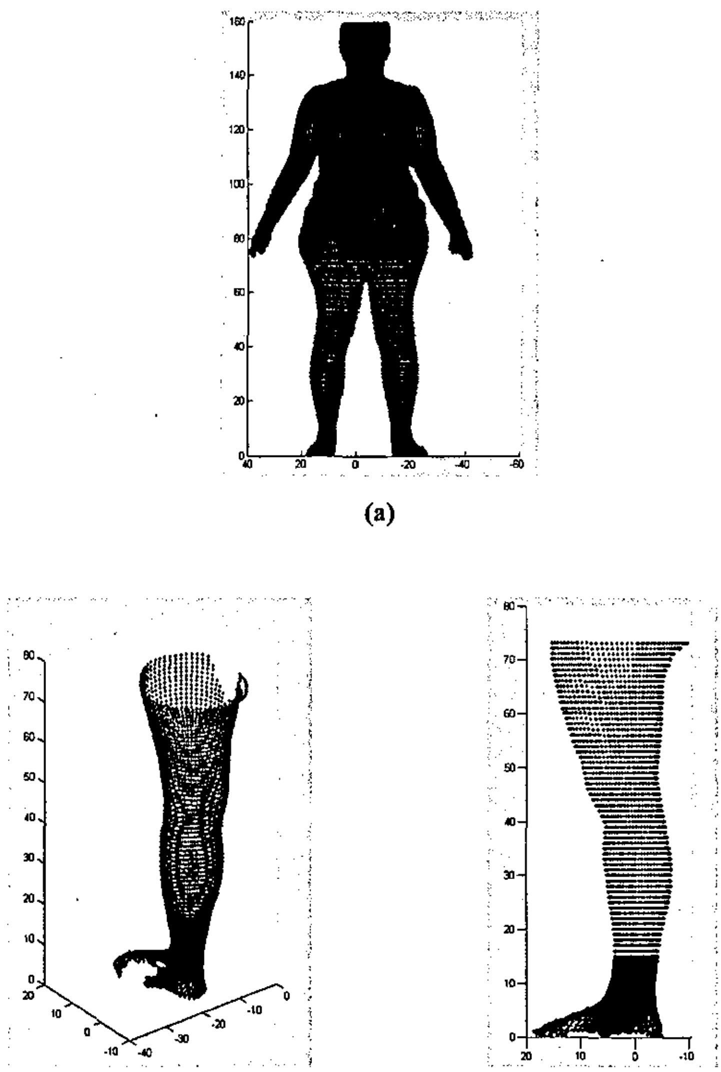

(a)

(b)

Figure 3.2 3D point cloud of (a) a body (b) a leg formed by using Matlab

Then, the data is examined, and only data for the wounded area is extracted. A computer program is developed so that the data can be gathered by selecting the height of the location of the wounded area (both top and bottom). For this research, an area below the knee was chosen as wounded area The data can be transformed to create a 3D wounded area model (refer Figure 3.3). Figure 3.4 shows the location of the wounded area on the leg.

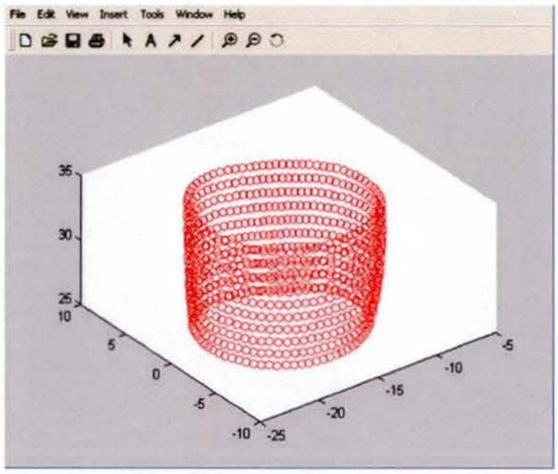

Figure 3.3 Extracted data from 3D body model

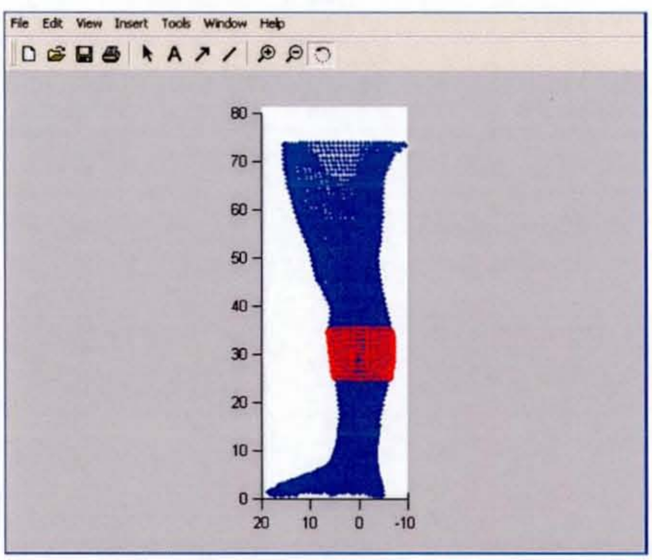

Figure 3.4 Location of selected wounded area

3.3 Methodology to develop 3D pressure garment model

This research uses the 3D body data generated by a body scanner to create the pressure garment. A flowchart of the process is shown in Figure 3.5.

First, the radius and centroid of each layer are determined from the 3D wounded data. By combining the radius with the fabric's modulus of elasticity and the pressure to be exerted, a reduction factor for each layer was obtained. Then, by joining together the reduction factor and the centroid of each layer and also the 3D wounded area, a 3D pressure garment is developed. Since the model is based on measured body shape, radius of curvature, the elastic modulus of the fabric used to create the pressure garment and the pressure required to be applied, it leads to an accurate calculation of the reduction factor at each layer, which in turn results in an accurate pressure garment.

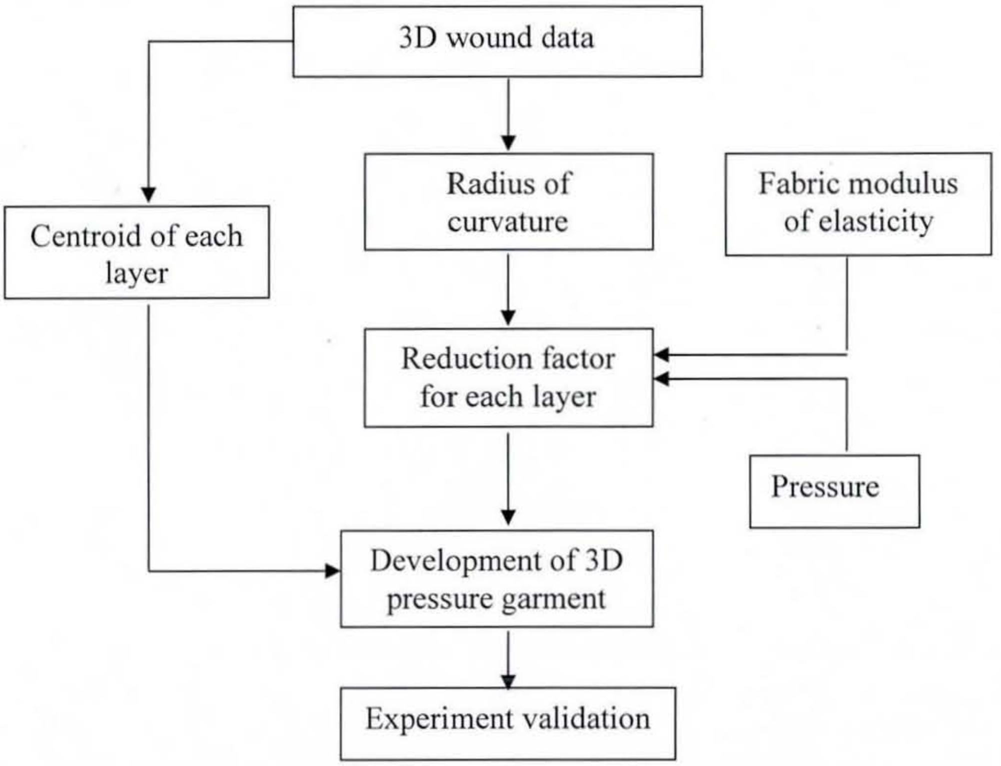

Figure 3.5 **3D pressure garment creation proposal**

3.3.1 Calculation of the reduction factor

The reduction factor is the factor that is needed by which to reduce the original body measurement. Thus, if C_0 is the original circumference of the wounded area at a certain layer, then the pressure garment's circumference at the layer, C_1, should be:

$$C_1 = (1 - \mathrm{Re})C_0$$

where Re is the reduction factor. According to Laplace's Law, the tension, the radius of curvature and the pressure have a definite relationship that is given by the formula:

$$P = \frac{T}{\rho}$$

where P is the pressure, ρ is the radius of curvature and T is the surface tension of the pressure garment. The latter can be calculated by using Hooke's Law. By assuming that the body's circumferences remains constant even after pressure has been exerted, the pressure generated by the pressure garment can be calculated as:

$$T = E\frac{(C_0 - C_1)}{C_1}$$

$$T = E\frac{(C_0 - (1 - \mathrm{Re})C_0)}{(1 - \mathrm{Re})C_0}$$

$$T = \frac{E\,\mathrm{Re}}{1 - \mathrm{Re}}$$

where E is modulus of elasticity (Ng and Hui, 2001). By substituting the above formula into Laplace's Law:

$$P = \frac{E\,\mathrm{Re}}{(1-\mathrm{Re})\rho}.$$

Thus the reduction factor is given by:

$$\mathrm{Re} = \frac{P\rho}{P\rho + E}$$

$$\mathrm{Re} = \frac{1}{1+\dfrac{E}{P\rho}} \tag{3.1}$$

Based on the equation 3.1, in order to calculate the reduction factor, there are three main parameters to be considered, the modulus of elasticity, the pressure to be exerted and the radius of curvature.

For the first parameter, every fabric has its own elasticity, which can be determined by using a tensile test experiment. Selected fabrics will be extended to a certain percentage, and the forces that are needed to extend the fabrics will then be recorded and plotted. The modulus can be determined by calculating the slope of the stress-strain curve, in the region where the Hooke's Law holds.

For the second parameter, the pressure to be exerted depends on how much pressure the garment is required to exert on the body. In this research, a pressure of 2666 Pa (20 mmHg) is selected.

The third parameter, the radius of curvature, is discussed in the next section.

3.3.2 Radius of curvature

The radius of curvature of a curve at a point is actually the radius of the osculating circle at that point. It is given by the formula:

$$\rho = \frac{1}{\kappa},$$

where κ is the curvature. However, in pressure garment research the radius is always calculated by dividing the circumferences of the body by 2π (pi), i.e. by determining the radius of a nominal circle that has the same circumference as the measured body part.

This is a very common practice because it is difficult to determine the suitable radius of curvature for each layer to be used. The radius of curvature for each point on the circumference of the cross section is different depending on its location. Its value ranges from very low to almost infinity in certain cases. For example, Figure 3.6 shows how a small number of the radius of curvatures in the wounded area is extremely high compared to others.

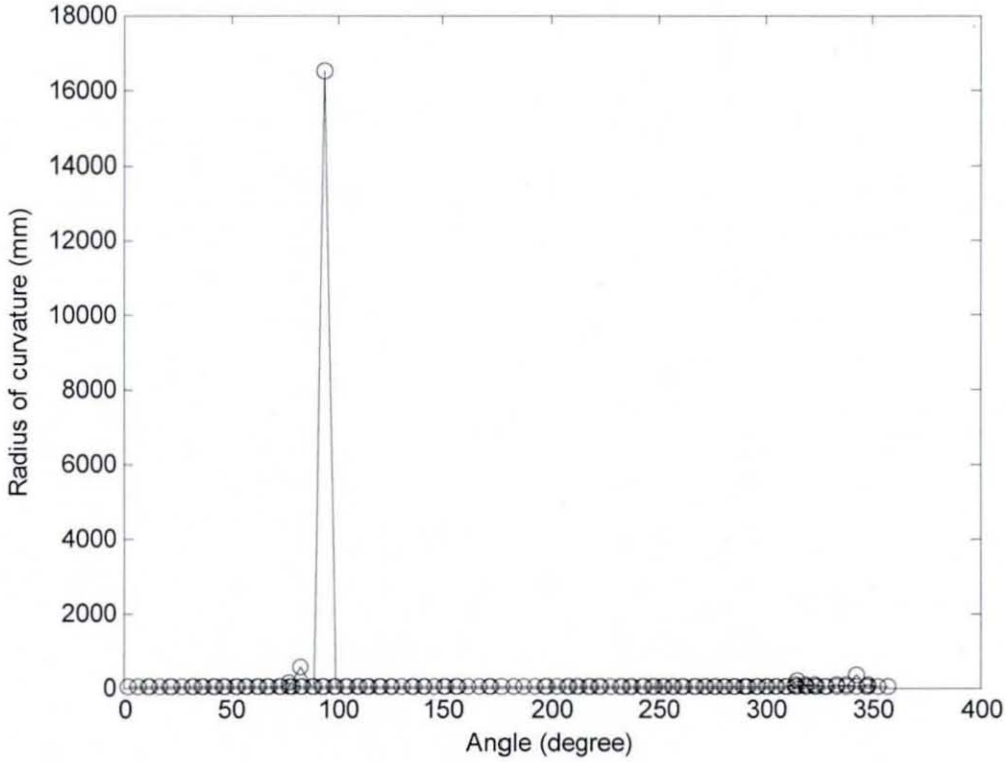

Figure 3.6 Radius of curvature (ROC) for the wounded area

Figure 3.7 shows the radius of curvature for every layer of the wounded area. The figures show that at all layers, there are points which can be considered as extreme compare to others.

Layer	Cross section	Radius of curvature
1	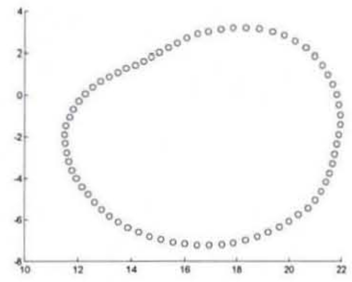	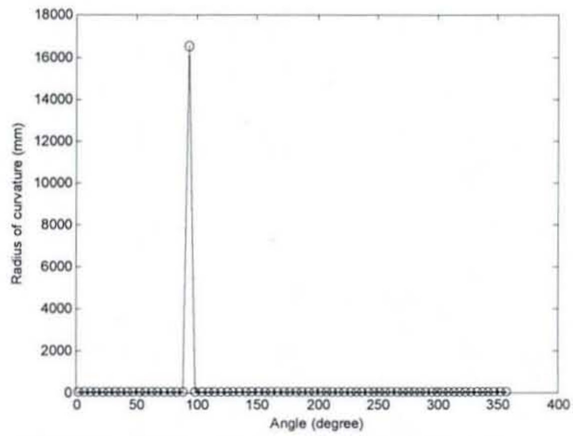
2	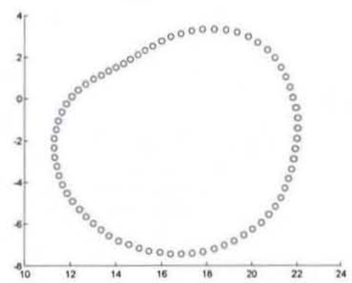	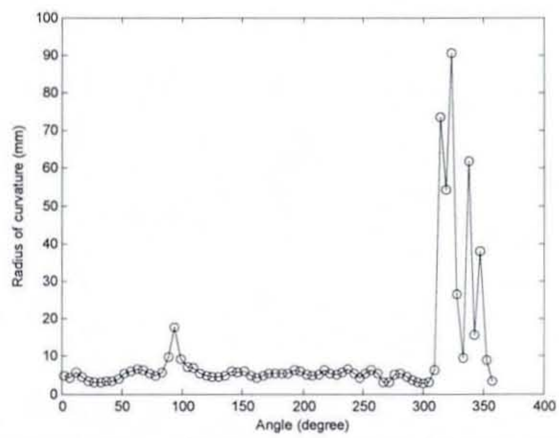
3	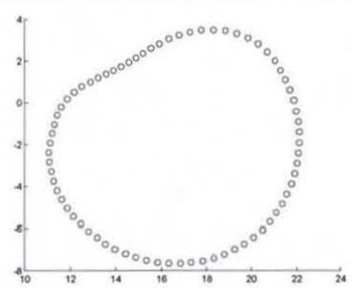	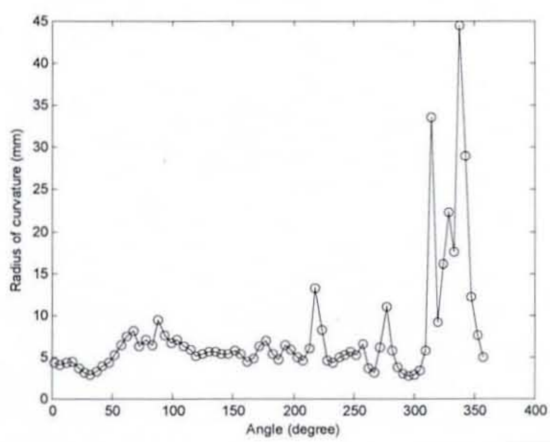

4	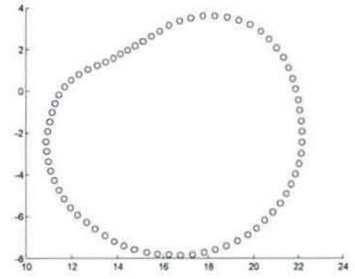	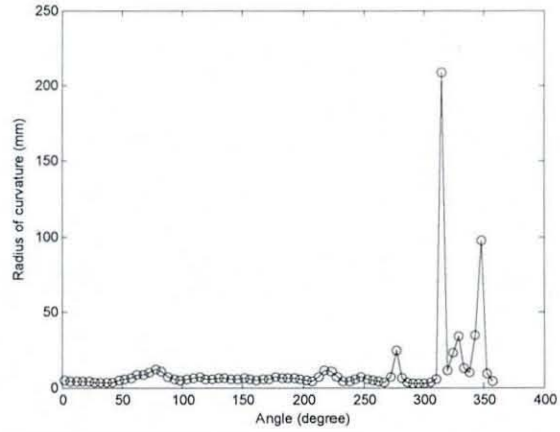Radius of curvature (mm) Angle (degree)
5	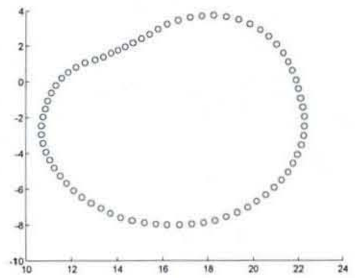	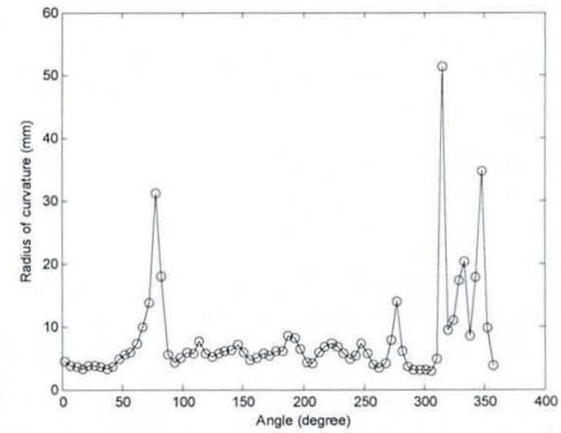Radius of curvature (mm) Angle (degree)
6	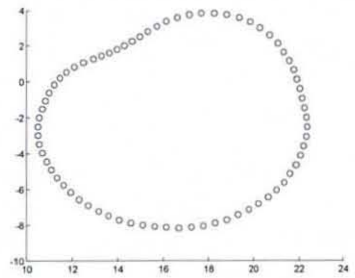	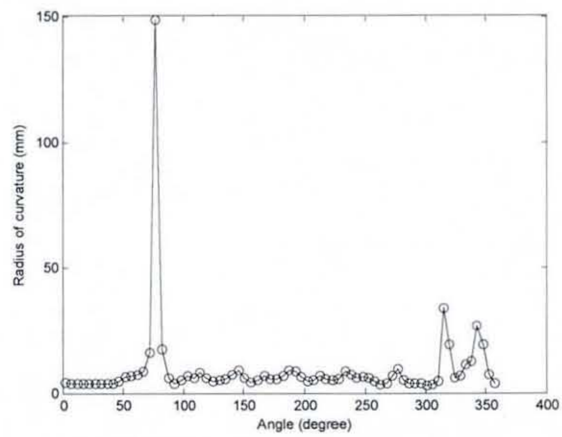Radius of curvature (mm) Angle (degree)

7	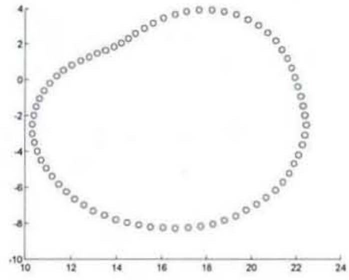	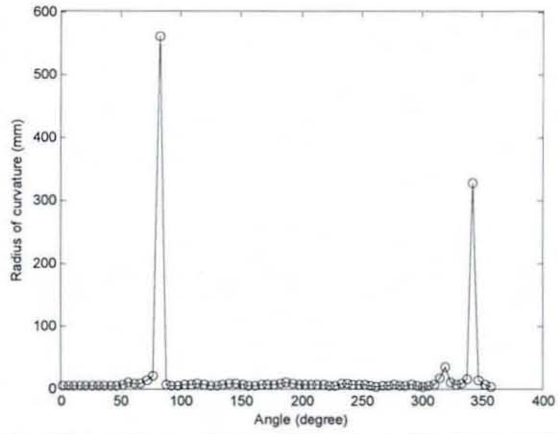Radius of curvature (mm) Angle (degree)
8	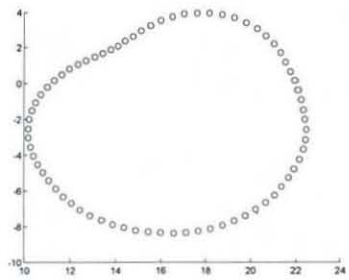	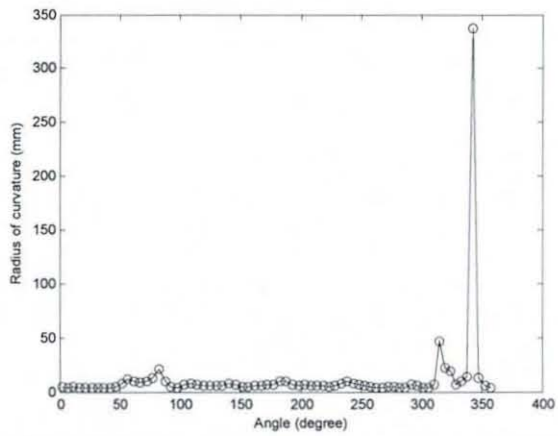Radius of curvature (mm) Angle (degree)
9	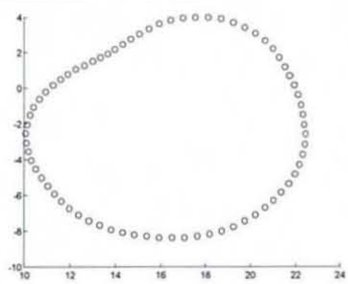	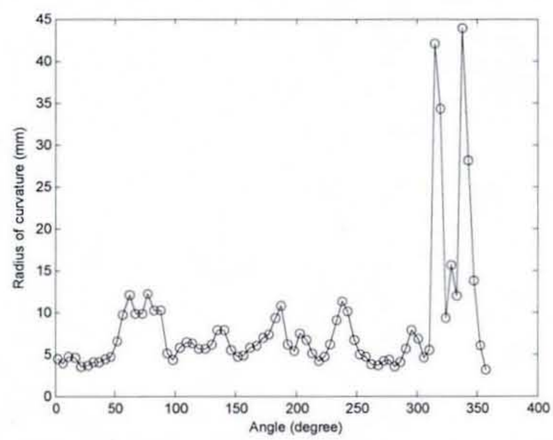Radius of curvature (mm) Angle (degree)

10

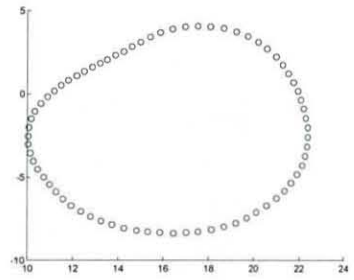

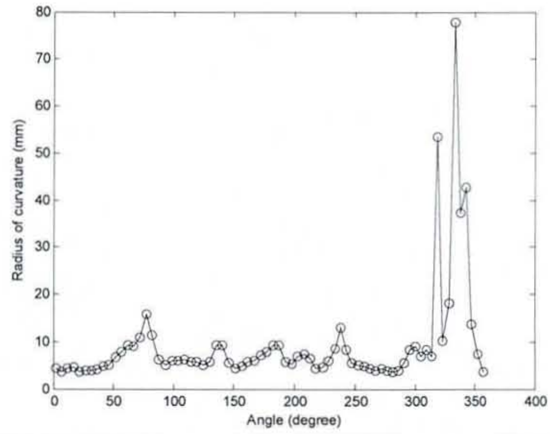

Figure 3.7 Reduction factor distribution at each layer (cm vs degree)

Since there only one reduction factor is computed for each layer, average radius of curvature is used. It can be obtained by dividing all the radius of curvature with the number of them in the layer. When averaging is used, these extreme values can affect the value of the average at their corresponding layers as shown in Table 3.1. These averages, if used, will influence reduction factor and 3D pressure garment model as shown in Table 3.1.

Average radius of curvature (metre)		Reduction factor (%)	
With extreme value	Without extreme value	With extreme value	Without extreme value
2.349	0.068	92.6	23.6
0.099	0.078	34.4	29.3
0.074	0.065	28.2	25.7
0.113	0.072	37.4	27.6
0.079	0.069	29.5	26.7
0.091	0.067	32.4	26.2
0.189	0.068	50.0	26.3
0.120	0.067	38.9	26.7
0.083	0.073	30.5	27.9
0.093	0.076	32.9	28.8

Table 3.1 Average radius of curvature and reduction factor for each layer with and without extreme value

To overcome the problem of reduction factor's extremity due to radius of curvatures factor, this research used the circumference of the body, measured by the body scanner to calculate the reduction factor. The circumferences of the body were calculated by adding up all the distances between two consecutive points in each layer. This can be easily done since the body scanner that this research used is a horizontal type, which means each layer will have the same z-coordinate. If P_1 (x_1, y_1) to P_n (x_n, y_n) indicate the points' number and coordinates in one layer, the circumference for the layer *j* is given by:

$$C_j = \sum_{i=1}^{n} \sqrt{(x_i - x_{i-1})^2 + (y_i - y_{i-1})^2} \tag{3.2}$$

However, this is only an approximation. The calculated circumference always underestimates the distances between two points. It is because equation 3.2 considered distances between the two points as straight line, but the fact is the line is a curvature. So the calculated circumference is smaller than the actual circumference. The higher the number of points used, the higher the accuracy of calculation.

3.3.3 Calculating the centroid location

The centroid is the point at the centre of any shape, sometimes called the centre of area or the centre of volume. The coordinates of the centroid (G) are the average of the coordinates of all the points of the shape, and its formula is shown below.

$$G_j = \left(\frac{\sum_{i=1}^{n} x_i}{n}, \frac{\sum_{i=1}^{n} y_i}{n} \right)$$

The centroid will become the 3D pressure garment's reference point.

3.3.4 3D pressure garment creation

By combining the wounded area data, the reduction factors and the centroids together, a 3D pressure garment can be developed.

By referring to Figure 3.8, if we assume that G_j is the centroid of a layer with coordinate of (x_G, y_G), A is one of a series of points that define the circumference of the layer. The reduction factor is Re. Then the location of A' (x_i', y_i') which determines the circumference of the pressure garment by using a reduction factor Re can be determined by using the following formula:

$$x_i' = x_G + GA'\cos\theta$$
$$y_i' = y_G + GA'\sin\theta$$
$$\theta = \arctan\left(\frac{y_i - y_G}{x_i - x_G}\right)$$
$$GA' = (1 - \mathrm{Re})GA$$
$$GA' = (1 - \mathrm{Re})\sqrt{(x_i - x_G)^2 + (y_i - y_G)^2}$$

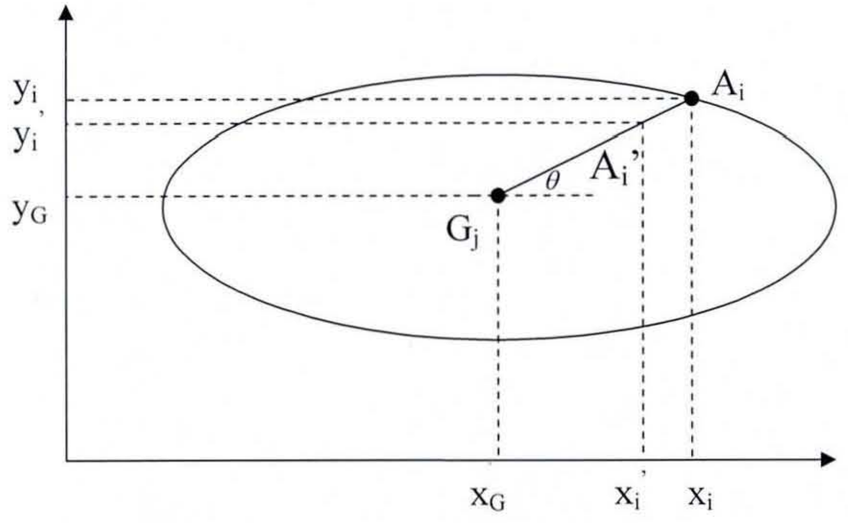

Figure 3.8 3D pressure garment points coordinates

By plotting x_i', y_i', points along circumference of the pressure garment at the layer can be obtained. By repeating this process at other layers of concern, a 3D image of the pressure garment can be achieved. This then can be used to develop a 2D pattern for the pressure garment.

3.4 Methodology to obtain a 2D pattern of the pressure garment

The method to generate a 2D pattern from the 3D model involves two steps: creating a triangulation for the points and flattening the triangulation.

3.4.1 Triangulation of the points

First, all the 3D coordinate data for the pressure garment must be rearranged to develop the triangulation. The triangulation is important because it will help to flatten the 3D pressure garment model to fit the body smoothly. This research manipulated the nature of the arrangement of existing data to develop it (refer Figure 3.9).

The arrangement of existing data begun with a data point (reference point) on the front of the body segment (marked in the figure), and moved in the clockwise direction to the rear, and has continued to the front again to complete a cycle. This process has been repeated for the next layers until all the layers have been processed. Each layer has the same number of data points. Thus, if number of points in each layer is k, then data point in first layer is P_1, P_2 … P_k, while for second layer is P_{k+1}, P_{k+2}, … P_{2k} (Figure 3.10). Third layer's points is P_{2k+1}, P_{2k+2}, … P_{3k} and so on. Since each layer on the body is a close loop, first data point and last data point in the layer is actually a neighbouring point.

As shown in Figure 3.11, triangle 1, or T_1, consists of points P_1, P_{k+1} and P_{k+k}, while triangle 2, or T_2, is made by points P_1, P_2 and P_{k+1}. Members of neighbouring triangles are shown in Table 3.2.

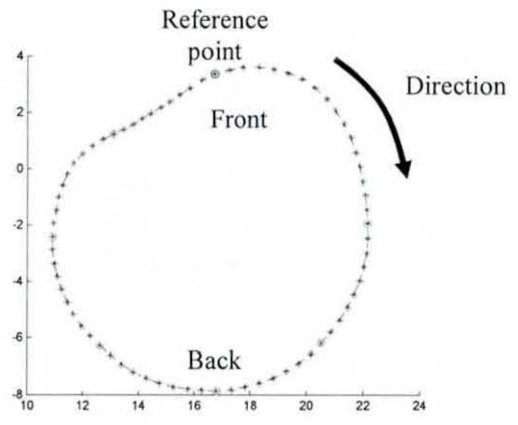

Figure 3.9 Arrangement of body points data

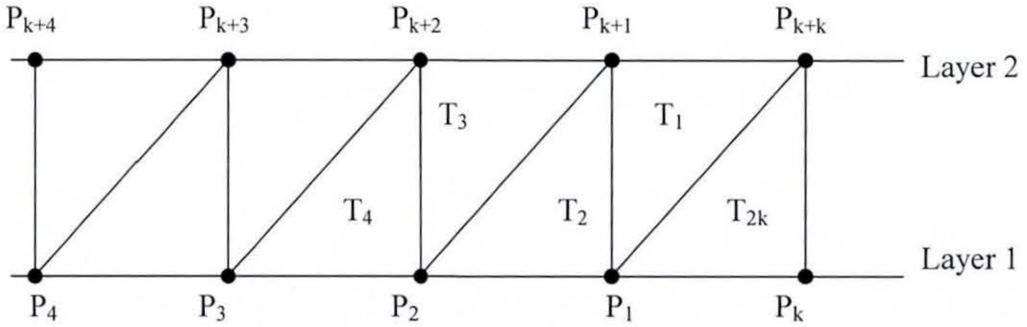

Figure 3.10 Arrangement of data in two layers

Table 3.2 Triangulation data arrangement

Triangle, T_i	First position	Second position	Third position
1	P_1	P_{k+1}	$P_{k+(k)}$
2	P_1	P_2	$P_{k+(1)}$
3	P_2	P_{k+2}	$P_{k+(1)}$
4	P_2	P_3	$P_{k+(2)}$
5	P_3	P_{k+3}	$P_{k+(2)}$
. . .	. . .	. . .	. . .
2k-2	P_{k-1}	P_k	$P_{k+(k-1)}$
2k-1	P_k	P_{k+k}	$P_{k+(k-1)}$
2k	P_k	P_1	$P_{k+(k)}$

A computer program was developed to arrange the points into these positions. By using this sequence, triangulation of the pressure garment was made (Figure 3.11).

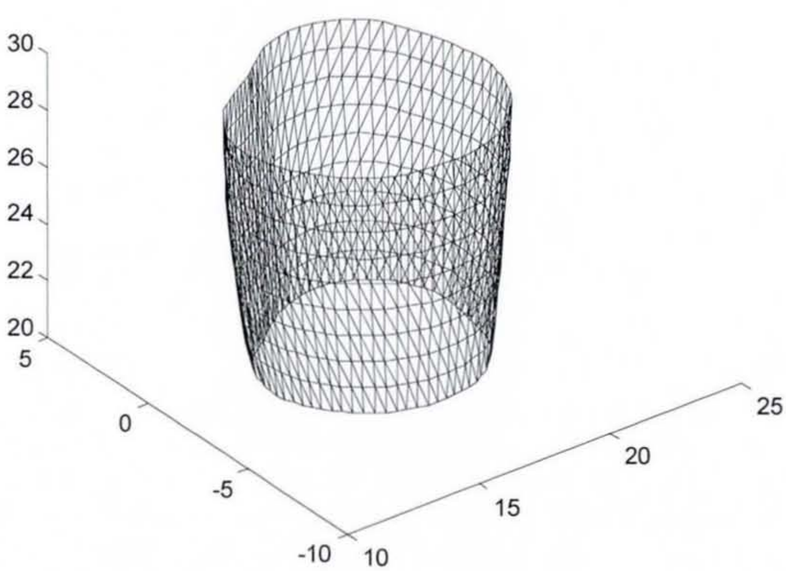

3.11 Triangulation of pressure garment

3.4.2 Flattening

After the triangulation of all the points has been completed, the next process is the flattening of the 3D image. The 3D pressure garment surface is flattened into a 2D pattern by using the method of intersection of two circles. The process is as follows:

Consider P_1, P_2 and P_3 are three points that make up a triangle in level 1 (Figure 3.12).

The next step is to calculate the distance between the points. The process starts with the reference point in the data. The first layer can be considered as the base layer, where no reference points yet exist. As Figure 3.13 shows, if P_1 is chosen as the base point, then P_2 can be determined by using the distance between P_1 and P_2. P_3 can be determined by using the intersection of two circles method. In this method, d_2 will be assumed as P_2's radius and d_3 is P_1's radius. However, it must be checked whether there is any intersection at all. If d_3 is longer than d_1+d_2 (d_3>d_1+d_2) or shorter than d_1-d_2 (d_3<|d_1-d_2|), then there is no intersection between these two circles. The former indicates that the two circles are separated and the latter shows that one circle is contained within the other. If both conditions were meet, the calculation for P_3 is as follows:

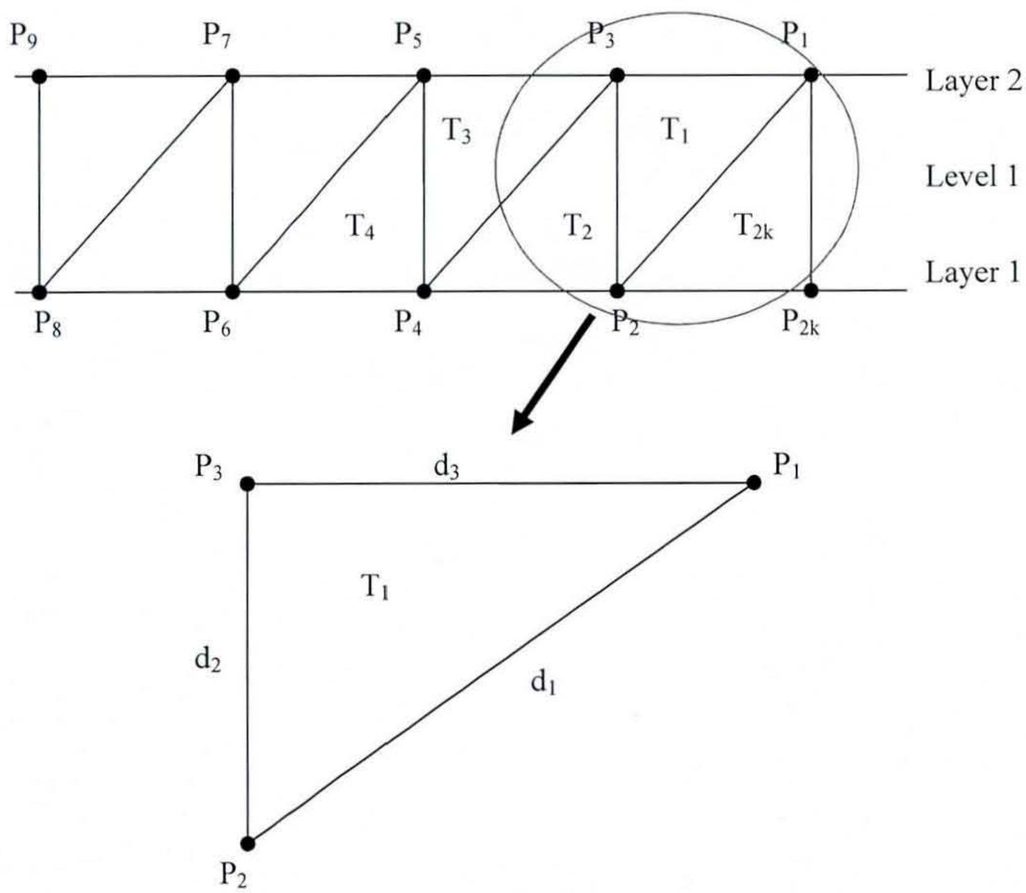

Figure 3.12 Triangulation of points

Referring to Figure 3.13; d_1, d_2 and d_3 can be described as:

$$d_1 = a + b;$$
$$d_2^{\,2} = a^2 + h^2;$$
$$d_3^{\,2} = b^2 + h^2;$$

By substituting the terms in the equations, a and h can be calculated;

$$a = \frac{\left(d_2^{\,2} - d_3^{\,2} + d_1^{\,2}\right)}{2d_1};$$
$$h = \sqrt{d_2^{\,2} - \frac{\left(d_2^{\,2} - d_3^{\,2} + d_1^{\,2}\right)^2}{4d_1^{\,2}}};$$

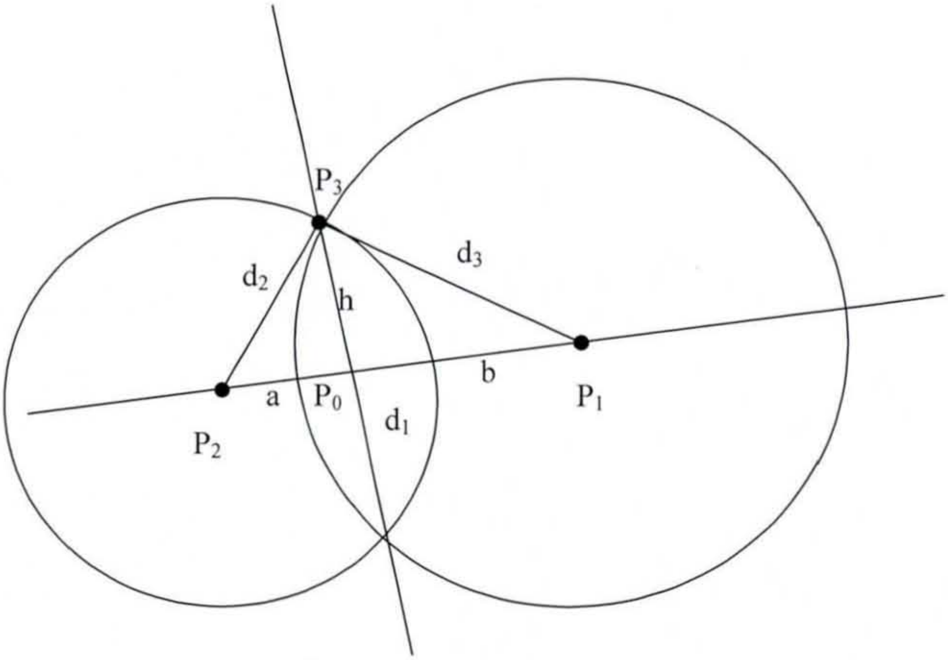

Figure 3.13 Intersection of two circles

P_0 is given by (Figure 3.13):

$$P_0 = P_2 + \frac{a}{d_1}(P_1 - P_2);$$

By referring to Figure 3.14, $\angle P_1P_2P_{1X}' = \angle P_{3X}'P_3P_0$. Thus x_3 and y_3 can be calculated by using ratio of a triangle.

$$\frac{x_0 - x_3}{h} = \frac{y_1 - y_2}{d_1};$$

$$x_3 = x_0 - h\left(\frac{y_1 - y_2}{d_1}\right);$$

and

$$\frac{y_3 - y_0}{h} = \frac{x_1 - x_2}{d_1};$$

$$y_3 = y_0 + h\left(\frac{x_1 - x_2}{d_1}\right)$$

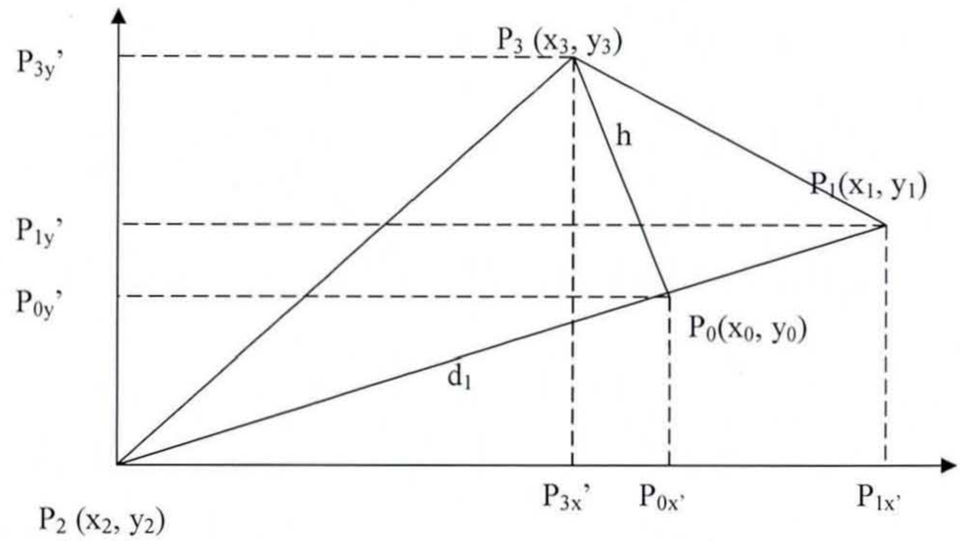

Figure 3.14 **Calculating the coordinates of the intersection of two circles**

After the location of P_3 is calculated, the next step is to use P_2 and P_3 to calculate P_4 (refer Figure 3.12). When location of P_4 is determined, then P_3 and P_4 are used to locate P_5. The same process is repeated to calculate the next point until all the points in the first level are flattened.

For flattening process in the next level (between layer 2 and layer 3), since some of the points in the first level will also form part of the next level, thus the flattened points must also be taken into consideration. For example, if triangles T_1-T_4 are located in the first level in Figure 3.15, which has already been flattened, in order to flatten triangles T_5- T_8 in the next level, points P_{21}, P_{22} and P_{23} must be considered. In this case, point P_{31} must be located first, by using the distance between it and P_{21}. Then, P_{31} and P_{21} can be used as reference points to search for P_{32}. After that, P_{32} will be used with P_{22} to locate P_{33}, and the process will be repeated until all points in the layer are flattened.

However, if the distance between P_{32} and P_{22} is longer than the sum of the distance of P_{32}, P_{33} and P_{22}, P_{33}, then a new point P_{22} must be searched for by using P_{32} and P_{21} as the base points.

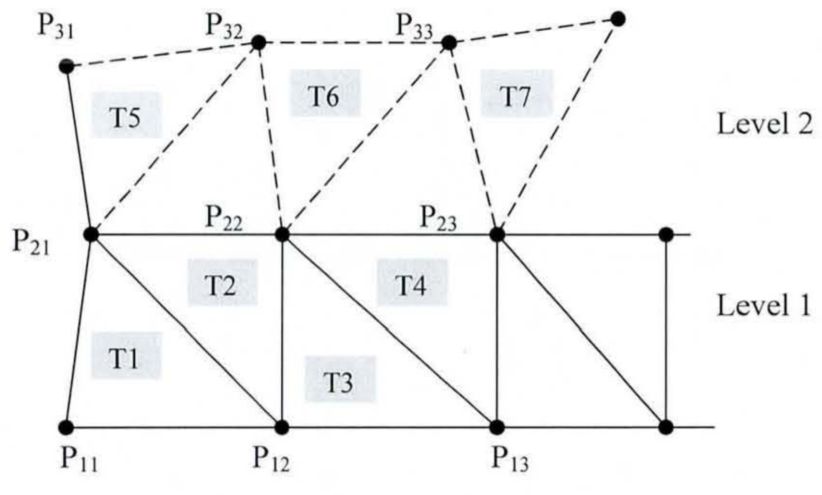

Figure 3.15 Flattening the triangle

For example, to flatten 3D pressure garment model shows in Figure 3.11, triangulation data in the first level is flattened first (Figure 3.16a). Then triangulation at the next level (Figure 3.16b) until all the triangulations were flattened (Figure 3.16c).

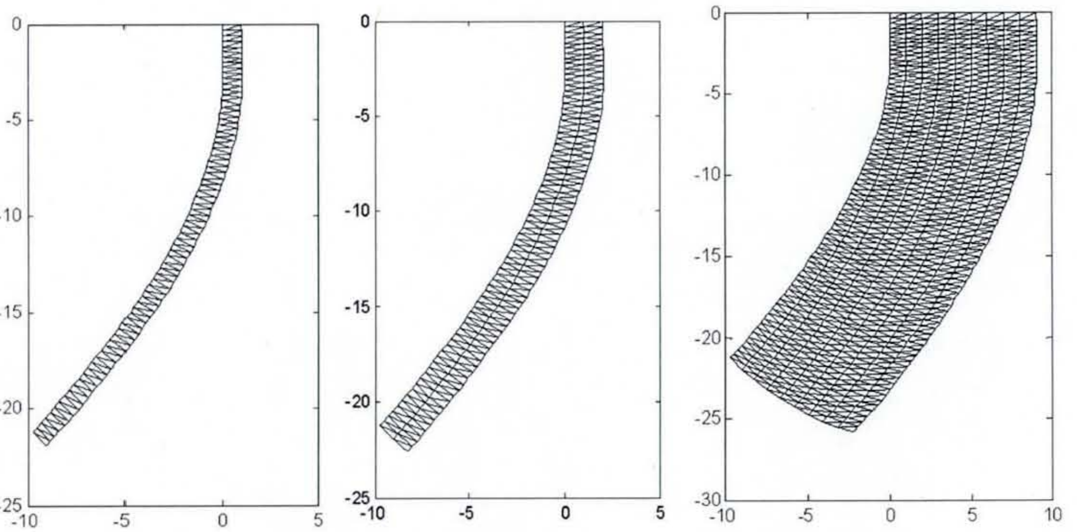

(a) (b) (c)

Figure 3.16 Flattening process for model in Figure 3.12

3.5 Experimental verification

The experimental method to verify the pressure garment pattern developed by the computer program is shown in Figure 3.17. A cylinder with a circumference of 31.5 cm has been used to represent a body part. Then a 3D pressure garment model has been developed following the process explained in the previous sections. Then this 3D model has been converted into 2D pattern. The pressure garment's fabric has been tested to determine their moduli of elasticity which was used in developing the pressure garment model. Based on the 2D pattern, a real pressure garment has been constructed and tested on the cylinder with a pressure sensor. The pressure distribution has been measured and compared with the intended pressure.

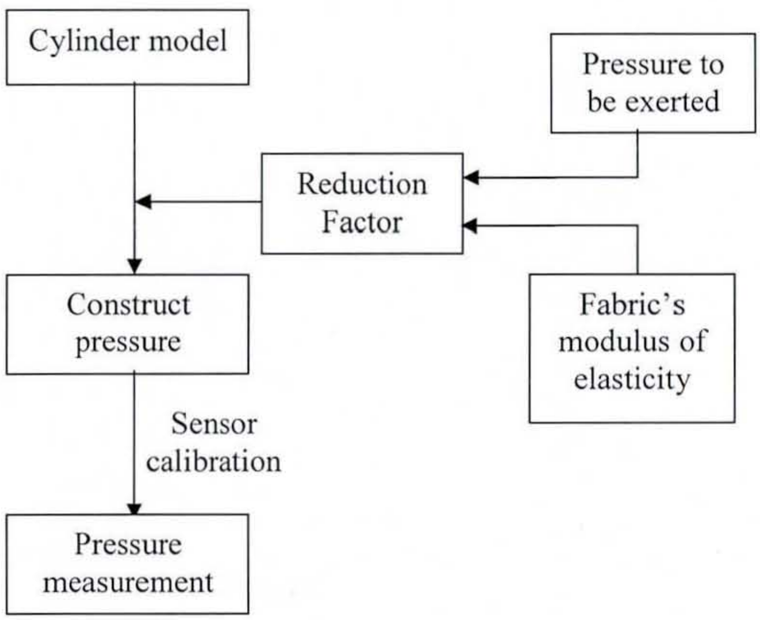

3.17 Flowchart of experiment to verify the developed pressure garment pattern

3.5.1 Cylinder model

First, a cylinder was used to replace the human body. A cylinder was chose because it has the same radius of curvature at each point on its surface which simplified the validation process. Thus, the pressure from the pressure garment is evenly distributed along its surface. The cylinder has a circumference of 31.5 cm (Figure 3.18). Its 3D model has been created, and its data is inputted into the computer program to generate its pressure garment pattern.

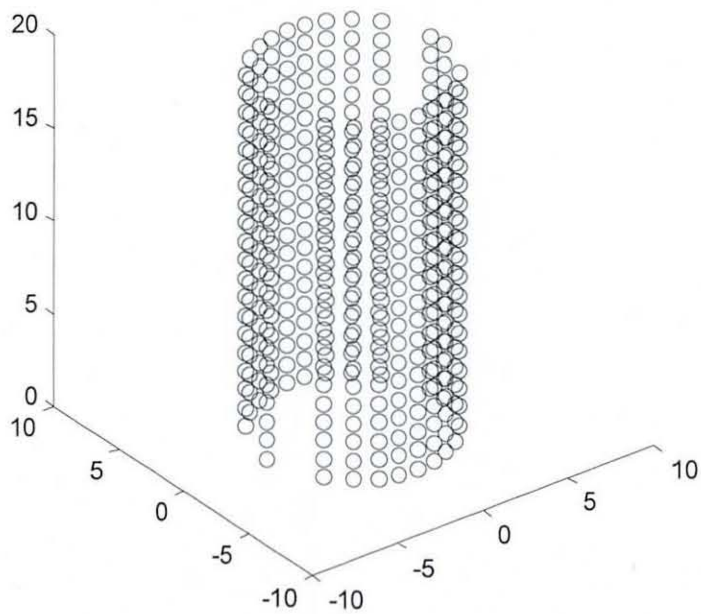

Figure 3.18 **Cylinder model with circumference and height of 31.5 and 20 cm respectively**

3.5.2 Modulus of elasticity of the fabrics

This experiment has been conducted to establish the modulus of elasticity of the pressure garment fabrics. Modulus of elasticity is measured in the direction of the circumference of the pressure garment. The experiment has been conducted according to BS-EN 14704-1: (2005) standards. Five test samples has been cut from the fabric, from region at least 150 mm from the edge of the fabric, with dimensions of 50 (± 1) mm wide and 250 (± 1) mm long. Since the fabric is warp-knitted, the specimens were cut with their length parallel to the wales of the fabric (Figure 3.19).

In order to ensure that the specimens are accurately removed, the fabric is measured using a ruler and marked with a coloured pen. Initially, each of the specimens was roughly cut from the fabric using scissors. Then, the specimens were further cut close to the dimensions by using a paper cutter. To ensure that the accuracy of the specimens was in the region of 50 (± 1) mm, each of them was manually checked and any excess yarn was taken out from the specimen using scissors.

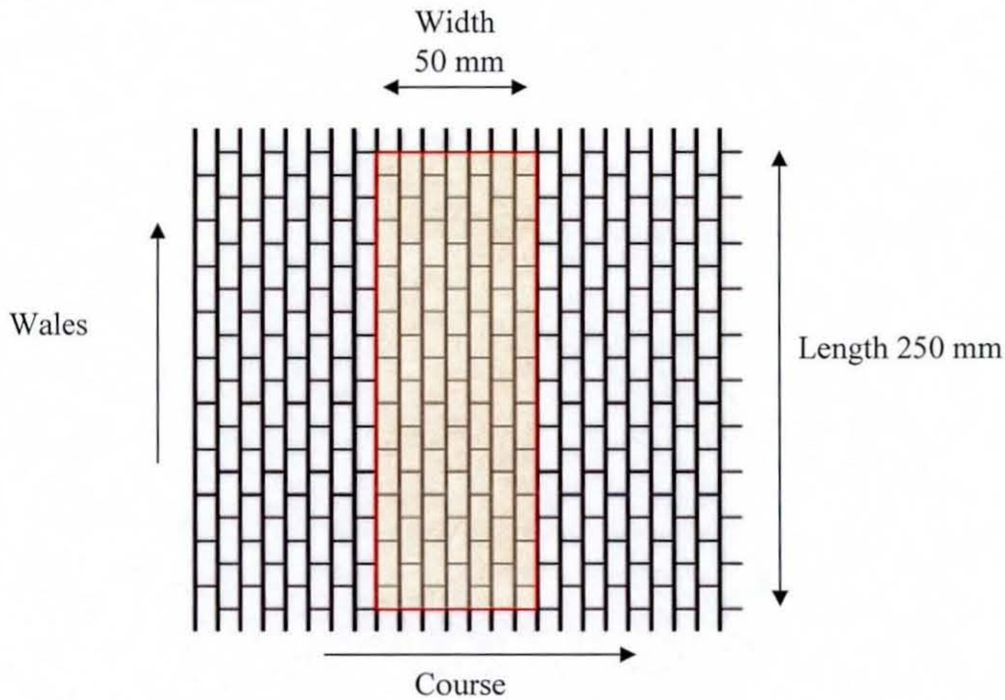

Figure 3.19 Position and dimension of sample in the fabric

When the specimens are ready (Figure 3.20), the next step is to measure their modulus of elasticity. A tensile testing machine (Hounsfield Test Equipment H5KS) was used in the experiment (Figure 3.21). The machine had been verified for tension and compression to BS EN ISO 7500-1: (1999) standard using verification equipment calibrated to ISO 376: (1999) and known masses that meet the requirement of BS EN 7500-1: (1999).

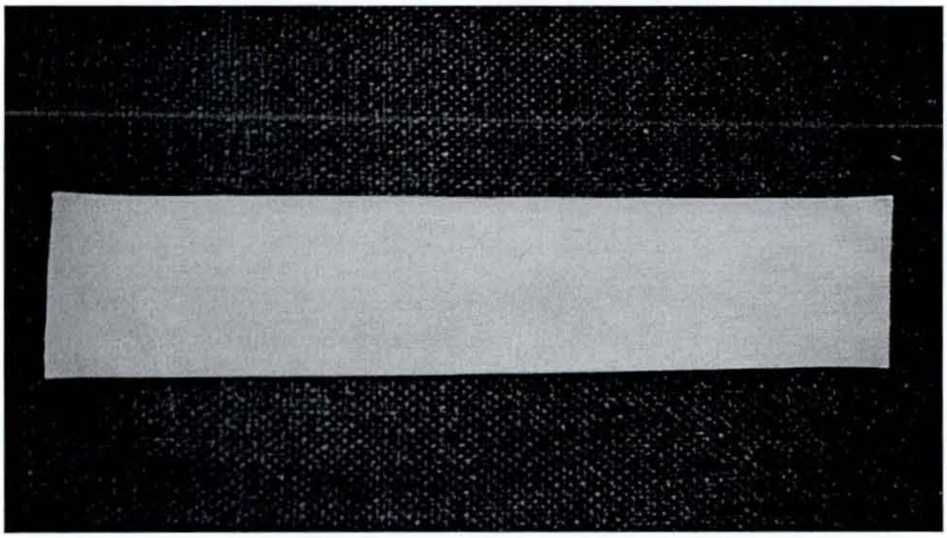

Figure 3.20 **Specimen for the fabric's modulus of elasticity investigation**

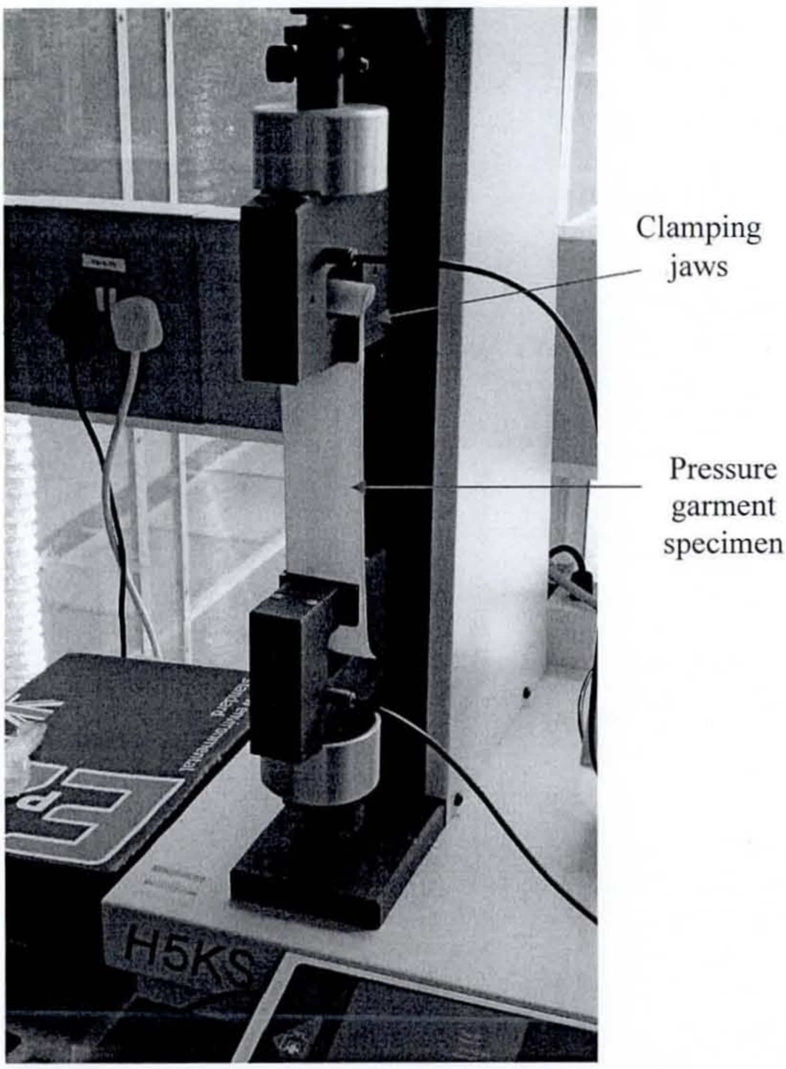

Figure 3.21 **Specimen on the tensile testing machine**

The clamping jaws of the machine were set 100 mm from each other using paper and carbon paper. The mark left on the paper was measured using a ruler.

The fabric was extended from 0 mm to 100 mm with a constant rate of 500 mm/min. Five cycles of extension and relaxation were run to obtain a stable load extension curve. The extensions were run within the elastic deformation load and below the plastic deformation load.

Each elongation and the force that was needed to stretch it have been plotted, and the slope of the graph was calculated using Microsoft Excel.

3.5.3 Pressure garment construction

The reduction factor formula, $\mathrm{Re} = \dfrac{1}{1+\dfrac{E}{PR}}$, was used to calculate the reduction factor. If the circumference of the cylinder is C_0, then the circumference of the pattern, C_1, is $C_1=(1-\mathrm{Re})*C_0$. This has been calculated by applying the reduction factor to each distance between the measurement points on the circumference of the body segment. A 2D pattern has been developed and cut out from the fabric, sewn together to form the pressure garment and then applied to the cylinder.

Pressure measurement experiments have been carried out to validate the process used in the development of the pressure garment pattern. Two separate pressure garments to exert pressure of 2666 Pa (20 mmHg) and 5000 Pa respectively on the cylinder has been developed. Although 5000 Pa is high for burn wound treatment, it has been used here to verify the method of designing and making pressure garments using the developed method. Such pressure are used in venous leg ulcers treatment.

The exerted pressure has been measured using the Tekscan Flexiforce A201-1 sensor. A sensor was inserted at four different locations on the cylinder and the average pressure was calculated.

The experiment procedure requires the following steps

a. Experiment to determine the modulus of elasticity.
b. Sensor calibration.
c. Pressure measurement.

3.5.4 Pressure sensor calibration

The Tekscan's Flexiforce A201-1 sensor has been selected because it is a single load cell, thin and flexible. All these characteristics are important to ensure that the sensor would not affect the accuracy of the pressure measurements. The sensor has a piezoresistive sensing device in which resistance is inversely proportional to an applied force. Ferguson-Pell *et al.* (2000) have evaluated the sensor and reported that it is suitable for direct measurement for surfaces with a radius of curvature more than 3.2 cm under static condition. A circuit for the sensor was constructed as recommended by the manufacturer and is shown in Figure 3.22.

An oscilloscope was used to gather the data from the sensor at a rate of 1250 data points per second.

First, in order to use the sensor, a calibration is needed. The calibration has been conducted by establishing the relationship between the pressure and the sensor output. A range of weights, from 10 g to 50 g, have been applied to the sensor. This range of weights has been chosen because the pressures exerted by the pressure garment are relatively low, between 20 – 30 mmHg (2666 - 3999 N/m^2), within the range of weight applied. A maximum pressure of 50 mmHg (6665 N/m^2) is assumed for the sensor. Since the sensing area diameter is 9.53 mm (as described by the manufacturer in its specification), then the active area of the sensor is, $A= 7.13*10^{-5}$ (m^2).

Thus, for a 50 mmHg, the mass of the weight that needs to be used is 48.37 (g) or close to 50 (g).

First 10g weight has been placed on the sensor, and its reading (in volts) has been taken 1 minute after the loading (Ferguson-Bell *et al*, 2000). Similarly, the same procedure has been used for weights of 20, 30, 40 and 50g (Figure 3.23).

All the weight and voltage readings have been plotted, and a linear equation was determined using MS Excel graph.

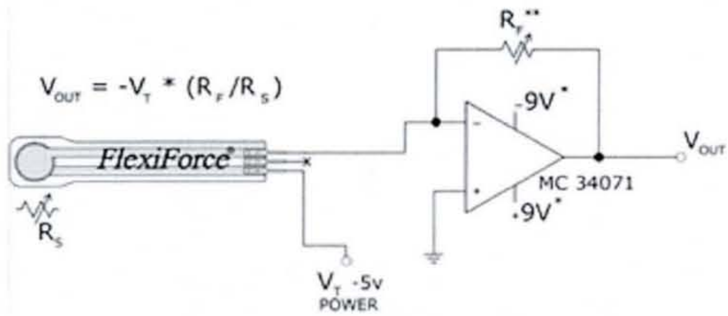

Physical Properties	
Thickness	0.008" (.203mm)
Length	8" (203mm) 6" (152mm) 4" (102mm) 2" (51mm)
Width	0.55" (14mm)
Sensing Area	0.375" diameter (9.53mm)
Connector	3-pin male square pin

Typical Performance		
Linearity Error	<+/-3%	<+/-1.2%
Repeatability	<+/-2.5% of full scale (conditioned sensor, 80% force applied)	<+/-3.5% of full scale
Hysteresis	<4.5% of full scale (conditioned sensor, 80% force applied)	<3.6% of full scale
Drift	<5% per logarithmic time scale (constant load of 90% sensor rating)	<3.3% per logarithmic time scale
Response Time	<5 microseconds	TBD
Operating Temperatures	15°F to 140°F (-9°C to 60°C)	15°F to 400°F (-9°C to 204°C)
Force Ranges	0-1 lb. (4.4 N) 0-25 lbs. (110 N) 0-100 lbs. (440 N)*	Low: 0-30 lbs. (133 N) High: 0-100 lbs. (445 N)*
Temperature Sensitivity	Output variance up to 0.2% per degree F (approximately 0.36% per degree C)	Output variance up to 0.16% per degree F

Figure 3.22 Circuit for pressure measurement sensor with specification and features

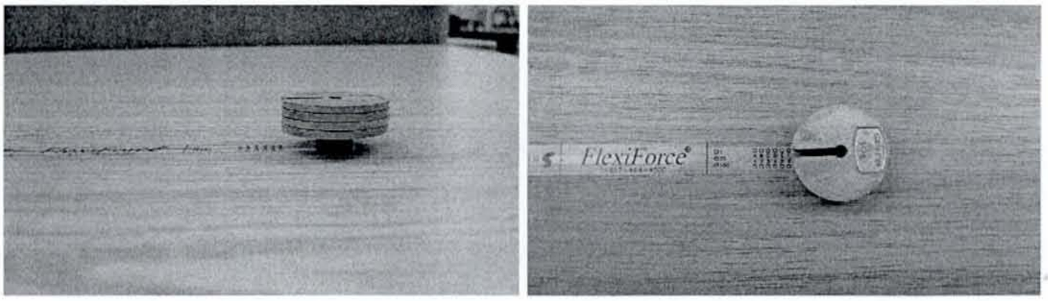

(a) (b)

Figure 3.23 Sensor calibration (a) side view (b) top view

3.5.5 Modulus of elasticity

a) Introduction

This experiment was conducted to investigate the fabric's modulus of elasticity. A sample of five fabrics was used and tested on the tensile test machine.

b) Results

Results of the experiment are shown in Figure 3.24.

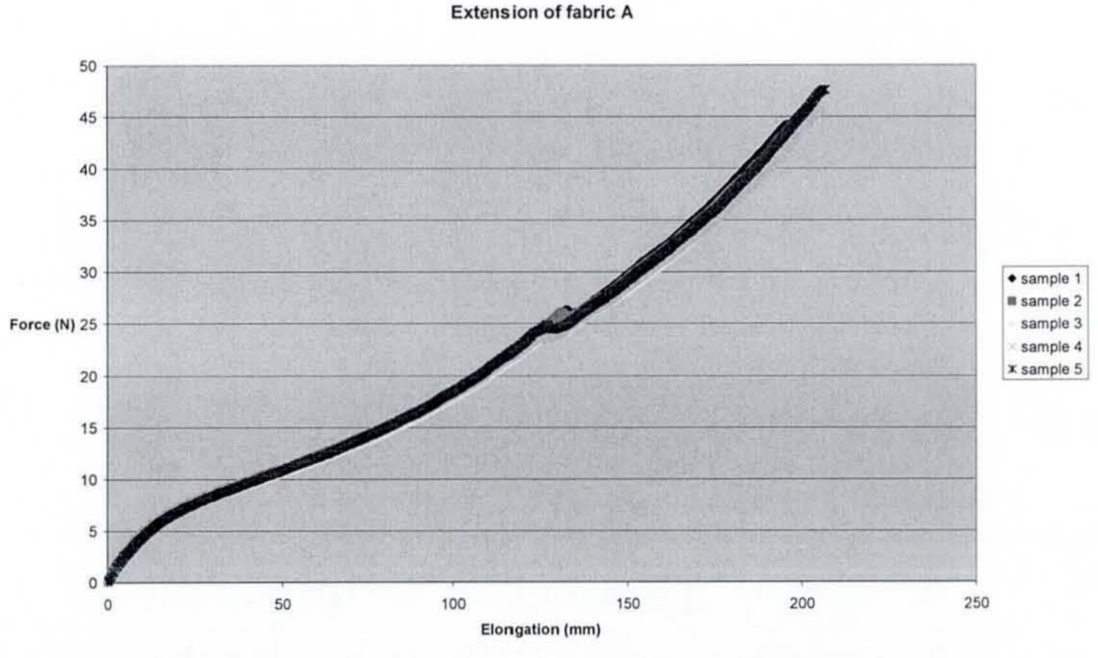

Figure 3.24 Stress-strain relationship for the fabric

c) Discussion

The stress strain curves are similar to the fabric tensile curve up to around 125 mm (or at 125%) extension where there is a disturbance to the curve. This was caused when the fabric became loose from the jaws of the tensile testing machine. However, since no pressure garment ever uses an extension of more than 100%, for this research, only data within an extension of 100% will be considered for estimation of the modulus of elasticity.

The graph from 0% to 100% of strain shows that the curve can be divided into three main linear parts. The initial linear segment has the steepest slope, and is usually referred to as the Young's Modulus. Stiffness at this part is the highest but its strain range is very small. In the figure, it is located within 0% to 10% of extension. The second linear part of the curve is almost flat. It is represented by an area within 10% to 100% of extension. The stiffness at the area is reduced significantly. The third linear part of the curve is represented by the area of extension of more than 100%.

To measure the rigidity of the fabric, this research will use only the first linear part of the curve. The reason for the selection is because, according to Zheng *et al*. (2000), it is where the modulus of elasticity, or Young's Modulus, can be calculated. The extension of the pressure garments are also likely to be in this range.

The area of the first 10% of the fabric A is shown in Figure 3.25. The tangents for each specimen are shown in Table 3.3. They are measured using '*polyfit*', a MATLAB function that computes a least squares polynomial for a given set of data.

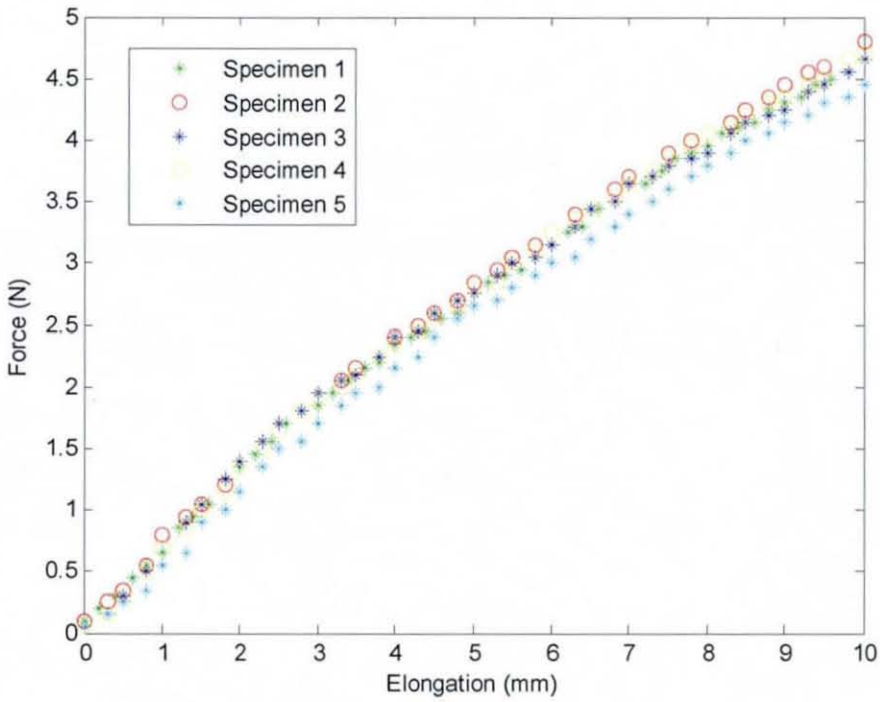

Figure 3.25 Stress strain curvature for first segment of the fabric

Table 3.3 Modulus of elasticity for fabric's specimen

Specimen	Modulus of elasticity (N/mm)
1	0.5054
2	0.5185
3	0.5058
4	0.5114
5	0.479

Based on the result, the fabric has an average Young's Modulus of 0.504 N/mm (in the context of these work, E is quoted as N/mm for a 50 mm wide sample)

3.5.6 Sensor calibration

a) Introduction

The experiment was conducted in order to calibrate the sensor so it can be used to measure pressure. The sensor was calibrated using the method explained in section 3.5.4.

b) Result

Figure 3.26 shows the result for the sensor calibration. There are 2500 data points for each measurement. Because of the huge amount of data, an average reading for each weight was used. These are shown in Table 3.4. In order to convert the mass, *m*, (kg) into pressure, *P*, (Pa), following formula was used.

$$P = \frac{F}{A} = \frac{mg}{A}$$

where g is the gravity force and A is the sensing area of the sensor. The diameter of the sensing area is 9.53 mm as describe by the manufacturer in its specification (refer Figure 3.22), then the active area of the sensor is $7.13*10^{-5}$ (m^2).

Thus, the conversion formula from mass into pressure is given by following equation.

$$P = \frac{9.81 * m}{7.13 * 10^{-5}}$$
$$P = (1.38 * 10^{5})m$$

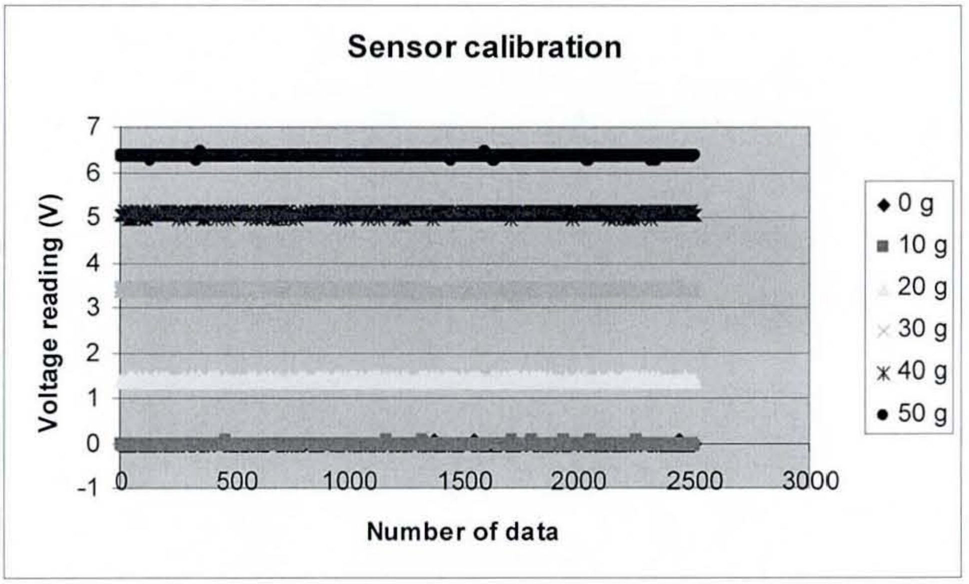

Figure 3.26 Sensor calibrations

Table 3.4 Average pressure

Weight (g)	0	10	20	30	40	50
Pressure (Pa)	0	1373.707	2747.414	4121.121	5494.828	6868.535
Voltage reading (V)	-0.0104	-0.00698	1.364064	3.381088	5.052416	6.363904

c) Discussion

Figure 3.27 shows the results in a graph. A tangent line for its result is also included in the Figure along with its linear equation.

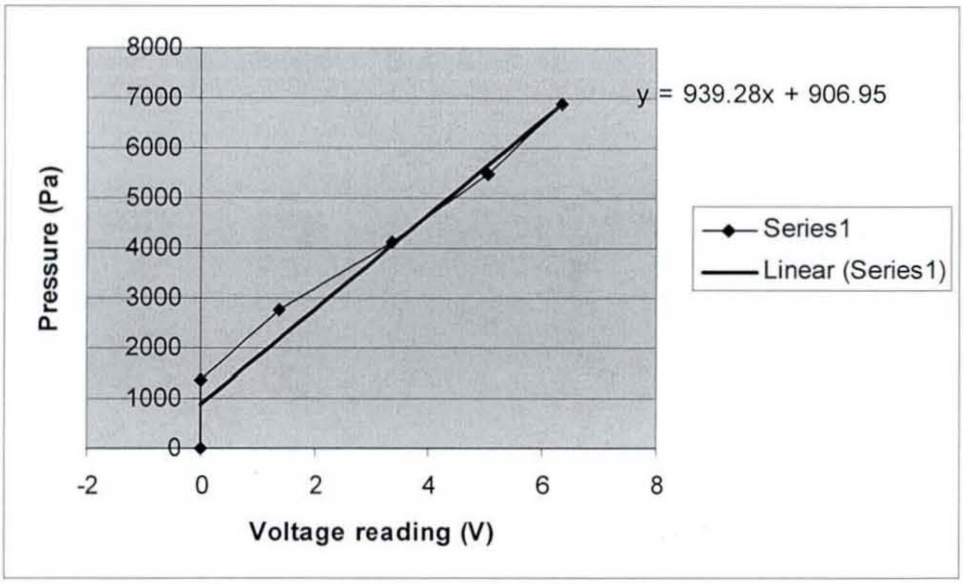

Figure 3.27 Graph for result of sensor's validation

However, based on the results, it is clear that the sensor can barely measure a weight less than 10 g. As shown in Table 3.4 and Figure 3.27, the results for weights of 0 gram and 10 gram are almost the same. The results agree with the findings by Ferguson-Pell *et al.* (2000), which stated that the Flexiforce sensor should not be used to measure weight of less than 10 g. Thus, in this research, a linear equation for the slope of weights of greater than 10 g has been used. The new graph and its linear equation are shown in Figure 3.28.

Based on the equations, the results of pressure measurements on subjects will be converted from volt into N/m^2 or Pascal (Pa).

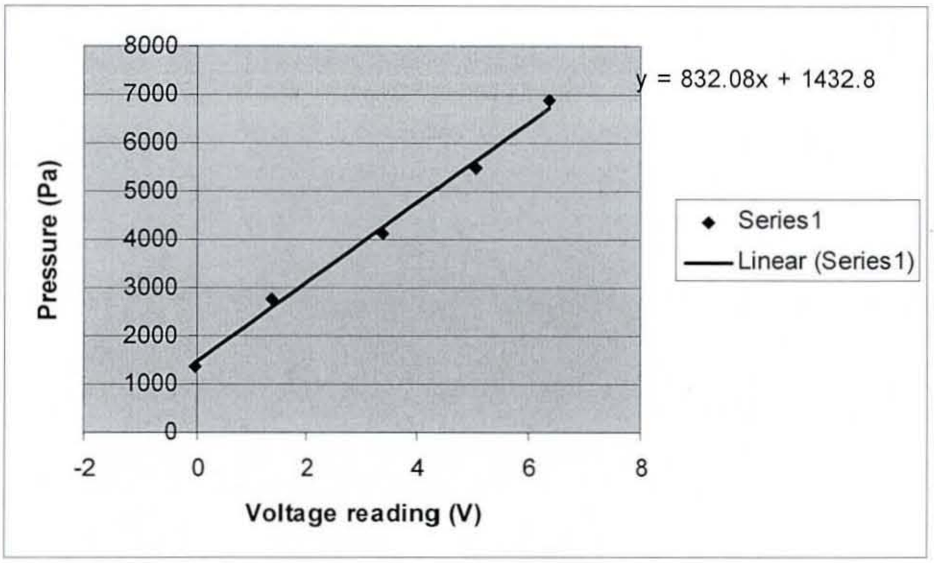

Figure 3.28 Linear equation

3.5.7 Result for experiment

a) Introduction

Experiments have been conducted to validate the model for the pattern development and the procedure for the pressure garment development. Two pressure garment patterns for a cylinder with a circumference of 31.5 cm has been developed to exert pressure of 2666 Pa and applied to the cylinder. The pressures have been measured at four locations, with a 90-degree interval.

b) Result

The results for both patterns are present in Table 3.5. Both measurements are in close agreement with their corresponding design pressure.

Table 3.5 Pressure on cylinder

Pressure to exert (Pa)	Location 1	Location 2	Location 3	Location 4	Average pressure
2666	2530.5	2671.5	2579.3	2606.7	2597.0
5000	4927.5	4941.2	5332.7	5024.9	5056.6

3.6 Discussion

This chapter has discussed how the 3D pressure garment model has been developed, and the method of transforming it into a 2D pattern.

The transformation process begins with data acquisition using a body scanner. A computer program, using Matlab, has been developed to transform the data into a 3D body model. The program uses a mathematical model to calculate the reduction factor. The model is based on Laplace's Law and Hooke's Law. Some discussions are included about parameters in the mathematical model, and the method to obtain them is explained.

The computer program to transform the 3D pressure garment model into a 2D pressure garment pattern involves two steps: creating triangulation for the 3D points and flattening the triangulated data using the intersection of two circles method.

An experiment has been conducted to validate the method. In the experiment, a cylinder with circumference of 31.5cm and height of 20cm was used. The results show that the program can develop a pressure garment pattern that can apply specific pressure on a cylinder with a similar radius of curvature.

However, since the human body is not a perfect cylinder, a program to predict pressure distribution on the human body needs to be developed. The next chapter describes the method to develop a computer program that can predict pressures based on 3D human body data and the radius of curvature.

Chapter 4 The 3D pressure distribution model

A pressure garment is designed to exert a certain amount of pressure on a wounded part of the body. Only the correct level of pressure on the wound assists the healing process, therefore it is important to apply the right pressure on the affected part. This can be achieved by designing and making a pressure garment to fit the body part correctly to apply the required pressure. In addition to the pressure garment modelling using 3D scanned body data and developing a 2D pressure garment pattern using the mechanical properties of the fabric, as well as the 3D model, it is also essential to make sure that designed and made pressure garment applied the right pressure. This can be verified by in situ pressure measurement. However, this is not practical and not possible with every patient. An alternative to this is the simulation of the pressure applied by the garment on the part of the body that it is designed for. This requires a pressure distribution model that can predict the pressure that the garment applies to the body part. This chapter deals with the development of the pressure tat the pressure garment exerts on the wounded part of the body.

Chapter 3 has reported a method that was developed to create a 3D wounded area model and a 3D pressure garment model. Data from these 3D wounded areas and the 3D pressure garment model have been used to develop the pressure distribution model. First, circumferences of the layers from both models were calculated. By using Hooke's Law, tension of each layer of the fabric can be obtained. Then, by using the radius of curvature at each point on the body model, pressure that the pressure garment exerts on the wounded area can be calculated using Laplace's Law.

4.1 Methodology to develop pressure distribution model

4.1.1 Pressure calculation and 2D pressure prediction model

Based on the theory of mechanics, clothing pressure at a particular position depends on the curvature of the body and fabric tension in the principal directions (Fan & Chan, 2005).

$$P = \kappa_x T_x + \kappa_y T_y$$

where κ_x and κ_y are the curvatures in the horizontal and vertical directions, and are given by following formula;

$$\kappa_x = \frac{1}{\rho_x}$$
$$\kappa_y = \frac{1}{\rho_y}$$

ρ_x and ρ_y are x and y components of radius of curvature. However, since ρ_y is close to infinity (due to the near-flat-surface in the vertical direction), then κ_y eventually become very small. Since T_y is almost zero (because usually the elongation in vertical direction is very small), the formula can be rewritten as:

$$P = \kappa_x T_x$$

To simplify the formula, κ_x is substitute with κ only, and its radius of curvature is ρ. The tension of the fabric in a horizontal direction, T_x, is given by the following formula:

$$T_x = \frac{E(C_0 - C_1)}{C_1}$$

where C_0 is the circumference of the body segment, C_1 is the circumference of the pressure garment and E is the rigidity or tensile modulus of the fabric.

By combining all the formulae, the pressure at a location n is,

$$P_n = \frac{E(C_0 - C_1)}{C_1 \rho_n} \tag{4.1}$$

For the circumferences of a body, since the body scanner is a horizontal type, each layer will have the same z-coordinate. As shown in Figure 4.1, by adding up all the distances between two adjacent measured-point on the periphery of the section in each layer, the circumference of the layer can be obtained. The process is explained in Section 3.3.2.

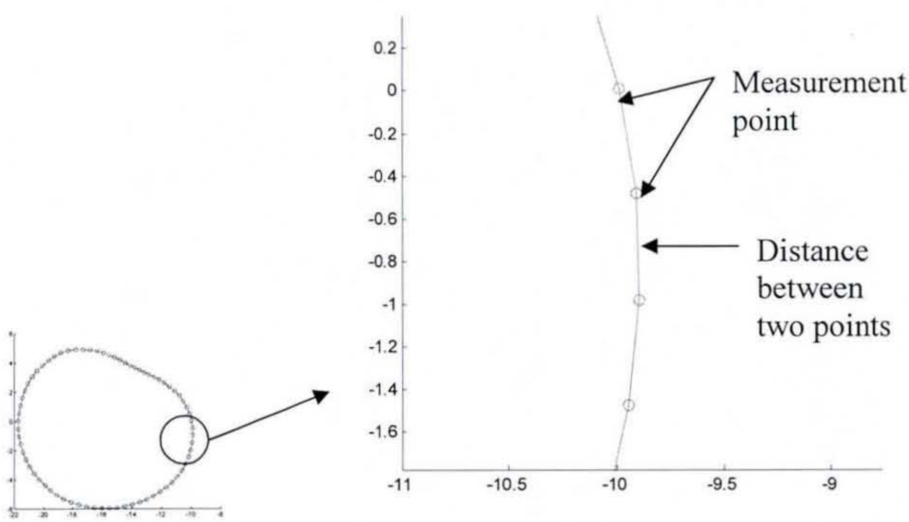

Figure 4.1 Measurement of circumference at one layer

As for circumferences for the pressure garment, it can also be calculated using a similar method by adding up all the distances between two adjacent points in the model.

As for ρ_n its formula is the following:

$$\rho_n = \frac{1}{\kappa_n},$$

where κ_n is the curvature at point n.

This research used the three points method to calculate the radius of curvature, in which the radius was estimated by using three points. Even though it is only estimation, the result can be a good indication of the real dimension. Since the same method is applied to both the scanned body segment dimension and the pressure garment model, the reduction factor between the two will not be affected by this process. The estimated results approximates to the actual values much closer when the distance between the points gets smaller (Figure 4.2).

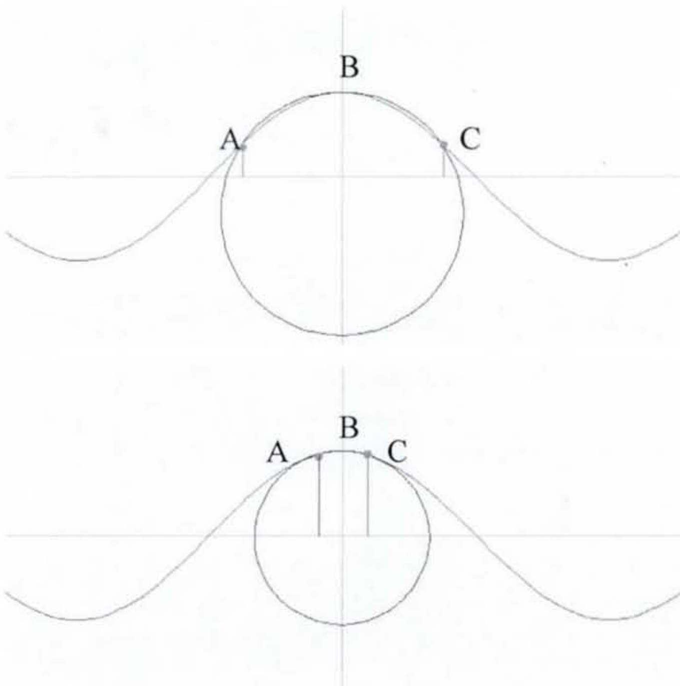

Figure 4.2 Radius of curvature when distance between points close to zero

The method used to calculate the radius of curvature is described below.

Suppose there are three points on the circle, $A(x_1,y_1)$, $B(x_2, y_2)$, $C(x_3, y_3)$ (refer to Figure 4.3). The slope between AB, m_{AB}, and BC, m_{CB}, can be calculated by using the following formula.

$$m_{AB} = \frac{y_2 - y_1}{x_2 - x_1},$$

$$m_{CB} = \frac{y_2 - y_3}{x_2 - x_3},$$

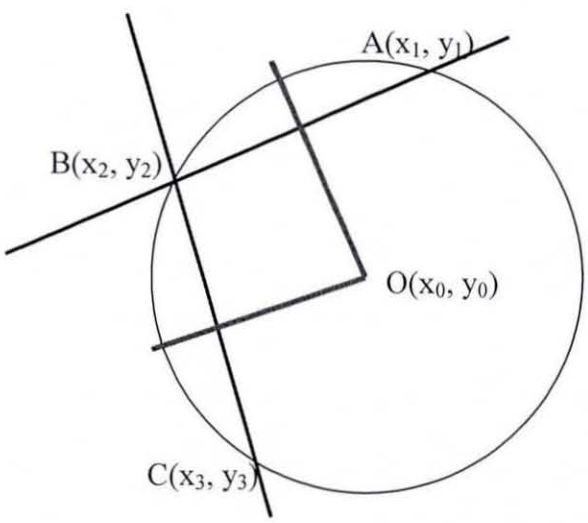

Figure 4.3 Three-point-method

The centre of the circle will lie on the perpendicular bisector of AB and BC. In other words they will lie on lines that pass through the midpoints of chords AB $\left(\frac{x_1 + x_2}{2}, \frac{y_1 + y_2}{2}\right)$ and BC $\left(\frac{x_3 + x_2}{2}, \frac{y_3 + y_2}{2}\right)$ and are perpendicular to each chord.

Lines that are perpendicular have negative reciprocal slopes $-\frac{1}{m_{AB}}$ & $-\frac{1}{m_{BC}}$. Thus, the equation for the perpendicular bisectors passing through the midpoints AB is,

$$\frac{y_1 + y_2}{2} = -\frac{1}{m_{AB}}\left(\frac{x_1 + x_2}{2}\right) + c,$$
$$\therefore c = \frac{y_1 + y_2}{2} + \frac{1}{m_{AB}}\left(\frac{x_1 + x_2}{2}\right),$$
$$y_{AB} = -\frac{1}{m_{AB}} x_{AB} + \left(\frac{y_1 + y_2}{2} + \frac{1}{m_{AB}}\left(\frac{x_1 + x_2}{2}\right)\right)$$

The y_{AB} linear equation was represented by thick green line on Figure 4.3. Equation for the perpendicular bisectors passing through midpoints AB is,

$$\frac{y_3 + y_2}{2} = -\frac{1}{m_{BC}}\left(\frac{x_3 + x_2}{2}\right) + c,$$
$$\therefore c = \frac{y_3 + y_2}{2} + \frac{1}{m_{BC}}\left(\frac{x_3 + x_2}{2}\right),$$
$$y_{BC} = -\frac{1}{m_{BC}} x_{BC} + \left(\frac{y_3 + y_2}{2} + \frac{1}{m_{BC}}\left(\frac{x_3 + x_2}{2}\right)\right)$$

The linear equation was represents by thick red line in Figure 4.3. These two lines will intersect at the centre of the circle where $y_{AB} = y_{BC} = y_0$ & $x_{AB} = x_{BC} = x_0$. By using both equations,

$$x_0 = \frac{m_{AB} m_{BC}(y_3 - y_1) + m_{AB}(x_2 + x_3) - m_{BC}(x_2 + x_1)}{2(m_{AB} - m_{BC})}$$

By substituting x_0 into one of the line equations for the perpendicular bisector, y_0 can be calculated.

The radius can be found by calculating the distance between the centre and any of the three points. For this research, the radius of curvature of at a point will be calculated by using two points adjacent to it. First the x_0 and y_0 of the centre of curvature using 3 points will be calculated as explained above. For example, if point n is to be calculated, then point n-1 and point n+1 will be used. Then, the radius of curvature for point n can be calculated using,

$$\rho_n = \sqrt{(x_n - x_0)^2 + (y_n - y_0)^2} \ .$$

The radius of curvature of each data point in a given layer is calculated using this formula. This is repeated for each scanned body layer. Now by substituting all the parameters into the pressure formula (4.1), the pressure at each point can be obtained.

After that, a 2D pressure distribution prediction model can be developed as shown in Figure 4.5.

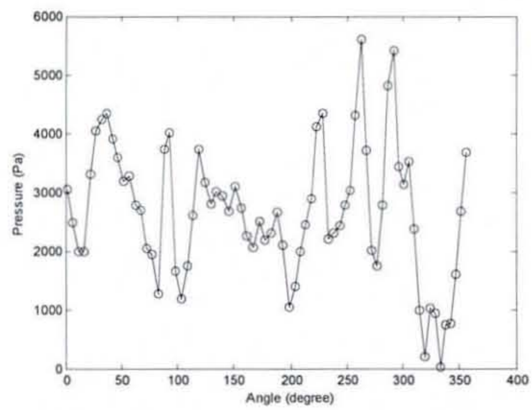

Figure 4.5 Pressure distribution at one layer

4.1.2 Development of 3D pressure distribution prediction model

Section 4.1.1 has shown method to calculate pressure at each point on the wounded area. Figure 4.5 shows 2D pressure distribution prediction model at one layer. It is very convenient to enable manufacturers or occupational therapists to assess pressure exerted by pressure garment. However, when the number of layer increases, the 2D model becomes more complex (Figure 4.6) and difficult to evaluate and to visualise the variations with respect to the neighbouring layers.

Layer		Layer	
1	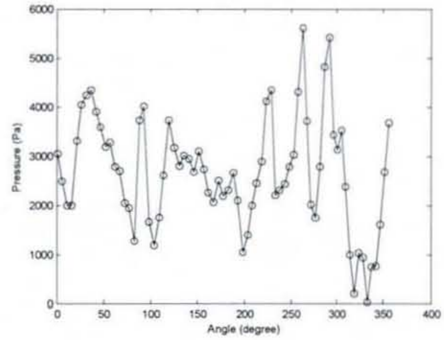 C_0=29.24 cm; Re=19.76%	6	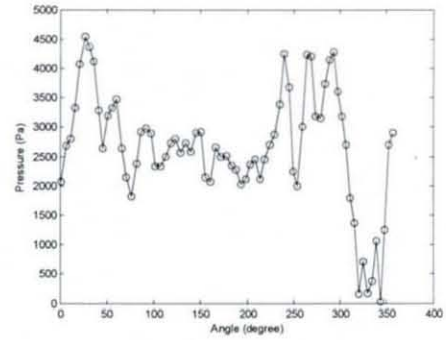 C_0=35.55 cm; Re=23.04%
2	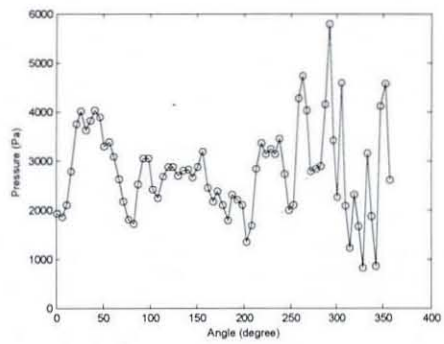 C_0=30.65 cm; Re=20.51%	7	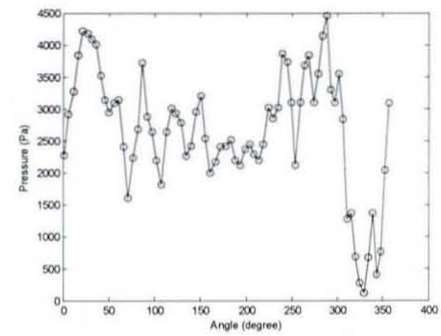 C_0=36.51 cm; Re=23.51%
3	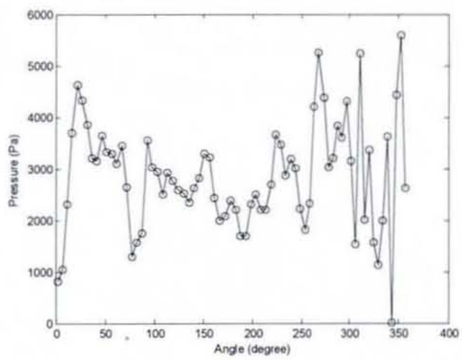 C_0=32.03 cm; Re=21.24%	8	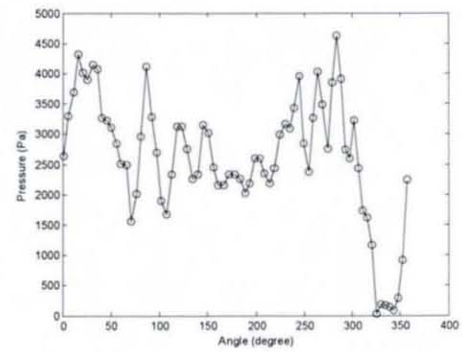 C_0=37.31 cm; Re=23.90%
4	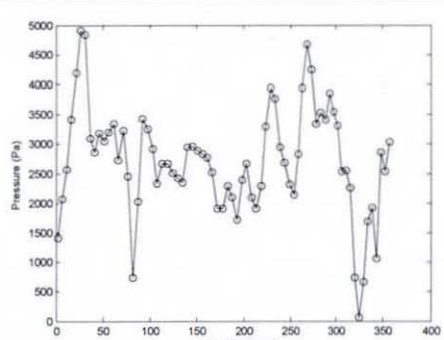 C_0=33.32 cm; Re=21.91%	9	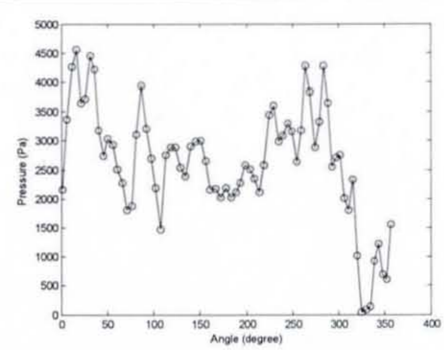 C_0=37.98 cm; Re=24.23%

5	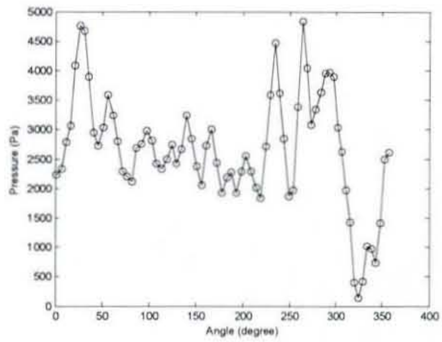 C_0=34.49 cm; Re=22.50%	10	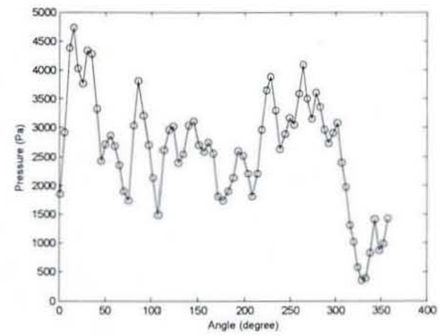 C_0=38.50 cm; Re=24.48%

Figure 4.6 2D pressure distribution prediction model for 10 layers

To overcome the problem, a 3D pressure distribution prediction model is needed. In order to develop the model, *fill3* function in MATLAB is used.

fill3(X,Y,Z,C) fills the three-dimensional polygon defined by vectors X, Y, and Z with the colour specified by C. The vertices of the polygon are specified by triples of components of X, Y, and Z. For example, triangle 1 (T_1) in Figure 3.11, can be defined as;

$$X = \begin{bmatrix} x_1 \\ x_{k+1} \\ x_{k+k} \end{bmatrix}$$
$$Y = \begin{bmatrix} y_1 \\ y_{k+1} \\ y_{k+k} \end{bmatrix}$$
$$Z = \begin{bmatrix} z_1 \\ z_{k+1} \\ z_{k+k} \end{bmatrix}$$

The files show that triangle 1 (T_1) is made up by three vertices, which is P_1 (x_1, y_1, z_1), P_{k+1} (x_{k+1}, y_{k+1}, z_{k+1}) and P_{k+k}(x_{k+k}, y_{k+k}, z_{k+k}). To show the pressure distribution, then the pressure at each vertex is included in another file, C, where:

$$C = \begin{bmatrix} \Pr essure_1 \\ \Pr essure_{k+1} \\ \Pr essure_{k+k} \end{bmatrix}$$

For example, if the first triangle of this research is made by points A, B and D, where the coordinates for point A is (0, 0, 20.37), B (1.01, 0, 21.37) and D (0.01, -0.31, 21.37), while the pressure at point A is 1991.3 Pa, at point B is 3383.7 Pa and at point D is 2240 Pa.

If all the parameters mentioned above is replaced with the first triangle in this research, where $X = \begin{bmatrix} 0 \\ 1.01 \\ 0.01 \end{bmatrix}, Y = \begin{bmatrix} 0 \\ 0 \\ -0.31 \end{bmatrix}, Z = \begin{bmatrix} 20.37 \\ 21.37 \\ 21.37 \end{bmatrix}, C = \begin{bmatrix} 1991.3 \\ 3383.7 \\ 2240 \end{bmatrix}$ its result is shown in Figure 4.7.

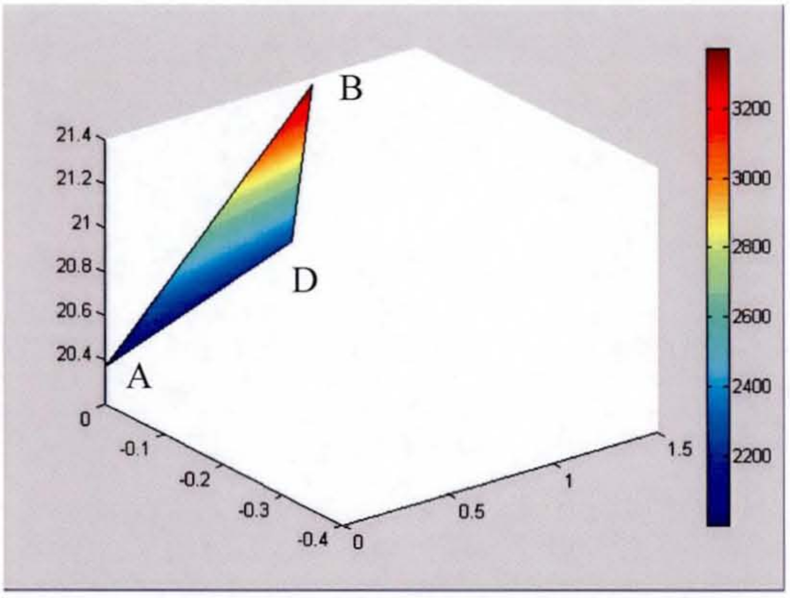

Figure 4.7 Results of triangle 1 (T_1) for this research

In order to develop 3D pressure distribution prediction model for the whole area, all points in the data must be arranged to be triangulated. The details of the triangulation process are explained in the previous chapter, Section 3.4.1.

After all the points that made up the triangulations are obtained, the next step is to arrange them so they can be used with the '*fill3*' function. In the '*fill3*' function, all the x-, y- and z- coordinates need to be separated into three files, X, Y and Z. In these files, the column number represents the triangle number, whilst the row number determines the position of the coordinate.

Thus, for triangle 1 (T_1) to triangle 2k (T_{k+k}), the X, Y, Z and C files should be;

$$X = \begin{bmatrix} x_1 & x_1 & . & . & . & x_k & x_k \\ x_{k+1} & x_2 & . & . & . & x_{k+k} & x_1 \\ x_{k+k} & x_{k+1} . & . & & . x_{k+(k-1)} & & x_{k+k} \end{bmatrix}$$

$$Y = \begin{bmatrix} y_1 & y_1 & . & . & . & y_k & y_k \\ y_{k+1} & y_2 & . & . & . & y_{k+k} & y_1 \\ y_{k+k} & y_{k+1} . & . & & . y_{k+(k-1)} & & y_{k+k} \end{bmatrix}$$

$$Z = \begin{bmatrix} z_1 & z_1 & . & . & . & z_k & z_k \\ z_{k+1} & z_2 & . & . & . & z_{k+k} & z_1 \\ z_{k+k} & z_{k+1} . & . & & . z_{k+(k-1)} & & z_{k+k} \end{bmatrix}$$

$$C = \begin{bmatrix} \Pr essure_1 & \Pr essure_1 & . & . & . & \Pr essure_k & \Pr essure_k \\ \Pr essure_{k+1} & \Pr essure_2 & . & . & . & \Pr essure_{k+k} & \Pr essure_1 \\ \Pr essure_{k+k} & \Pr essure_{k+1} . & . & & . \Pr essure_{k+(k-1)} & & \Pr essure_{k+k} \end{bmatrix}$$

Then, by using *fill3*(X,Y,Z,P) function, a 3D pressure distribution model has been developed for level 1. Figure 4.8 shows 3D pressure distribution prediction model for level 1 of this research. By repeating the process, 3D pressure distribution prediction model for the whole area of body can be visualized (Figure 4.9).

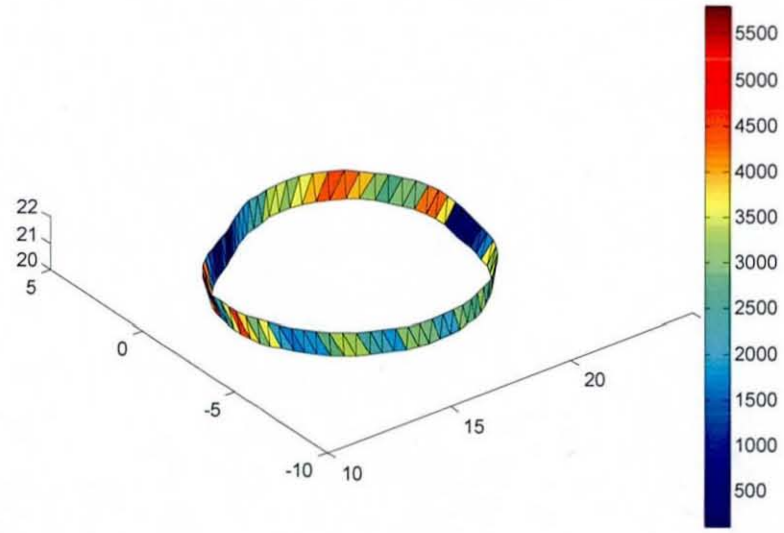

Figure 4.8 **3D pressure distribution prediction model for level 1**

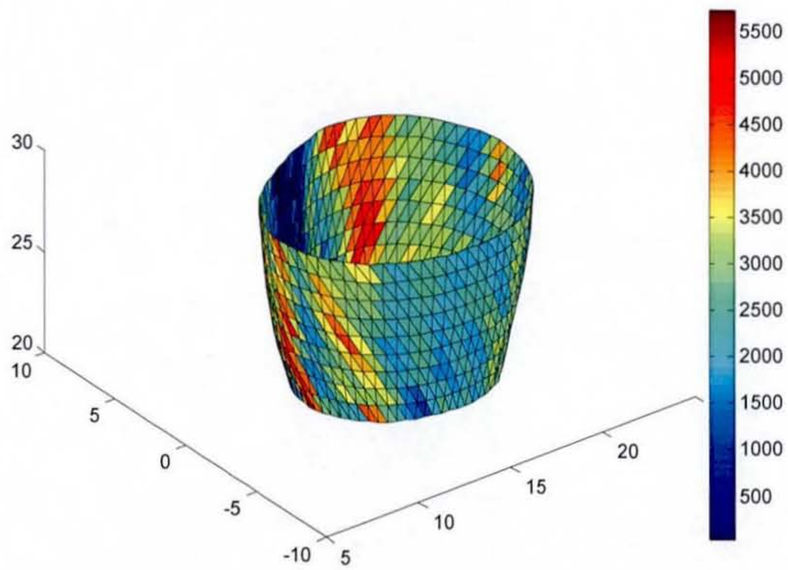

Figure 4.9 **3D pressure distribution prediction model for whole area**

4.2 Experimental methodology

The second experimental methodology for verifying the pressure distribution model is shown schematically in Figure 4.10. The steps are similar to the experiment in section 3.5, but instead of a cylinder, human subjects were used as a model. The subjects have been scanned using a 3D body scanner. Appendix B shows their leg figure. Then, pressure garments for the scanned body parts have been constructed using the method explained. Then, the experiments to measure the pressure exerted by the garment on the body has been conducted using the same volunteers. The pressure that the garment exerts on the body part has been calculated by using the pressure model developed. Then the results from the experiments were compared with those from the pressure model.

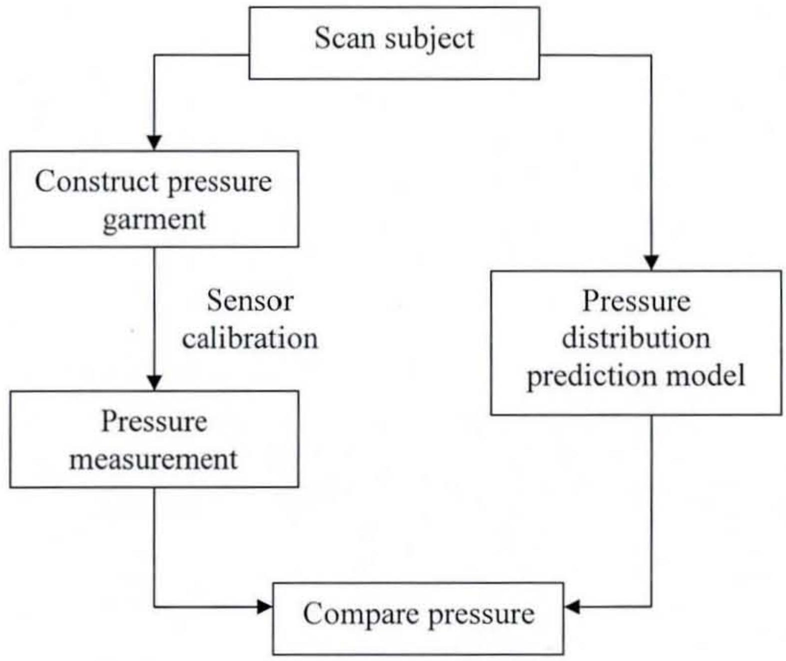

Figure 4.10 Flowchart of experiment to verify pressure distribution model

4.2.1 3D body scanning

Ten volunteer subjects have been used in this research. All of the subjects are male and their ages are in the range between 28 to 33 years old. Their whole body has been scanned and their body model was acquired.

The location of their body to represent a wounded area has been chosen not to be too intrusive for the volunteer subjects. Part of a leg below the knee has offered a convenient and less intrusive body part. Therefore this part of the body has been used with each subject. Then, the size of the generated pressure garment's pattern must be within the size of a sheet of A4 paper since this research uses A4 paper for printing the pattern.

4.2.2 The fabric's modulus of elasticity

The previously calculated modulus of elasticity of the fabric (see Section 3.5.5) has been used in this experiment since the same fabric was used in constructing the pressure garment in the experiments.

4.2.3 Pressure garment construction

By using the procedure developed, the pressure garment's pattern model for the volunteer subjects has been developed. In printing the pattern on hard copy, care must be taken that the dimensions on the printed pattern are the same as the actual, intended dimensions. Depending on the printer used and the software that supports it, different procedures may apply in order to obtain the true dimensions in print. Figure 4.11 shows original pattern size inside an A4 paper without any alteration. The size is smaller than its true size. Figure 4.12 shows the pattern size after its true dimension was obtained.

Once a hard copy print of the pattern with the actual dimensions is obtained, a pressure garment with an exact shape and size can be cut from the fabric with margins for sewing purposes. Before the pattern was cut, the paper patterns were aligned on the fabric so that the fabric pattern was mostly made from straight yarn (refer Figure 4.13). The pattern has then been sewn together to make the pressure garment.

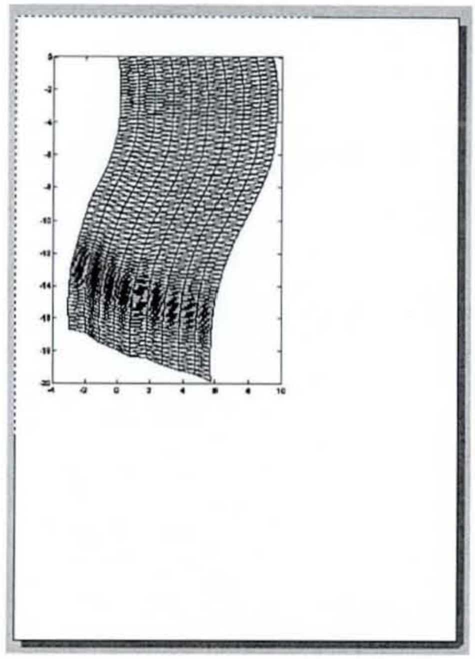

Figure 4.11 Pattern may be printed smaller than its true size

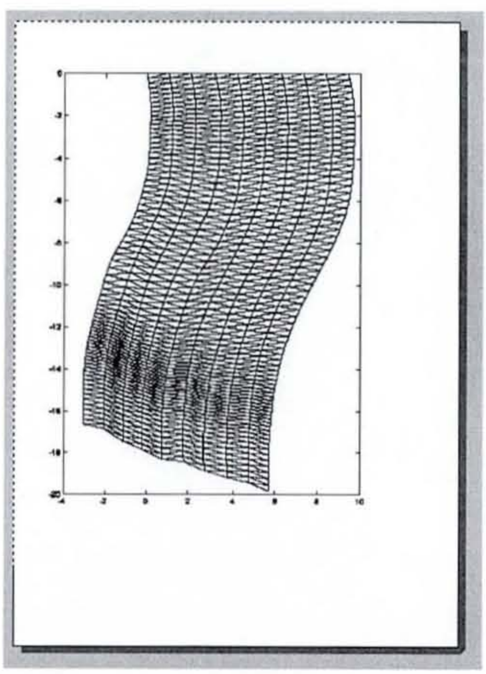

Figure 4.12 The size of the print needs to be adjusted to reflect the true size of the pattern

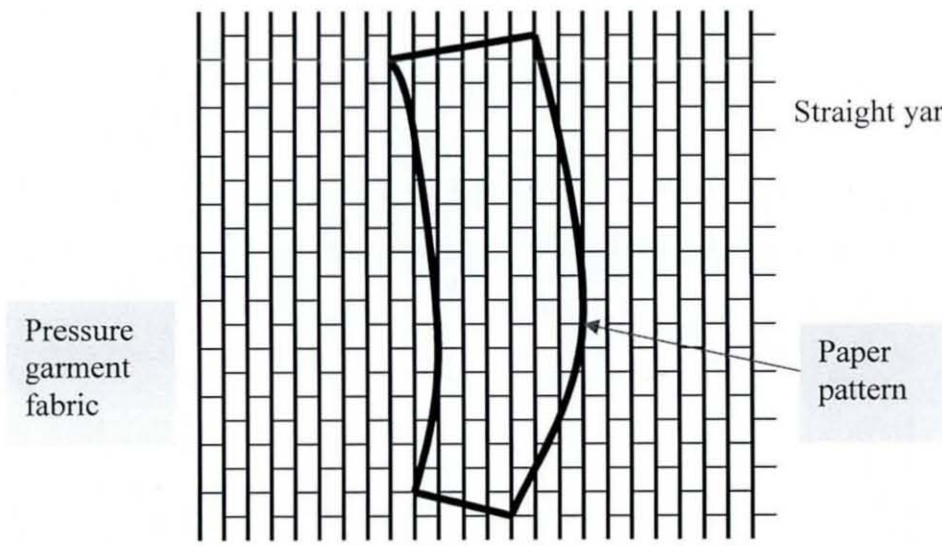

Figure 4.13 Paper pattern laid on the pressure garment fabric and adjusted before cutting

4.2.4 Sensor calibration

In the experiment, a single load cell, thin and flexible Flexiforce A201-1, a piezoresistive sensor made by Tekscan, has been used to measure the pressure exerted by the pressure garment on the body. The sensor's calibration, which was explained in Section 3.5.4, has been used to calibrate the sensor.

4.2.5 Pressure measurement to validate the pressure distribution

Subjects were fitted the pressure garment at the right part of their leg. They were given 15 minutes to move their leg freely so that the garment could become comfortable on the subject's leg. A rubber string was attached at the top end of the pressure garment and the location of the pressure garment on the body was checked regularly to ensure that it stayed at the intended area.

Then a pressure sensor was used to measure the pressure exerted on the leg by the pressure garment. Eight pressure measurements with equal angular separation were taken at each layer corresponding to θ= 0, 45, 90, 135, 180, 225, 270 and 315 degrees. Each layer is 1 cm apart from each other in the vertical direction. The angles, where the sensors were placed, were determined by using a computer program that can show the positioning, as in Figure 4.14. The lines shown there represent the mentioned angles, or a close approximation (to within 1 degree) to the angle. The blue line indicates the location of 0 degree, the reference point, while the yellow line represents the 45-degree location. The green lines show the other locations separated by 45^0. To ensure that all the readings were taken from the same height, a loose rubber string was used. The string was attached at the measuring height, and by referring to the Figure 4.14, the locations for the sensors on the pressure garment were marked. When finished, the string was removed. The sensor was attached inside the pressure garment on the mark.

The sensor was left on the location for one minute to settle prior to pressure measurements. Inspections were carried out regularly to ensure that the sensors were on the right spot, and the voltage readings were taken. Based on the linear calibration graph from the earlier calibration process, the voltage is converted to pressure. All the measurements were taken with the human subject standing with the legs straight and hands hanging down in a natural posture (Figure 4.15).

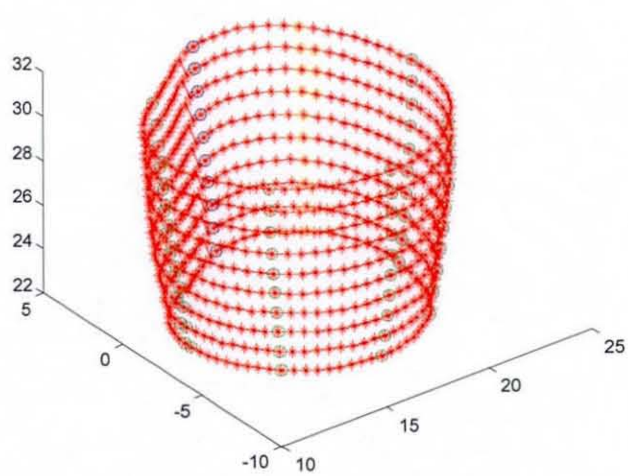

Figure 4.14 Location of sensors

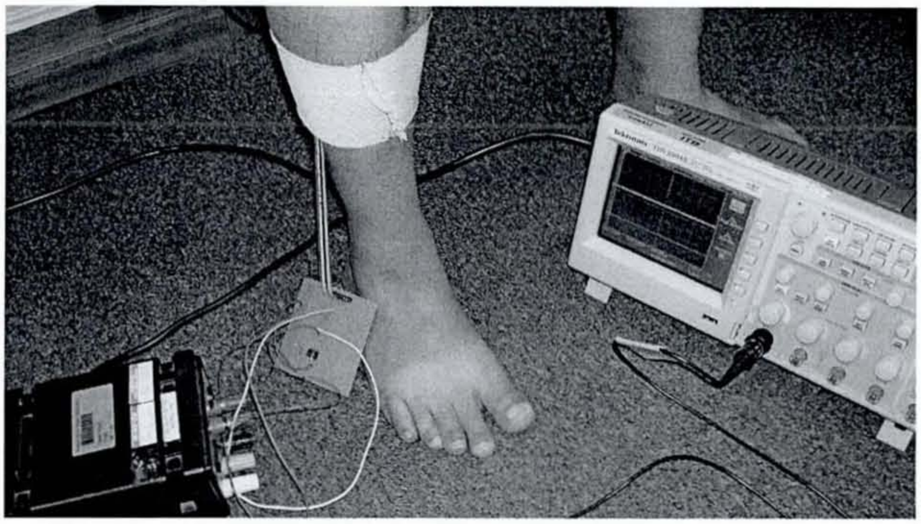

Figure 4.15 Measurement process

4.3 Result for verification of pressure distribution model

4.3.1 Scanning

The experiment was conducted to scan the body of the ten subjects in order to gather 3D digital body data. Then a location on the body was chosen for pressure garment development. Figure 4.16 shows the selected body part for pressure garment development for all ten subjects. Body parts corresponds the leg to below the knee.

4.3.2 Modulus of elasticity

The modulus of elasticity results from Section 3.6.2 was used in this experiment. Based on modulus of elasticity of five specimens from the same fabric, the average modulus of elasticity is 0.504 N/mm.

4.3.3 Sensor calibration

The experiment was conducted in order to calibrate the sensor so it can be used to measure pressure. The sensor was calibrated using the method explained in Section 3.5.4. The experiment was conducted over three days, so there are three sensor calibrations, one for each day. Figure 4.17 shows the results for the sensor calibrations.

Sub ject	Wounded area	Subj ect	Wounded area
1	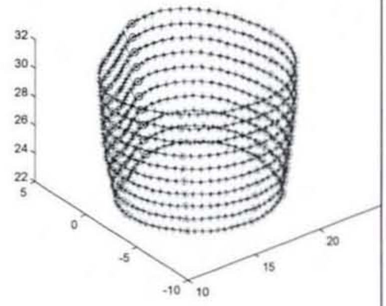	6	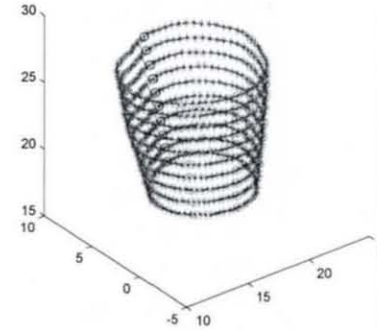
2	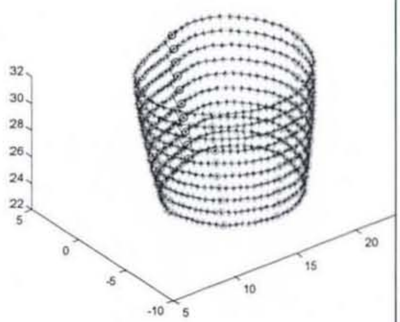	7	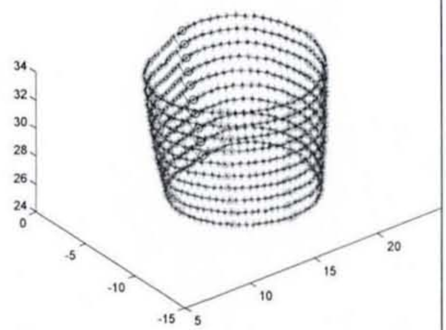
3	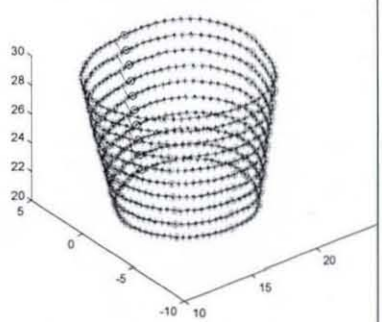	8	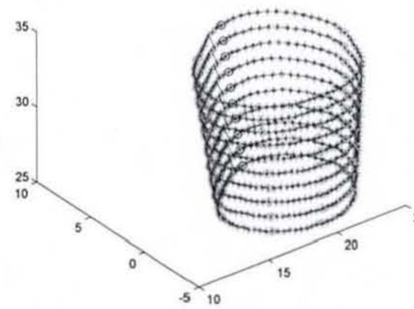

4	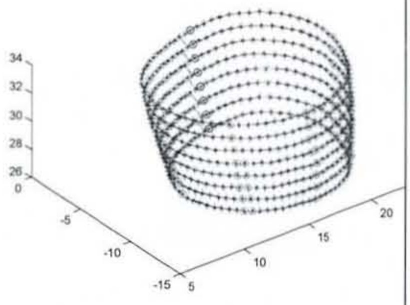	9	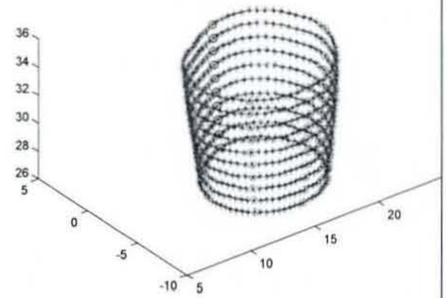
5	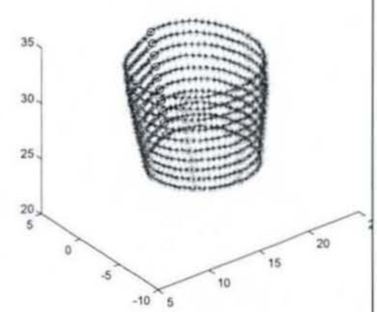	10	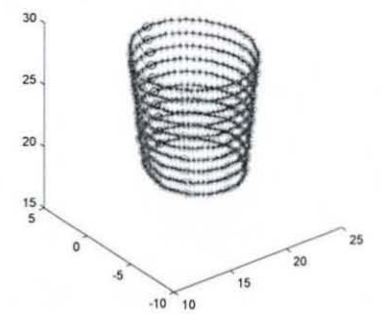

Figure 4.16 Wounded region for pressure garment of each subject

Day	Sensor calibration
1	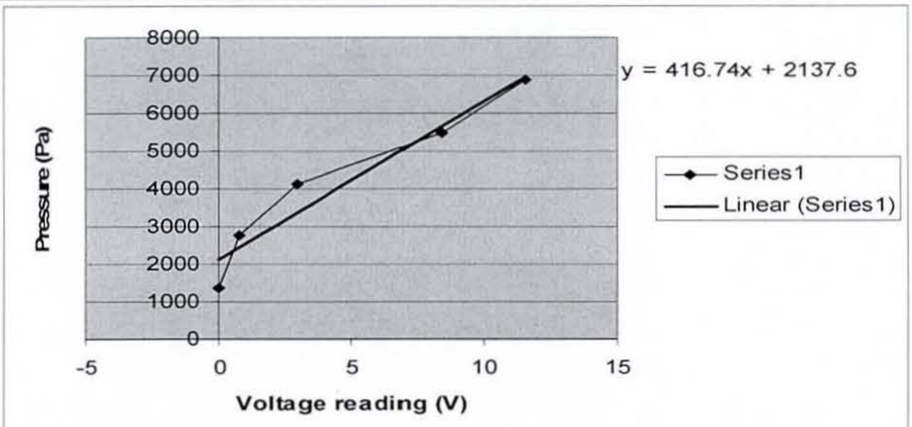

2	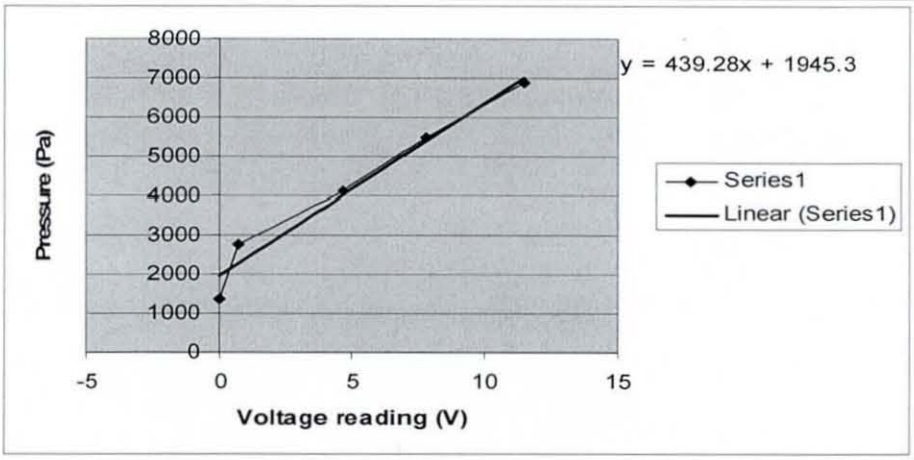
3	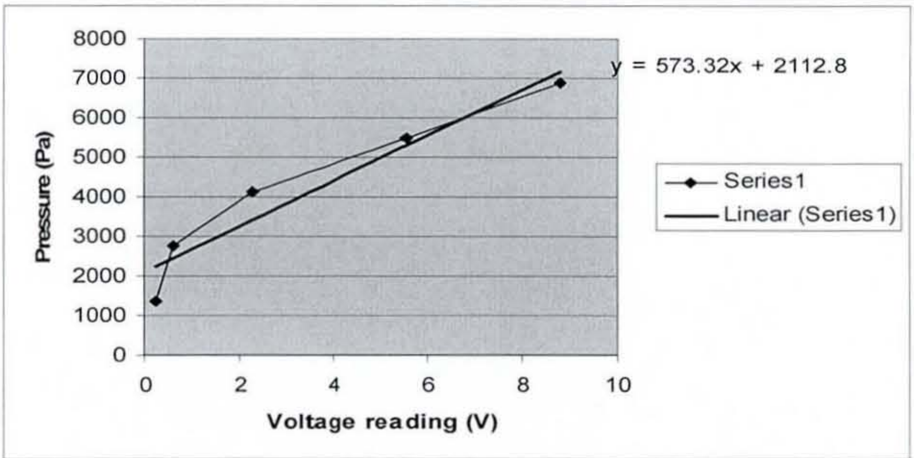

Figure 4.17 Sensor calibrations' result

4.3.4 Result for experiment to validate pressure distribution model

This experiment was conducted to validate the pressure distribution model developed by the computer program. Based on data for the fabric's modulus of elasticity and the 3D geometric data of the wounded area, a reduction factor for each layer of each subject was calculated. Results of the reduction factor are shown in Table 4.1. Then, the 3D pressure garment model was created based on the reduction factor and transformed into the 2D pressure garment pattern. Results for the developed pressure garment pattern are shown in Figure 4.18. The pressure garment patterns were generated copied on fabric and cut out to make a pressure garment.

Table 4.1 **Reduction factor at each layer for each subject**

Layers	Subject									
	1	2	3	4	5	6	7	8	9	10
1	0.21575	0.20671	0.19262	0.235	0.19884	0.16675	0.20643	0.18247	0.18743	0.16692
2	0.2212	0.21222	0.19737	0.24074	0.20426	0.1711	0.21094	0.18594	0.19188	0.17125
3	0.22626	0.21711	0.20223	0.24595	0.20965	0.17632	0.215	0.18986	0.19665	0.17598
4	0.23094	0.22184	0.20716	0.25048	0.21477	0.18163	0.21884	0.19341	0.20126	0.18093
5	0.23505	0.22651	0.21219	0.25432	0.21947	0.18696	0.2227	0.19653	0.2053	0.18528
6	0.23859	0.23111	0.21736	0.2571	0.22375	0.1924	0.22622	0.20004	0.2091	0.18908
7	0.24151	0.23531	0.22247	0.25879	0.22713	0.19735	0.22913	0.20341	0.21254	0.19286
8	0.24362	0.23873	0.22746	0.25952	0.2296	0.20191	0.23141	0.20741	0.2146	0.19637
9	0.24483	0.24134	0.2324		0.23139	0.20631	0.23328	0.21136	0.21544	0.19985
10	0.24523	0.24324	0.23694		0.2324	0.21046	0.23448	0.21509	0.21548	0.20356

For the first day, four subjects were measured. On the second day, one subject was measured and on the last day, five subjects were available. Their measurement locations are shown in Figure 4.16.

The pressure distribution results from the model are shown in Figure 4.19. In the second column, a 3D pressure distribution at the wounded area is presented. In the third column, the pressure distributions at a given layer, and at the layers located just below and above it, are presented graphically.

The pressure distribution model uses 72 data points at each layer, which was determined by the scanning instrument. This means that the data points in a given layer is separated by approximately 5 degrees or around 0.5 cm. On the other hand, in the experiments, only eight locations were measured, with a 45-degree interval. The sensor's sensing area's radius is 0.5 cm, which can span across an area corresponding to three scanned data points on the same layer, i.e. the intended data point and two adjacent ones on either side.

Sub ject	Pattern shape	Subje ct	Pattern shape
1	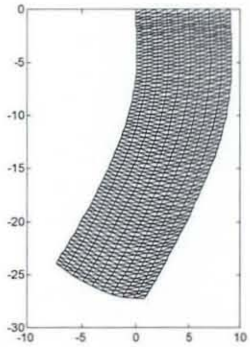	6	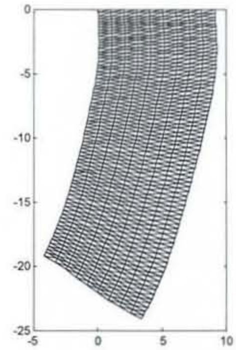
2	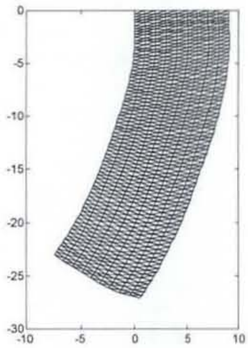	7	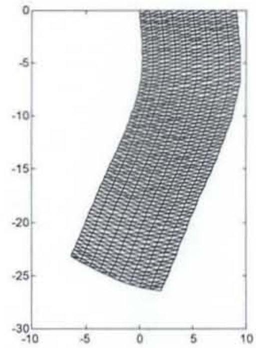
3	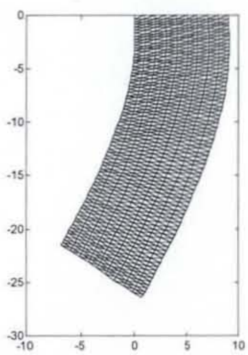	8	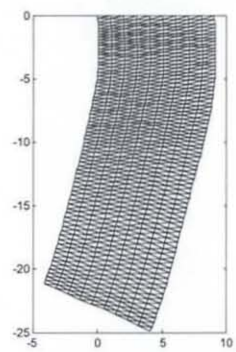
4	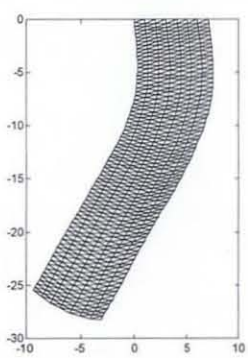	9	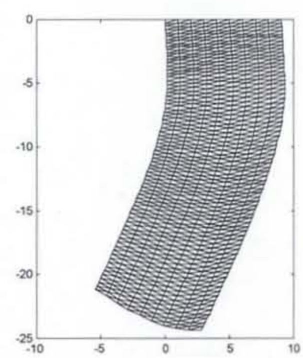

5	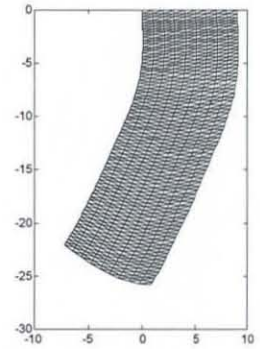	10	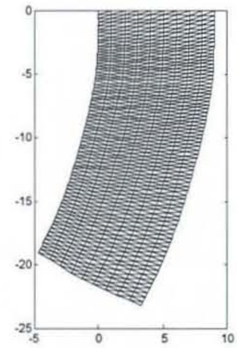

Figure 4.18 Pattern's shape for each subject

Subject	Pressure distribution in 3D	Pressure distribution in 2D
1	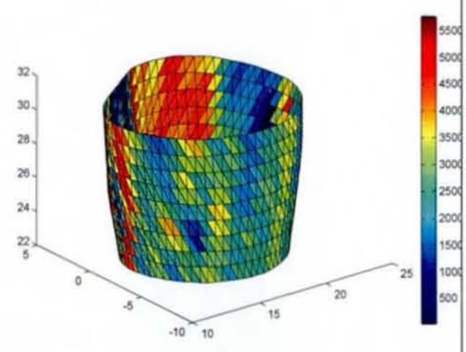	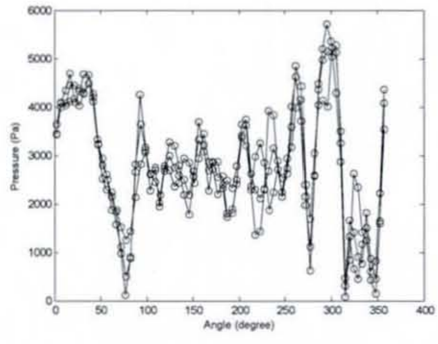
2	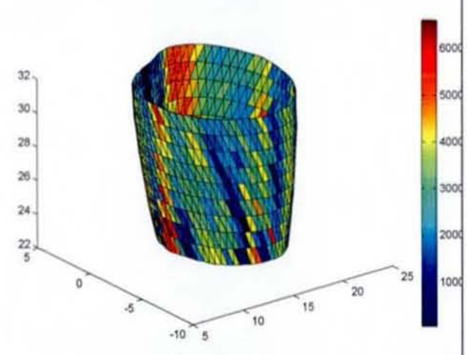	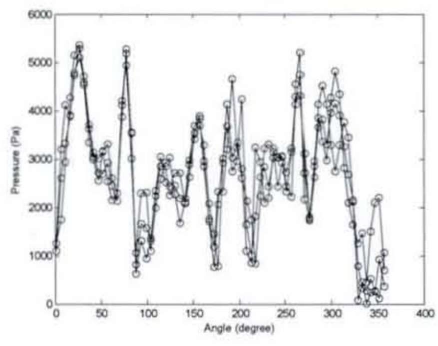
3	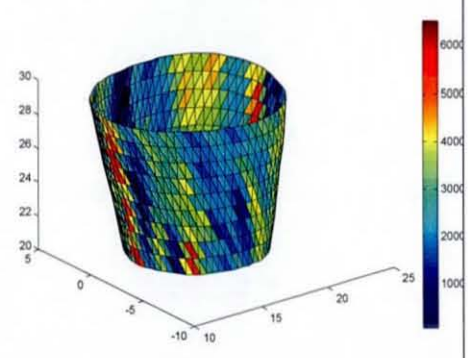	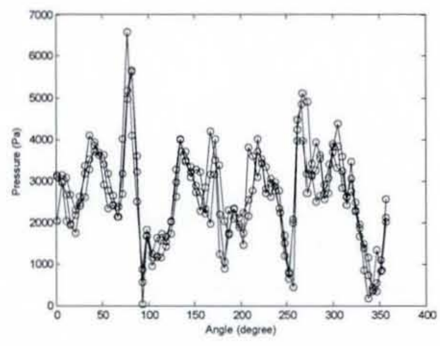

4

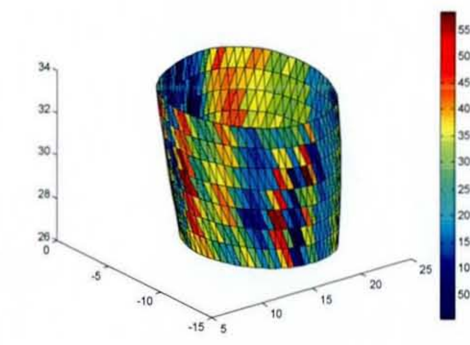

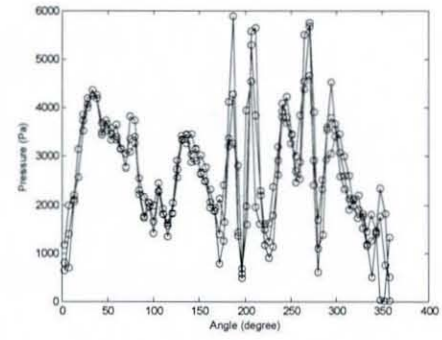
Pressure (Pa)
Angle (degree)

5

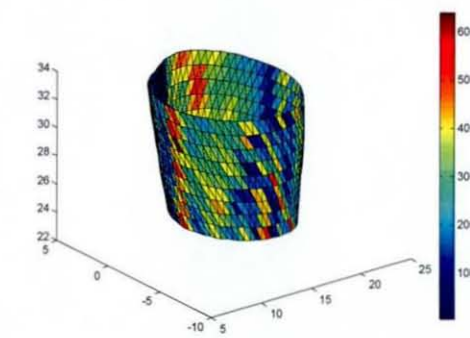

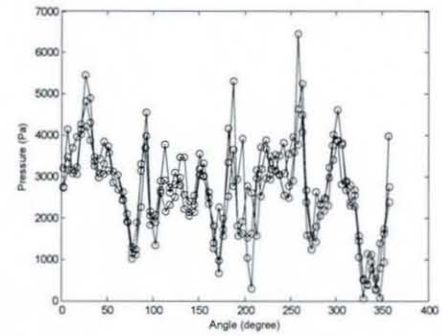
Pressure (Pa)
Angle (degree)

6

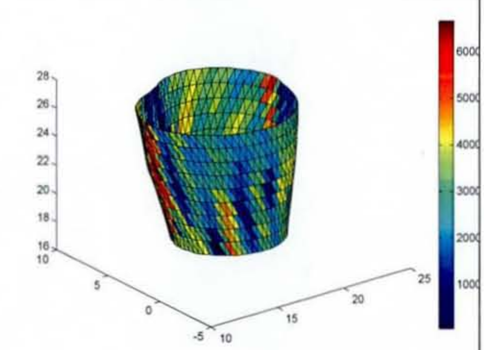

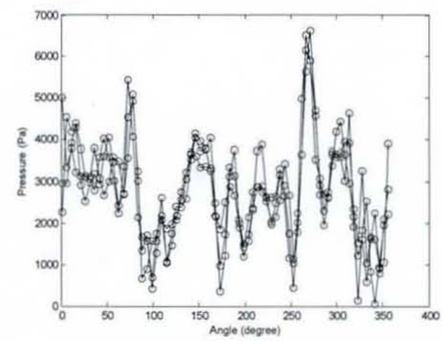
Pressure (Pa)
Angle (degree)

7

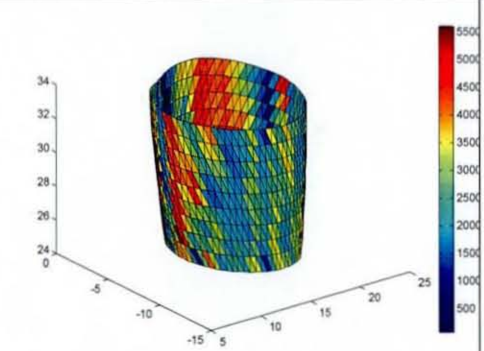

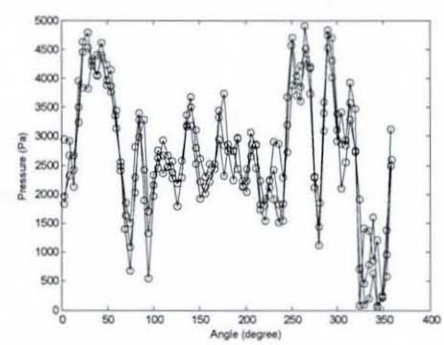
Pressure (Pa)
Angle (degree)

8	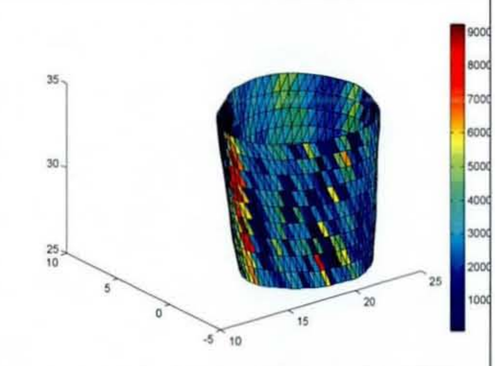	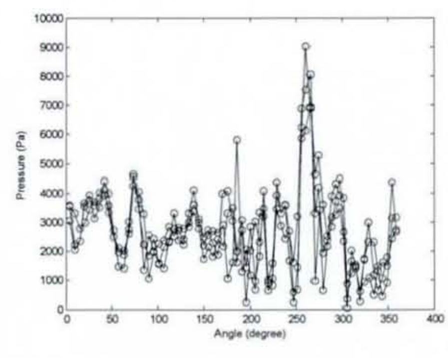
9	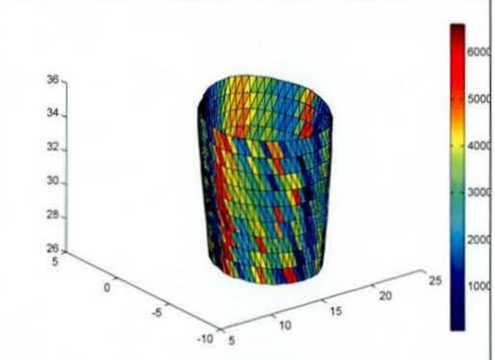	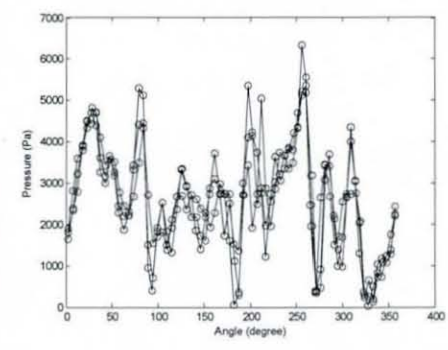
10	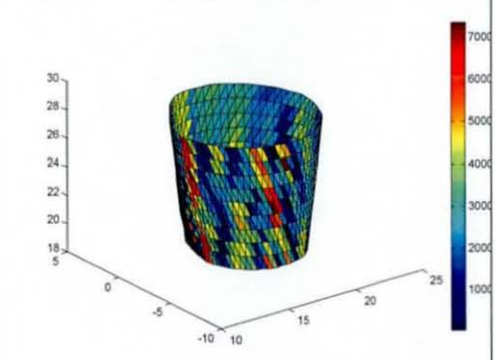	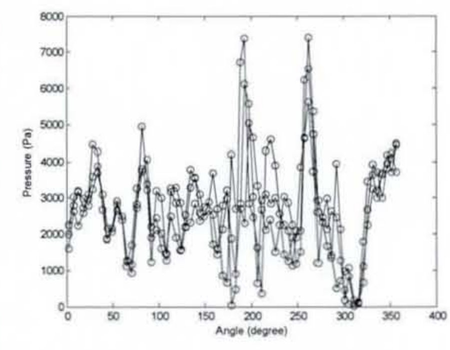

Figure 4.19 3D pressure distribution model and 2D graph

In measuring the pressure during the experiment, care was taken to place the sensor at correct data point. Since the sensor's sensing area covered neighbouring points, the average pressure from the pressure point with its two neighbouring points at a given layer was calculated. Then, the average pressures from pressure points at layers above and below were also calculated to include other areas that might influence the result (Figure 4.20). The results for the average prediction pressure on the body are presented in Table 4.2.

Table 4.3 shows result of pressure measured by the experiment. The comparisons of the results between the predicted and the experimental pressure are shown in Figures 4.21 and 4.22. In Figure 4.21, the experimental pressure is compared with the predicted pressure at the measured layer and the layers located below and above it. Figure 4.22 shows the experimental data compared with the average pressure from the three layers.

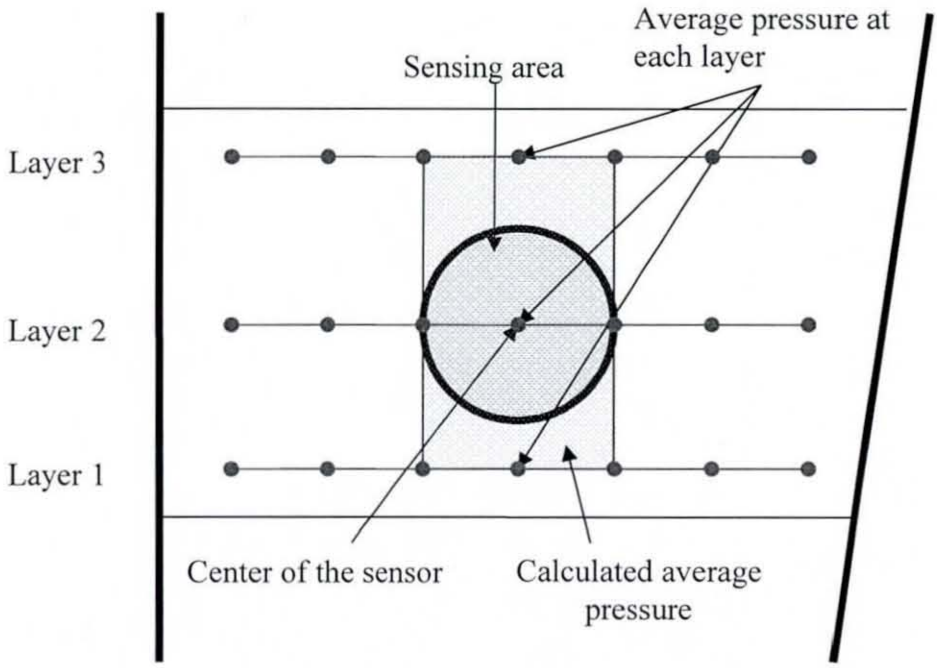

Figure 4.20 Intended location of the sensor

Table 4.2 Average pressure predicted by the model

Subject	0	45	90	135	180	225	270	315
1	4009.92	3362.41	2436.70	2656.04	2254.94	2781.14	2871.71	1601.00
2	1433.41	2938.34	1987.11	2263.41	1869.27	2427.61	3063.69	3288.86
3	2289.41	3928.23	1898.65	3582.23	2483.70	3082.53	4388.53	3148.96
4	867.97	3792.94	2073.73	3369.29	3028.79	1729.23	4408.97	2205.43
5	2373.78	3546.28	3111.80	2932.88	3080.11	3086.29	2026.90	2714.19
6	3738.06	3488.98	1645.95	2949.40	1894.44	2660.11	5218.34	3155.69
7	1633.49	4390.81	1879.04	2976.88	2736.69	2045.18	3709.76	3019.92
8	3259.73	3627.23	2092.04	2978.68	2683.99	2312.09	5042.80	1425.07
9	2198.02	3497.13	2414.31	2493.60	1863.61	2532.81	1417.82	2817.60
10	3002.51	2215.28	2457.37	2988.03	1544.68	3173.12	3870.84	832.89

Table 4.3 Pressure measured by the experiment

	0	45	90	135	180	225	270	315
1	3749.44	2144.77	2572.52	2723.18	2137.69	2392.43	2135.39	2152.50
2	2144.77	2390.23	2138.57	2138.91	2138.88	2187.97	2141.33	2368.15
3	4179.09	3519.02	2272.58	2131.77	2621.69	2132.05	2132.11	2460.16
4	2154.24	2205.79	2176.51	2581.32	2138.35	2301.82	2141.03	2294.87
5	2427.41	1940.32	1940.70	3041.14	1945.22	1943.33	2423.76	2996.14
6	3810.05	1469.57	1434.11	1439.56	1461.50	1435.78	2788.36	1540.74
7	2130.94	2196.72	2111.68	2206.92	2344.50	2565.75	2284.91	2396.03
8	2697.00	2655.12	2794.47	2111.59	2435.00	2110.45	2110.60	2111.13
9	2444.28	3214.07	2144.98	2246.86	2120.96	2582.12	2273.83	2104.75
10	5799.17	2912.94	2454.39	2517.52	2104.43	2136.50	2151.07	2381.21

Subject	Result
1	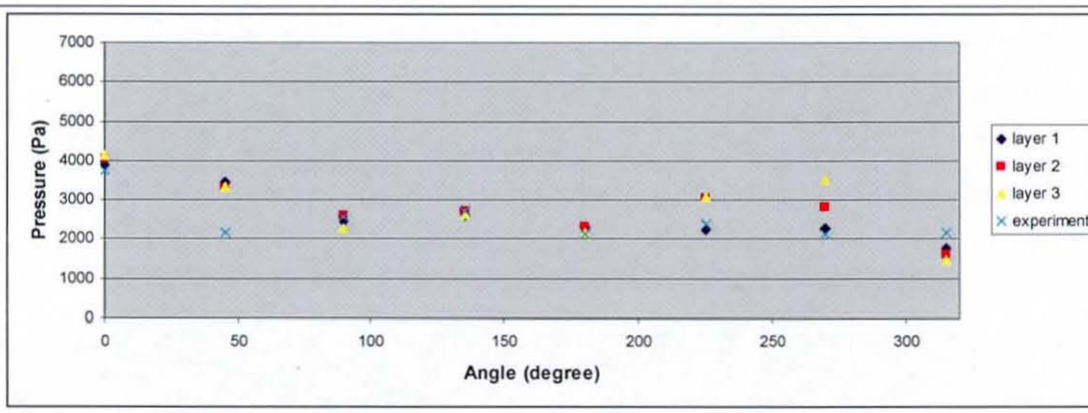
2	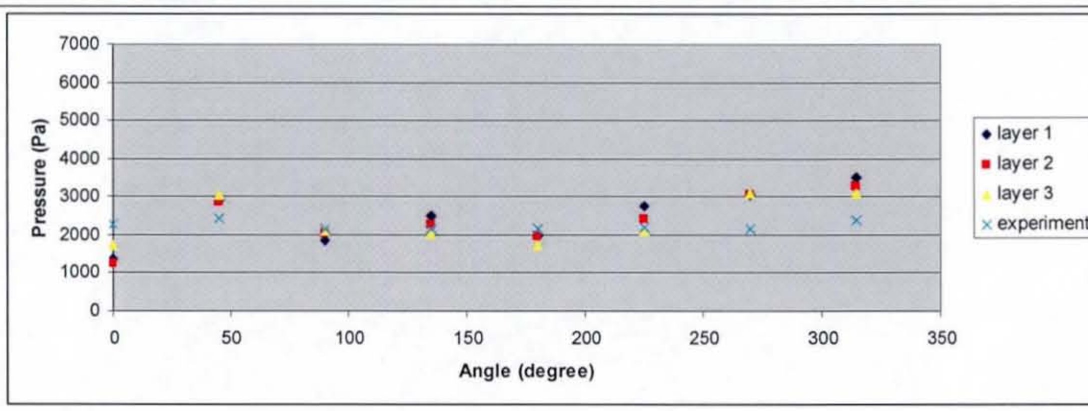

3	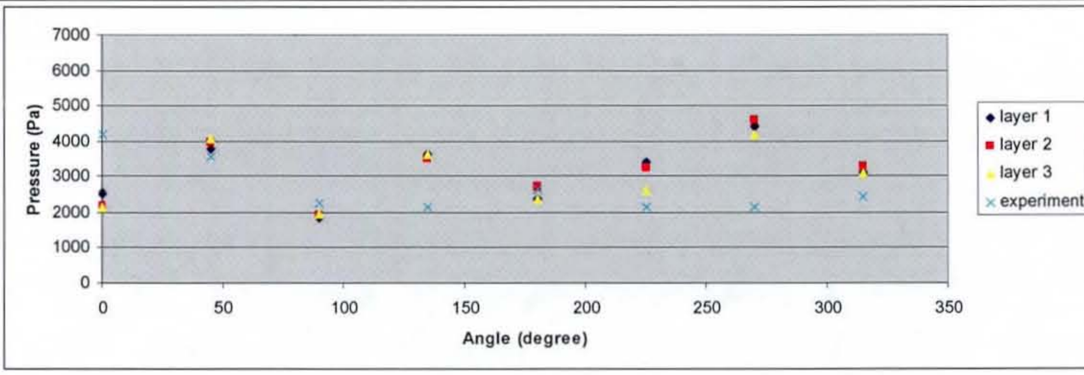Pressure (Pa) Angle (degree) layer 1 layer 2 layer 3 experiment
4	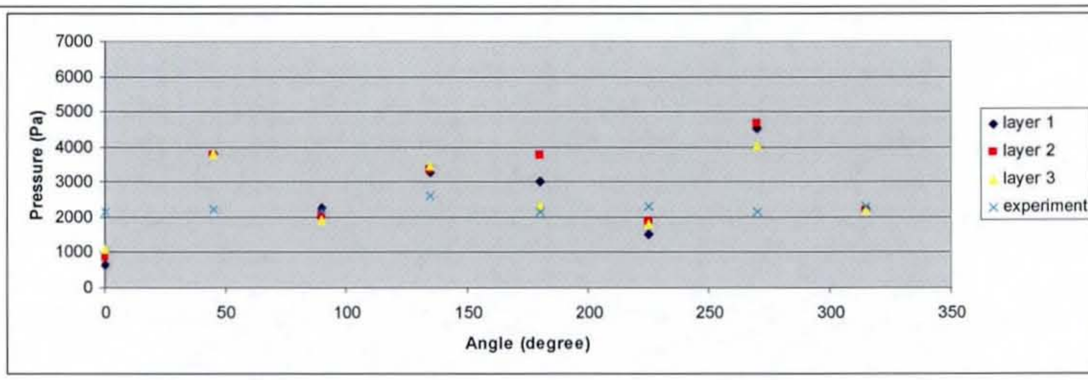Pressure (Pa) Angle (degree) layer 1 layer 2 layer 3 experiment
5	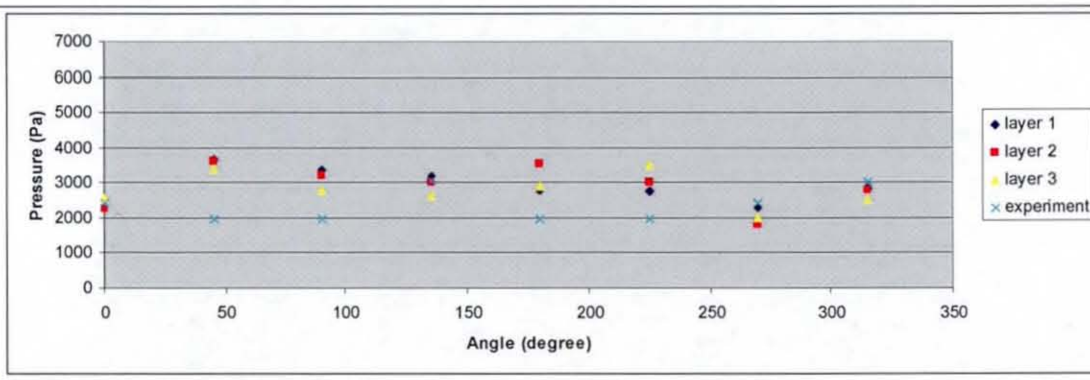Pressure (Pa) Angle (degree) layer 1 layer 2 layer 3 experiment
6	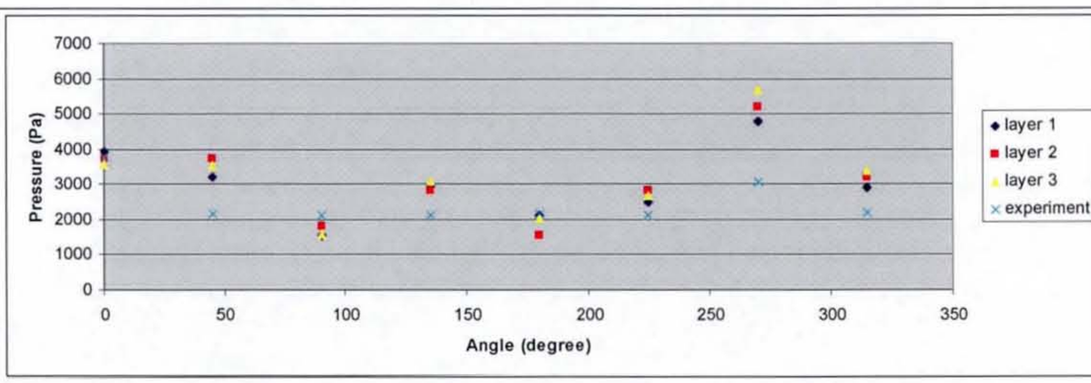Pressure (Pa) Angle (degree) layer 1 layer 2 layer 3 experiment

7

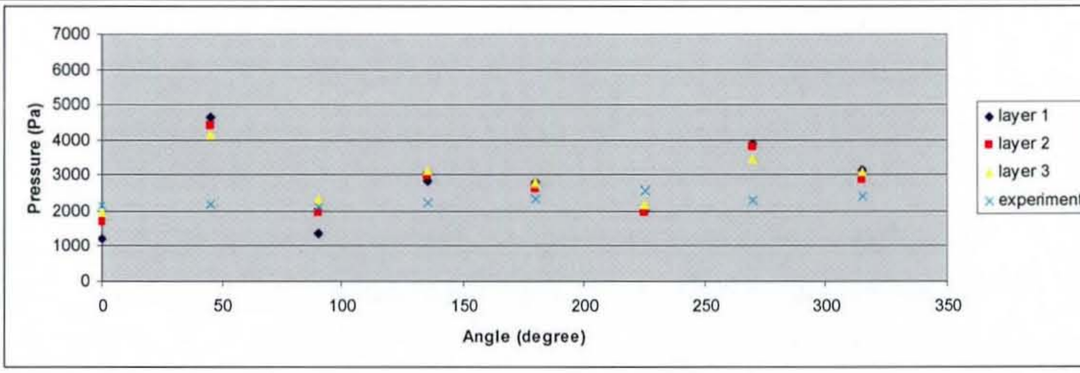

8

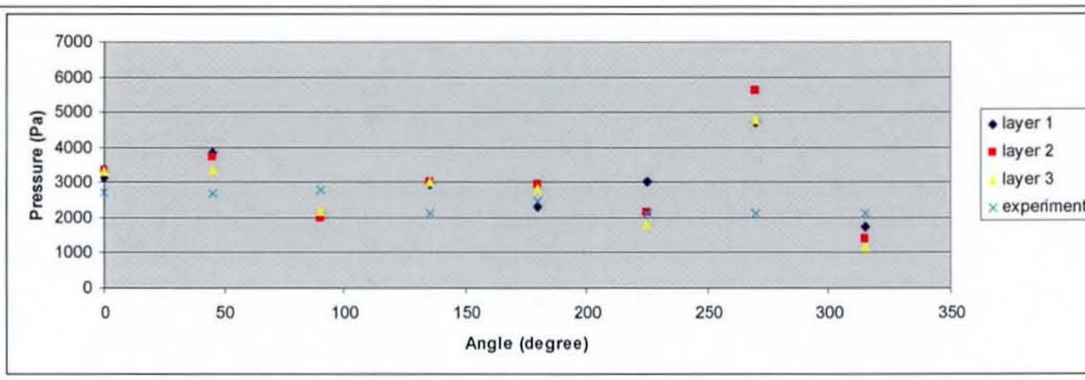

9

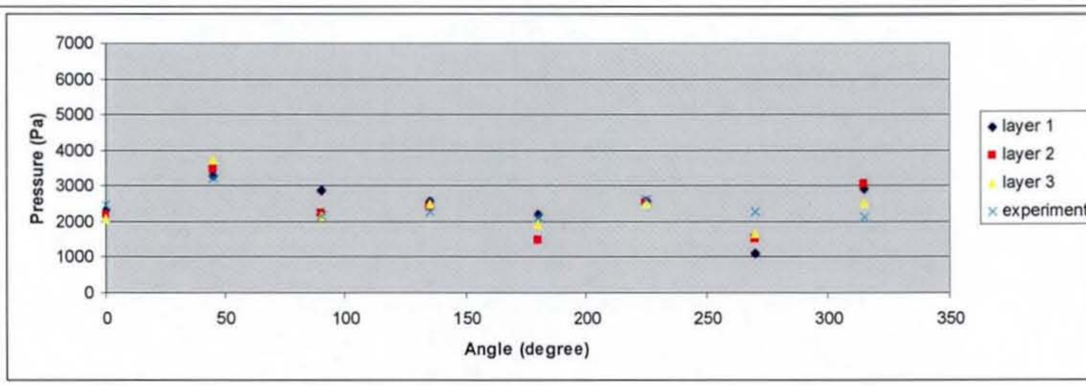

10

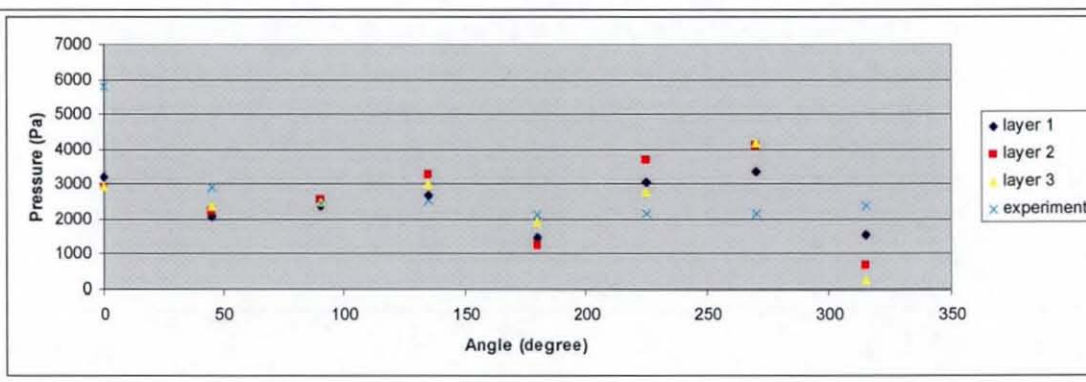

Figure 4.21 Comparison of pressure distribution with pressure at three layers

Subject	Result
1	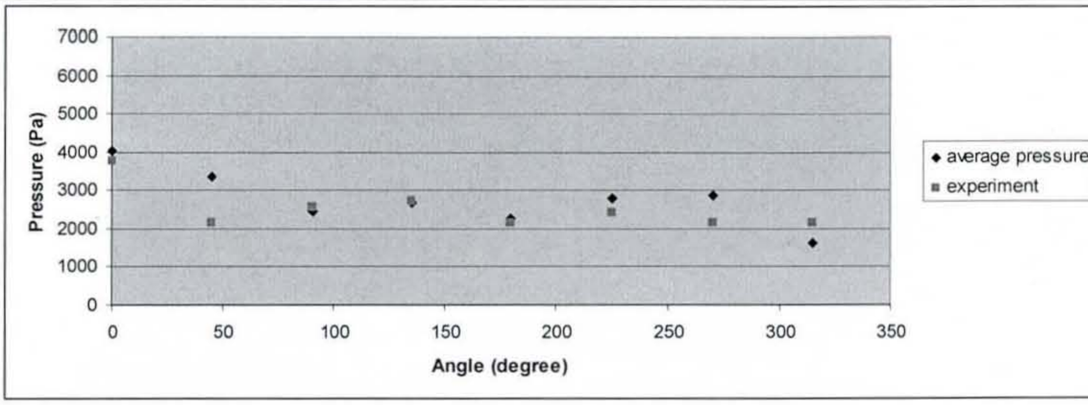
2	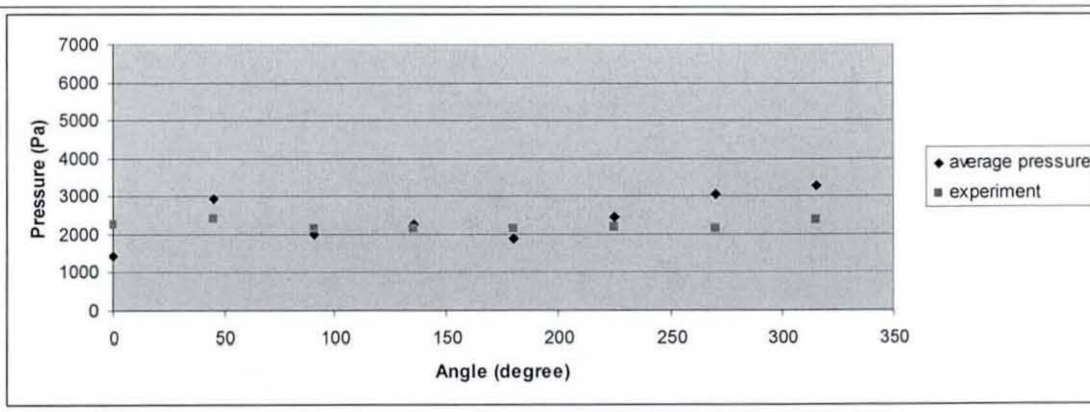
3	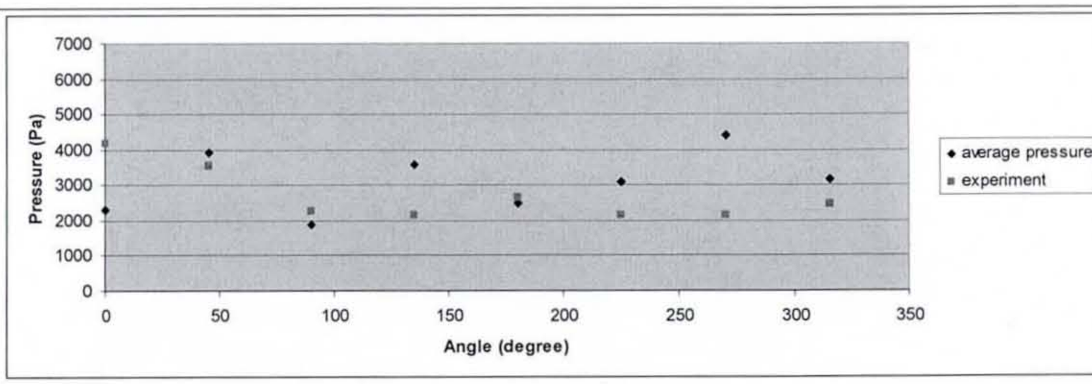

4

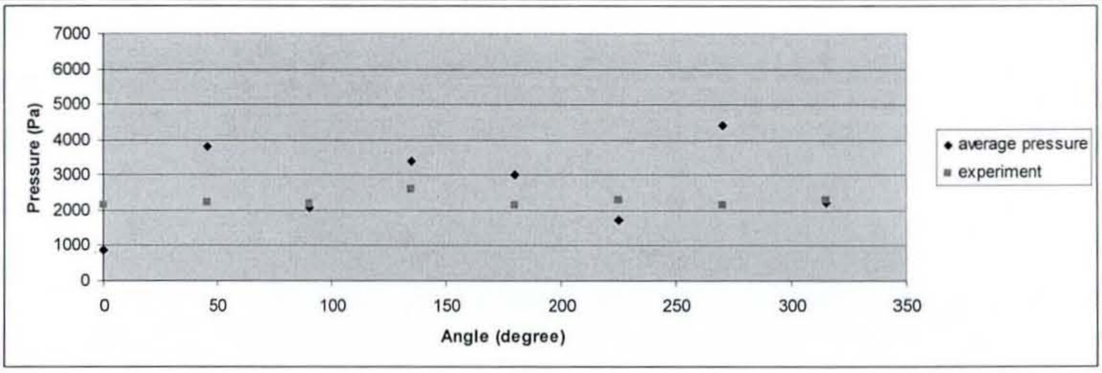
Pressure (Pa)
7000
6000
5000
4000
3000
2000
1000
0
0
50
100
150
200
250
300
350
Angle (degree)
average pressure
experiment

5

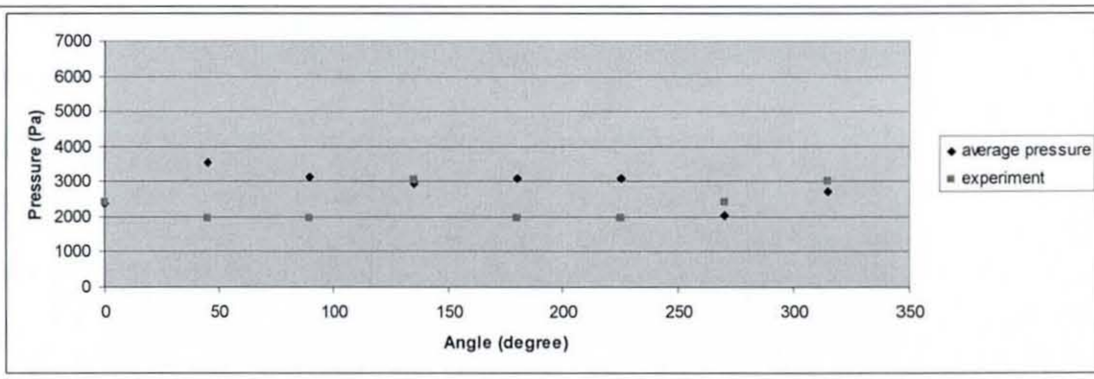
Pressure (Pa)
7000
6000
5000
4000
3000
2000
1000
0
0
50
100
150
200
250
300
350
Angle (degree)
average pressure
experiment

6

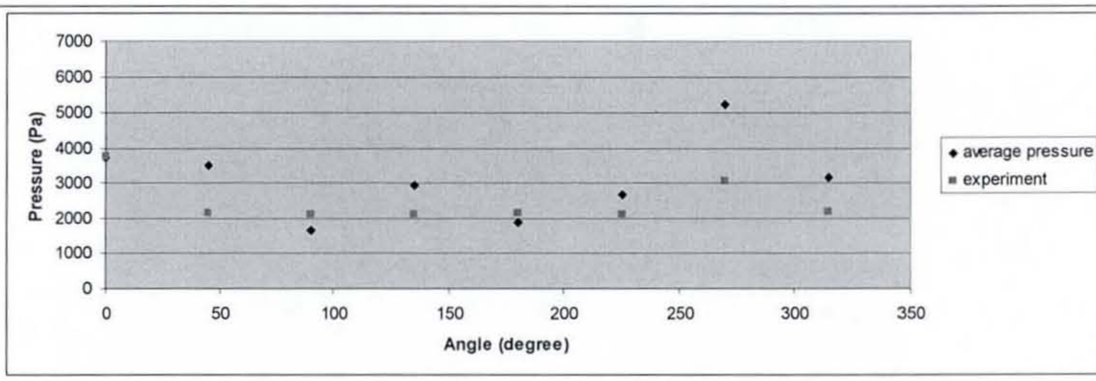
Pressure (Pa)
7000
6000
5000
4000
3000
2000
1000
0
0
50
100
150
200
250
300
350
Angle (degree)
average pressure
experiment

7

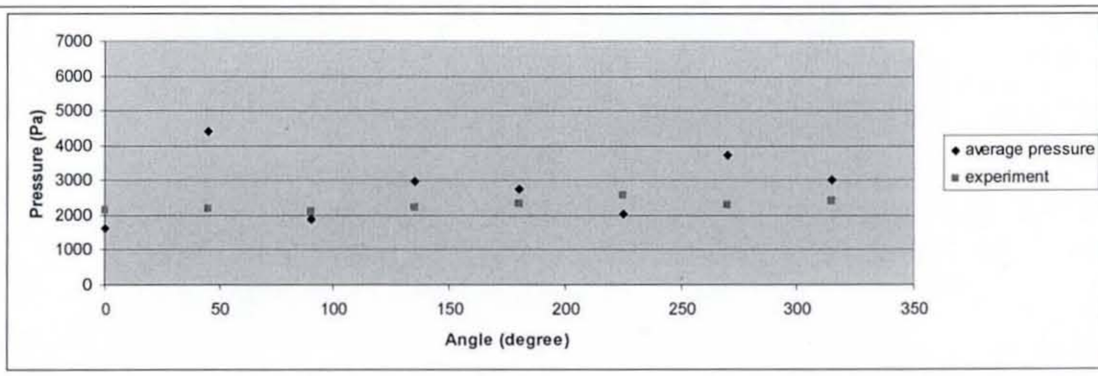
Pressure (Pa)
7000
6000
5000
4000
3000
2000
1000
0
0
50
100
150
200
250
300
350
Angle (degree)
average pressure
experiment

8

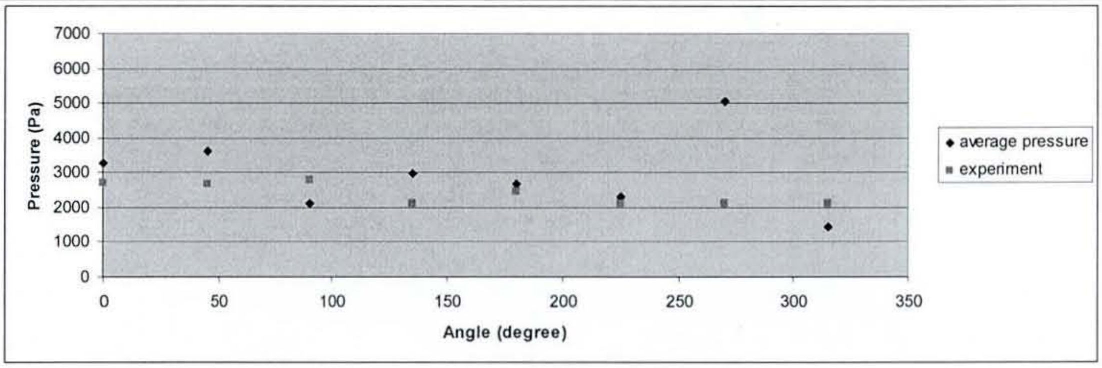

9

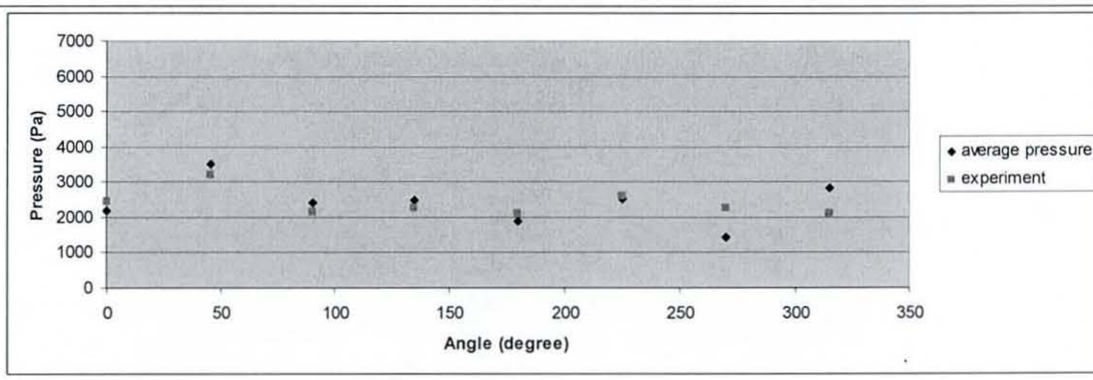

10

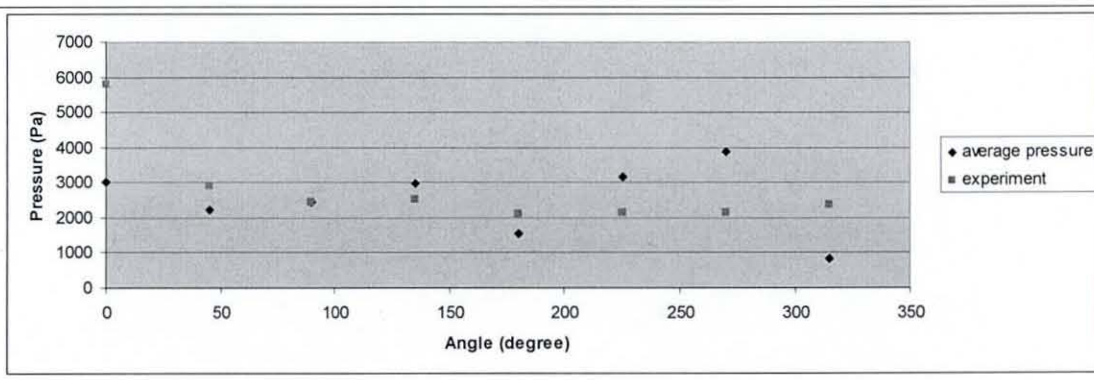

Figure 4.22 Comparison of experiment pressure with average pressure from the three layers

4.3.5 Data analysis

Table 4.4 shows the differences between estimated pressures and experimental pressures.

Table 4.4 **The differences between estimation pressures and experiment pressures (Pa)**

	Angle (degree)							
Subject	0	45	90	135	180	225	270	315
1	260.48	1217.64	-135.82	-67.14	117.25	388.71	736.32	-551.50
2	-711.36	548.11	-151.46	124.50	-269.61	239.64	922.36	920.71
3	-1889.68	409.21	-373.93	1450.46	-137.99	950.48	2256.42	688.80
4	-1286.27	1587.16	-102.78	787.97	890.44	-572.59	2267.94	-89.44
5	-53.63	1605.96	1171.10	-108.26	1134.89	1142.96	-396.86	-281.95
6	-71.99	2019.41	211.85	1509.84	432.94	1224.33	2429.98	1614.95
7	-497.45	2194.09	-232.64	769.96	392.20	-520.57	1424.85	623.89
8	562.73	972.12	-702.43	867.09	248.99	201.64	2932.20	-686.06
9	-246.26	283.06	269.33	246.74	-257.35	-49.30	-856.01	712.85
10	-2796.66	-697.66	2.98	470.51	-559.75	1036.62	1719.77	-1548.31

As shown by the Table 4.4, the model tends to overestimate the pressure that the pressure garment exerts on body except at location 0^0 and at 90^0 to an extent, where the measured pressures are generally higher that prediction pressure.

To measure the differences between pressure values predicted by the model and the value actually taken by experiment from the body being modelled, mean absolute error (MAE) was used. MAE is the average over the verification sample of the absolute values of the differences between forecast and the corresponding observation. The MAE is a linear score which means that all the individual differences are weighted equally in the average. MAE is negatively-oriented scores, lower values are better.

If pressure estimate from model is f_i and pressure obtained by the experiment is y_i, MAE is defined by the following formula.

$$MAE = \frac{1}{n}\sum_{i=1}^{n}|f_i - y_i|$$

$$MAE = \frac{1}{n}\sum_{i=1}^{n}|e_i|$$

Based on the formula, MAE for every subject was calculated. For f_i, the average pressures at three layers were used as estimated pressure.

Table 4.5 **MAE for each subject**

Subject	MAE
1	434.36
2	485.97
3	1019.62
4	948.07
5	736.95
6	1189.41
7	831.96
8	896.66
9	365.11
10	1104.03

The MAE's result shows that pressure estimations on some of the subjects significantly varied while for some others, the variations were small. These variations were contributed by several factors which will be discussed in Section 4.4.

4.4 Discussion

There are five main factors that affect the pressure distribution results, thus contributed to the differences between experiment pressure and predicted pressure. The first factor is the soft tissue that makes up the body. The second factor is the location of the sensor. The third factor is the pattern shape. The fourth factor is the sensor itself. And the last factor is the effect of calculating the circumference.

4.4.1 Soft tissue

The human body is made from hard tissues (bones) and soft tissues. The soft tissues is compressed and disturbed under pressure. However, the shape of the body that was obtained during the scanning process was free from pressure. Thus, when pressure is applied, the shape of body is changes. According to Yu *et al.* (2006), Young's modulus for human soft tissues on average is around 9.3 kPa. When pressure from the garment is applied, these tissues will contract. The greater the pressure, the more the tissues will compress, thus their surface becomes flatter and increasing their radius of curvature. According to Laplace's Law, pressure is inversely proportional to the radius of curvature. This phenomenon is one of the causes of the difference in pressure between the measured pressure using the fitted pressure garment on the actual leg and the predicted pressure at corresponding locations. For example, for subject 4, the experimental pressure at location 45^0 is just above 2000 Pa. However, the predicted pressure is at this point more than 3000 Pa.

An experiment was conducted to prove the effect of the changing body shape due to the soft tissue under pressure. A mannequin, instead of a human volunteer, was scanned and its leg is used to develop and fit a pressure garment. Since its body is made of hard material, the mannequin would not deform under the pressure from the pressure garment. Two pressure garment patterns were developed to exert 2666 Pa and 5000 Pa of pressure on the leg at an area between 20 cm to 30 cm height from the floor. The results are shown in Figure 4.23.

The results show that there is a better agreement between the pressure predicted by the model and the measured pressure. The results proved that the model more closely predict the pressure for a body part that does not change its shape or compress under the pressure garment pressure. However, all parts of body is covered by soft tissue at a varying degree; therefore the model predictions need to take this into account or the pressure garment patterns need to be adjusted to provide a better fit.

<table>
<tr><th>Pressure to be exerted(N)</th><th>Pressure distribution</th></tr>
<tr><td>2666</td><td>
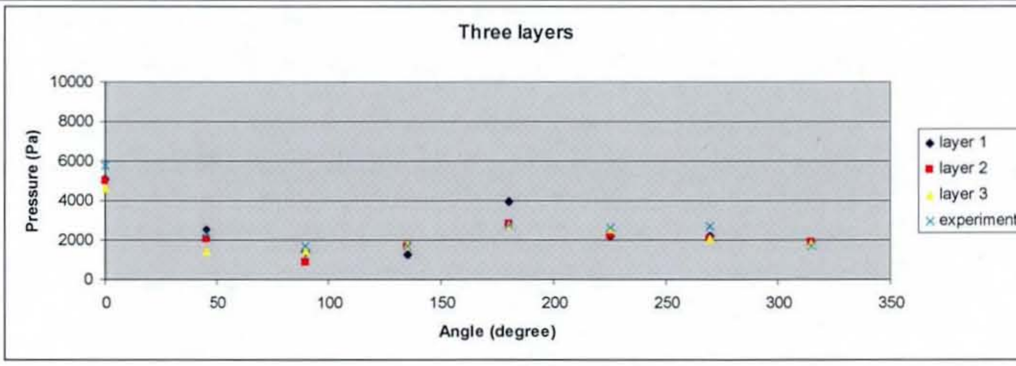

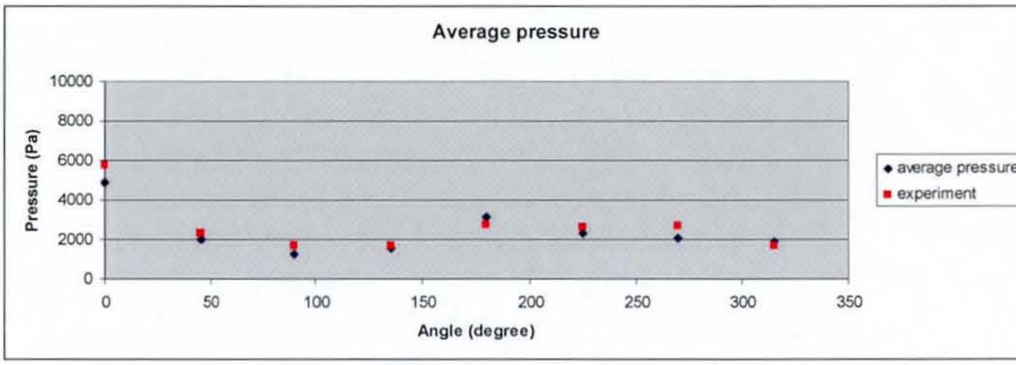

</td></tr>
<tr><td>5000</td><td>
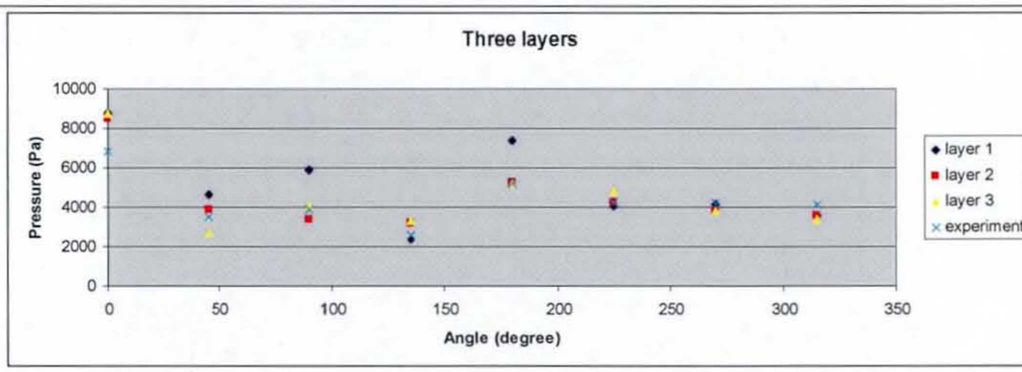

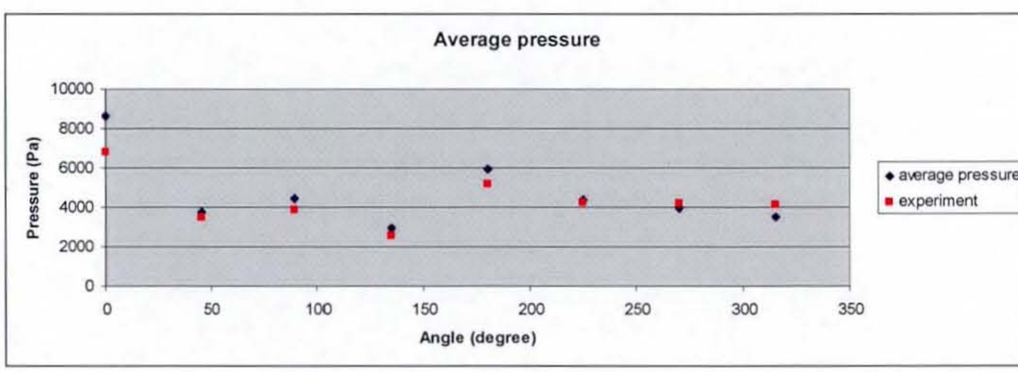

</td></tr>
</table>

Figure 4.23 Pressure distribution on mannequin's leg

4.4.2 Sensor location

It is difficult to position the sensor exactly at the right spot on the body due to reasons such as soft tissue deformation, migration of the sensor between the body part and the pressure garment and the inability to see the body part because of its being covered by the pressure garment.

For example, if the centre of the sensor is intended to be inserted at location 1 (Figure 4.20), there are possibilities that the centre of sensor is inserted at location 2, which covers only two points, Point 2 and Point 3 (Figure 4.24), at each layer. Even though the displacement of the location of sensor is small, it affects the result.

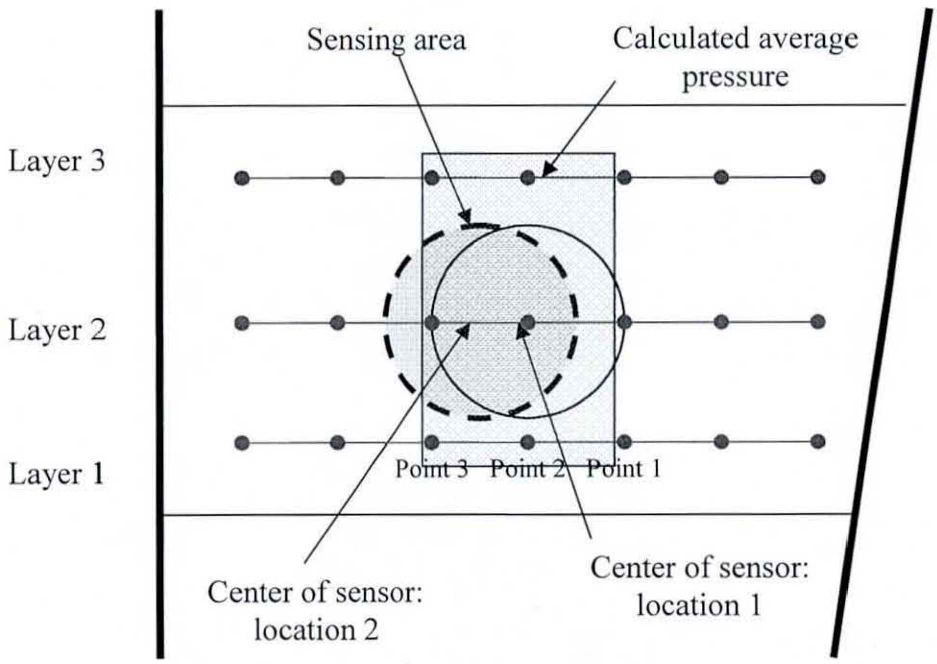

Figure 4.24 Location of the sensor

4.4.3 Pattern shape

The subject's pattern shape also has an influence in the pressure's differences. The fabric that was used in the research is the warp-knitted type. During the stress strain test to determine its modulus of elasticity, the specimens were cut with their length parallel to the wales of the fabric, which made it a rectangle shape (refer Figure 3.20).

However, when patterns were developed from the subject data, the shapes were not rectangle, instead their shapes are as shown in Figure 4.18. The differences in shape eventually will change the modulus of elasticity. To reduce the problem, before pattern was cut, paper patterns were adjusted on the fabric so the fabric pattern was mostly made from straight yarn. However, some of the subject's patterns are difficult to locate on the fabric, thus it will affect the modulus of elasticity of the fabric.

4.4.4 Sensor

The sensor also contributes to the differences in the measured pressure and the predicted pressure by the model, especially when the pressure is low. Ferguson-Bell et al. (2000) stated that the sensor is not suitable for measuring pressure less than 10 gram. Hence comparison of the predicted and measured pressures less than this value is not possible. Furthermore, there could be inaccuracies in the pressure measurements which contribute to the differences in pressures. The location of the pressure sensor has already been discussed which is also a contributing factor. The calibration lines, which are linear, should theoretically pass through zero pressure at zero loads but this is not the case (Figure 3.28 and Figure 3.29) due to the inaccuracy of the pressure sensor at low pressures. This also contributes to the difference in pressures.

4.4.5 Effect of circumferences calculation

The distance between two data points are calculated. These distances are always smaller than the arc between the two data points, hence the circumference calculated by this method is smaller than the actual circumference. When this is used to calculate the circumference of the pressure garment by using a reduction factor, this will inevitably be smaller. Hence the pressure predicted by a garment that has smaller circumferences at each layer than the ones corresponding to the actual design circumference will be higher. This is another reason for higher predicted pressure.

4.5 Conclusion of the chapter

This chapter has discussed a method to develop a pressure distribution model. The model is important because it enables therapists to evaluate the effectiveness of the designed pressure garment. It also enables the development of simulation of the pressure distribution.

The model has been developed using data from a 3D wounded area and pressure garment model. From the 3D wounded area data, the circumference and radius of curvature are calculated, and converted into a 3D pressure garment data, using the required reduction factor to achieve the desired pressure. By using both 3D wounded area and pressure garment data, the fabric's modulus of elasticity, the tension in the fabric is calculated. Then by using Laplace's Law, the pressure distribution at the wounded area is calculated.

Pressure garment are customized for a given body part, made using the above data and applied to the subjects. Then the pressure is measured to obtain experimental distribution. Then the predicted pressure results have been compared with the experimental results. They showed reasonable agreement. The differences between the two self of pressure distribution and their causes have been discussed.

For some subjects, the variations in pressure are small, but for some others, they are significant. The factors that are believed to be causing the differences are the nature of human soft tissue, the sensor, the location of the sensor, and the fabric pattern.

The pressure distribution model enables a manufacturer or therapist to predict the pressure that the garment applies on the body part without requiring an in-situ pressure measurement. This is a novel, powerful and useful tool. It can also identify the locations that have high or low pressure. For a high-pressure area, effort can be made to reduce the pressure by easing the fabric's tension. For a low-pressure area, especially at concave and flat areas, there is no convenient method of increasing the pressure. This can be achieved by applying padding to the area. There is no published research reporting the use of padding even though one paper has revealed that padding can help to reduce the formation of scar on a burn injury patient. Although padding is not normally used for pressure garments for burn injuries, but it is common for compression garments used for treating to venous leg ulcers. In the next chapter, a method to develop customized padding for the wounded area to even out the pressure is discussed.

Chapter 5 Development of the Pressure Garment Padding

The pressures exerted by a pressure garment at a flat or concave area are very low due to large radius of curvature or absence of contact between the garment and the body. This results in non-uniform pressure distribution on the body, which is not good for scar treatment. Padding can be inserted into such areas, to even out the radius of curvature causing a more even pressure distribution. The size and shape of the padding must be carefully determined. This would require modelling the mechanics of the forces applied in conjunction with the pressure distribution model.

The mechanics of pressure delivery to the body by the padding is shown in Figure 5.1. The tension in the pressure garment will press the padding, and the padding will exert a force to wounded area. The force applied by the garment on the padding and by the padding on the body part will be distributed as shown in Figure 5.1.

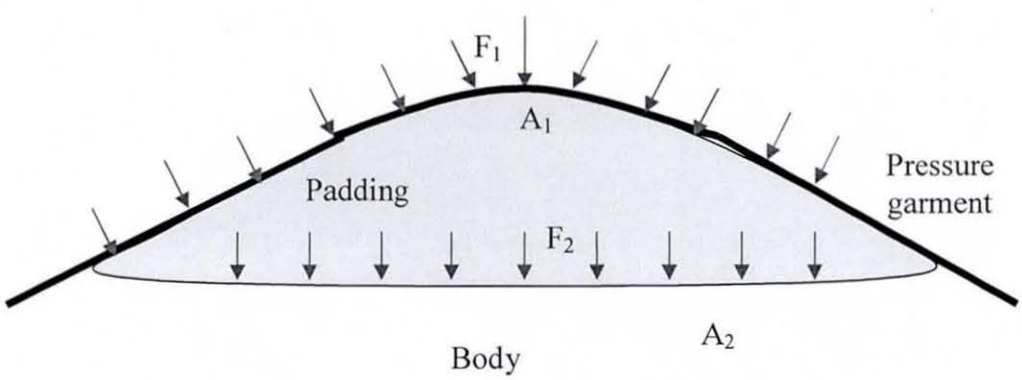

Figure 5.1 **The mechanics of pressure delivery by the padding**

If the resultant force exerted by the pressure garment to the padding due to the tension in the garment is F_1, and the resultant force from exerted to the wounded area by the padding is F_2

$$\sum F_1 = \sum F_2$$

Since F=PA, then the equation can be rewrite as;

$$P_1 A_1 = P_2 A_2$$

where the pressure from the pressure garment to the padding is P_1 and the contact area of pressure garment and the padding is A_1 while P_2 is the pressure from padding to the wounded area and A_2 is the contact area between padding and wounded area. Area, A, is equal to length, l, times width, h, thus the equation becomes;

$$P_1 l_1 h_1 = P_2 l_2 h_2$$

where l_1 is contact length between pressure garment and padding, while l_2 is contact length between padding and wounded body. h_1 and h_2 are the width of the pressure garment and padding respectively. Since h_1 is equal to h_2, then

$$P_1 l_1 = P_2 l_2$$

$$P_2 = P_1 \frac{l_1}{l_2}$$

P_1 can be calculated using Laplace's Law used in the development of the pressure distribution model.

There are four main stages for constructing the padding. The first stage is to determine the location where the padding is needed. The second stage is to develop the padding model. The third stage is to construct the padding pattern for the experiment. The last stage is to generate a pattern for the padding.

5.1 Determining the area for padding

As shown in Section 3.6.3, specific pressure can be easily delivered if the shape of the area is a cylinder, since it has a similar radius of curvature at each level. However, the human body is not naturally cylindrical in shape, thus the pressure it receives varies depending on the radius of curvature of the point. By manipulating this phenomenon, the padding that will be developed must make the shape of the wounded area appear cylindrical.

In order to do that, a circle was developed to surround the body area. Points of the circle must overlap the points on the body or be in their close vicinity. The radius and centre of the circle can be calculated by either of two methods: using the centroid or by finding the middle point of the longest chord.

5.1.1 Radius and centre of the circle calculation

The method used in determining the radius and centre of the circle, is the longest chord method. A chord can be drawn between any two of the n points on the circumference of the scanned body cross section, and the longest chord can be determined. The longest chord is taken as the diameter of the circle and the centre of the chord is taken as the centre of the circle (Figure 5.2).

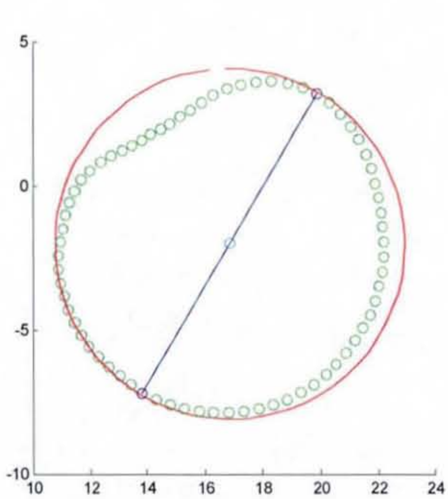

Figure 5.2 **The developed circle (red line) using middle point of longest Chord (blue line) as the centre**

If $(d_{ij})_l$ is the distance between points i and j of layer 1, and there are n-points in a layer, then all the distances in layer 1 can be represented as A_l, where A_l is:

$$A_1 = \begin{bmatrix} (d_{11})_1 & (d_{12})_1 & . & .(d_{1n})_1 \\ (d_{21})_1 & (d_{22})_1 & . & .(d_{2n})_1 \\ . & . & . & . \quad . \\ (d_{n1})_1 & (d_{n2})_1 & . & .(d_{nn})_1 \end{bmatrix}$$

A computer program was developed to determine the maximum distance in a given layer. This process is repeated for each layer to determine the longest chord and its middle point.

The maximum distance will become the diameter while its middle point is the centre of the circle (Figure 5.2).

5.1.2 Determine the padding area

After both the centre and the radius of the circle have been determined, the next step is to obtain the circle coordinate at same radial position; i.e. angle (α), as the body point. If the centre of the circle is located at (x_0, y_0) at a given layer, then, based on Figure 5.3, the location of the circle (x_c, y_c) is:

$$\begin{aligned} x_c &= x_0 + r_{\max} * \cos(\alpha); \\ y_c &= y_0 + r_{\max} * \sin(\alpha); \\ \alpha &= \tan^{-1}\left(\frac{y_b - y_0}{x_b - x_0}\right); \end{aligned}$$

where x_b and y_b is coordinate of the body point and r_{max} is the maximum radius.

Figure 5.4 shows the cross section of body and circle for each subject.

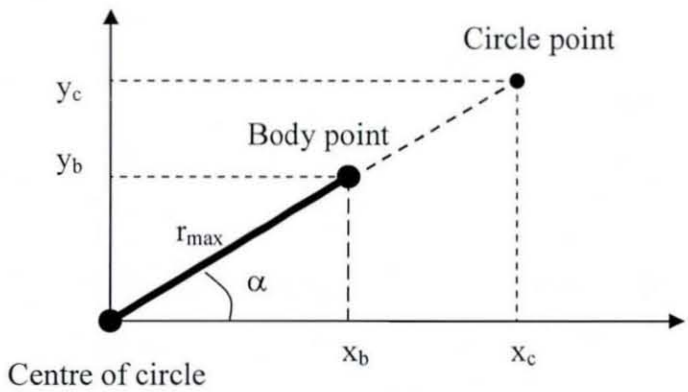

Figure 5.3 Calculate coordinate of the circle

Subject		Subject	
1	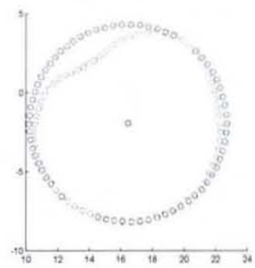	6	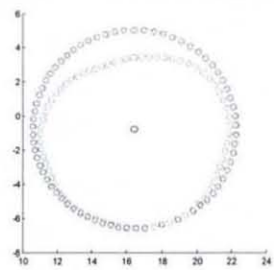
2	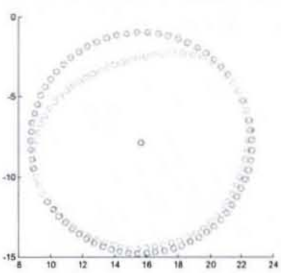	7	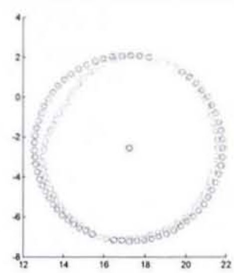
3	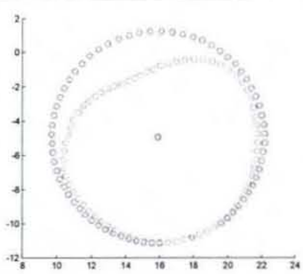	8	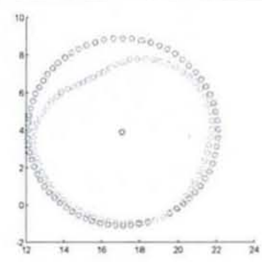

4	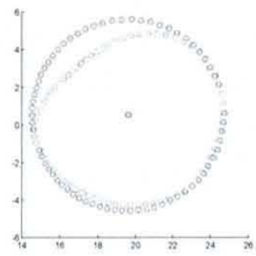	9	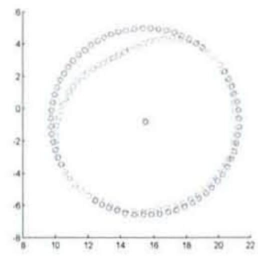
5	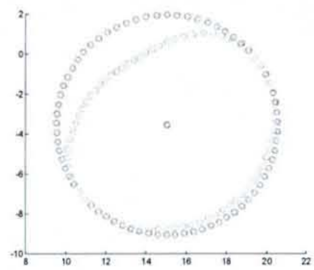	10	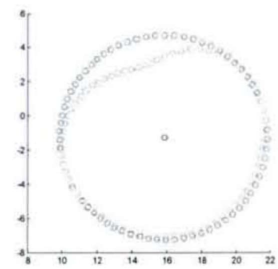

Figure 5.4 Cross section of body and circle for each subject

After all the circle coordinates were obtained, the distance differences (δ) between the body and the circle points of each layer are calculated and averaged (δ_{ave}). If r_{ci} is distance between center of the circle to circle point i, and r_{bi} is distance between center of the circle to body point i, the distance difference and its average can be represent by the following formula;

$$\delta_i = | r_{ci} - r_{bi} |$$

$$\delta_{ave} = \frac{\sum_{i=1}^{n} \delta_i}{n}$$

Any points on that layer that have δ greater than δ_{ave} can be considered as padding points. Figure 5.5 shows a cross section of the shape of padding for each subject. A comparison with the simulated pressure distributed at the corresponding points confirmed that this area needs padding. Figure 5.6 shows the 3D pressure distribution model at the location where the padding is required. Low-pressure areas, represented in blue, are the locations where the padding is needed.

Sub ject		Sub ject	
1	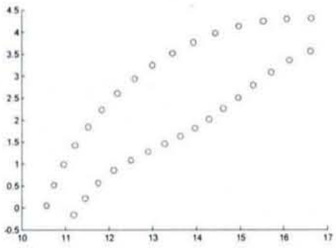	6	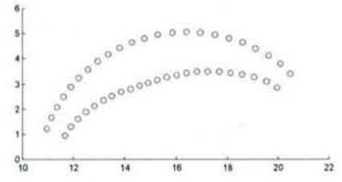
2	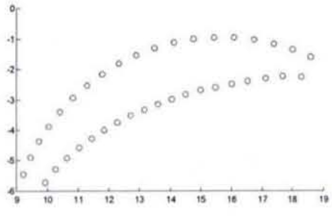	7	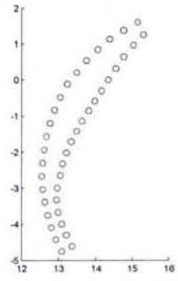
3	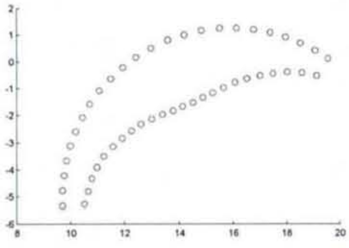	8	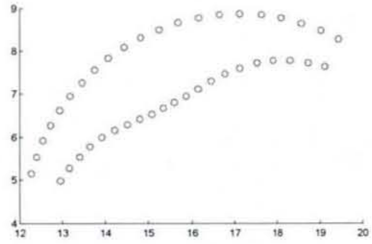
4	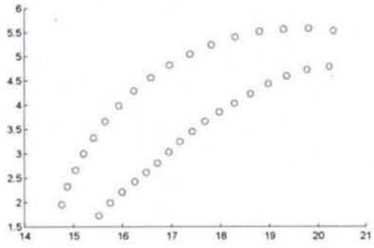	9	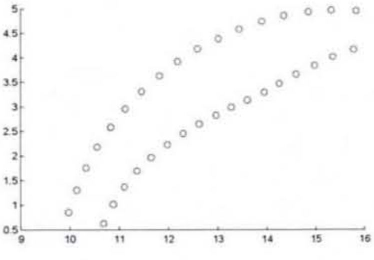
5	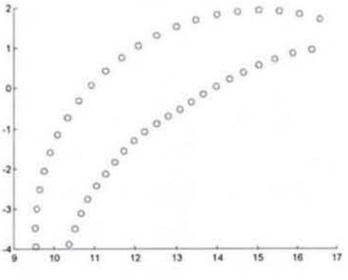	10	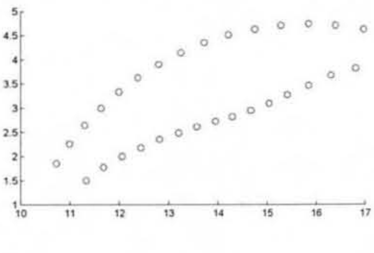

Figure 5.5 The padding cross section for each subject

Sub ject		Sub ject	
1	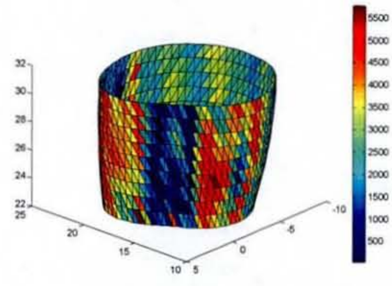	6	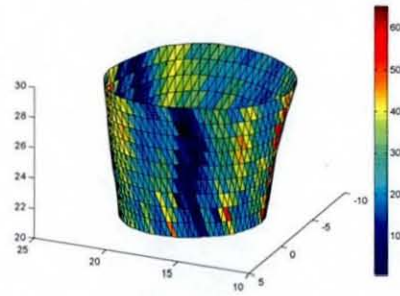
2	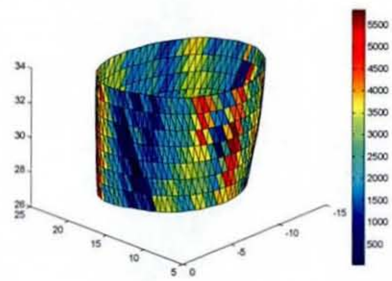	7	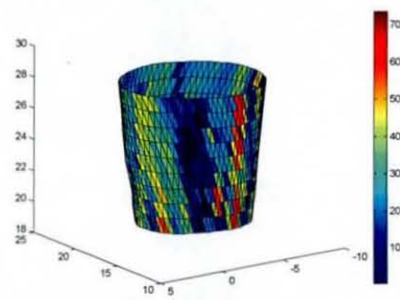
3	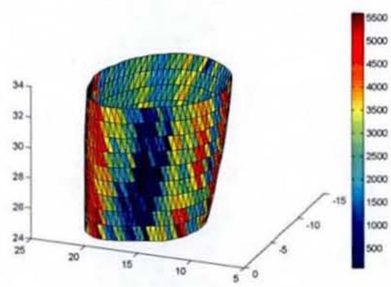	8	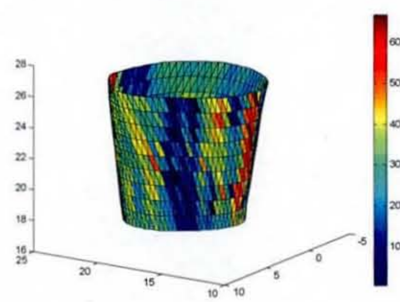
4	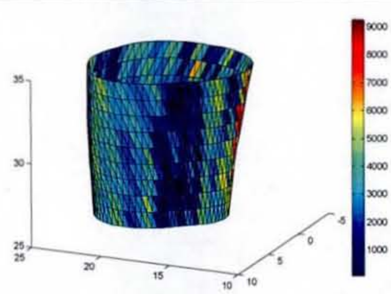	9	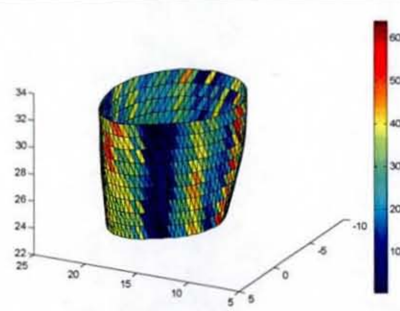
5	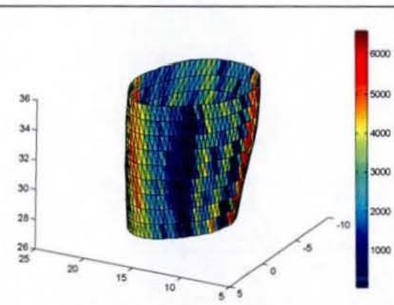	10	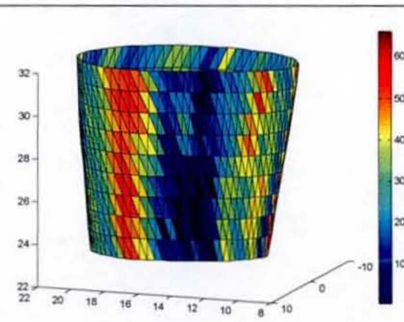

Figure 5.6 Low-pressure area in the 3D pressure distribution model (Pressure units is in Pascal)

5.2 Creating the padding model

The data from both the circle and the body still need to be modified to create the shape of the padding for the area of low level pressure that has been determined.

Problem that needed to be solved is the number of data points for each layer. As the number of data points is different at each layer, effort was made to make them the same because the computer program developed by this research can only create the triangulation using the same number of data points in each layer. As shown in Figure 5.7, the number of data points at each layer is different between each other. To overcome the problem, the number of points in each layer of padding was counted and the minimum number of points, n_{min}, selected.

Then, middle point for each layer of padding was determined. Any points located within $\pm n_{min}/2$ from the middle point are considered to be part of the padding. Points that are located beyond that range are excluded. The result was shown in Figure 5.8.

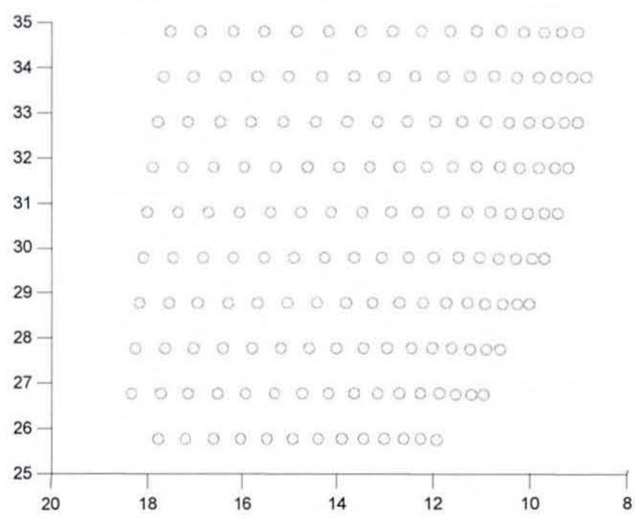

Figure 5.7 Number of data at each layer before exclusion

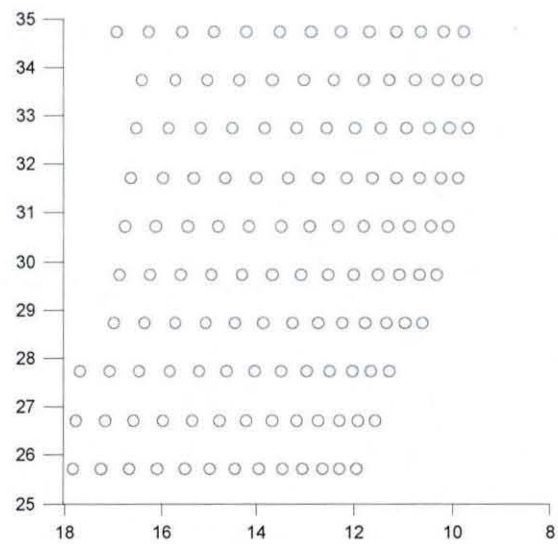

Figure 5.8 Number of data at each layer after exclusion

5.3 Pattern development for padding

In order to construct the padding, the padding model is divided into two parts, outer and inner surfaces. The body data becomes the inner surface, while the circle points represent the outer surface (refer Figure 5.9). By using the flattening method discussed in the previous chapter, both parts have been transformed into a 2D flattened design (refer Figure 5.10). Both patterns were cut and combined together to create the padding. The method of constructing the padding is explained in detail in the next section.

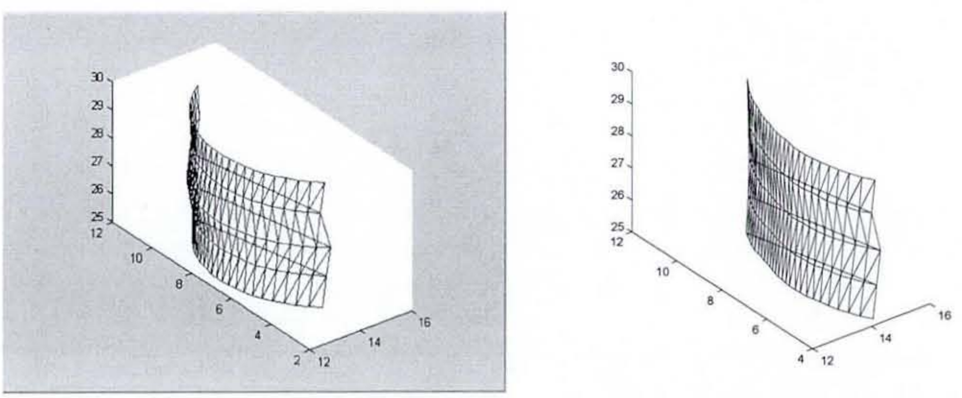

(a) (b)

Figure 5.9 3D model of (a) outer and (b) inner parts of the padding

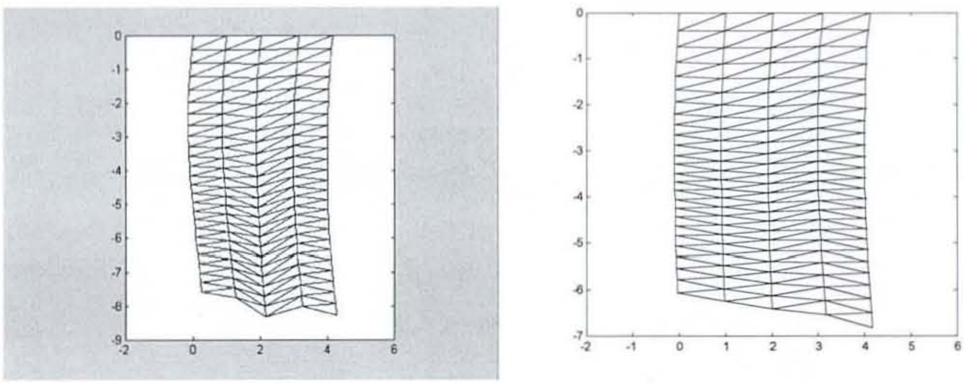

(a) **(b)**

Figure 5.10 Pattern for the padding's (a) outer and (b) inner parts

5.4 Experimental methodology for padding creation

This experiment was conducted to verify the model used to develop the padding. The flowchart of the process is shown in Figure 5.11.

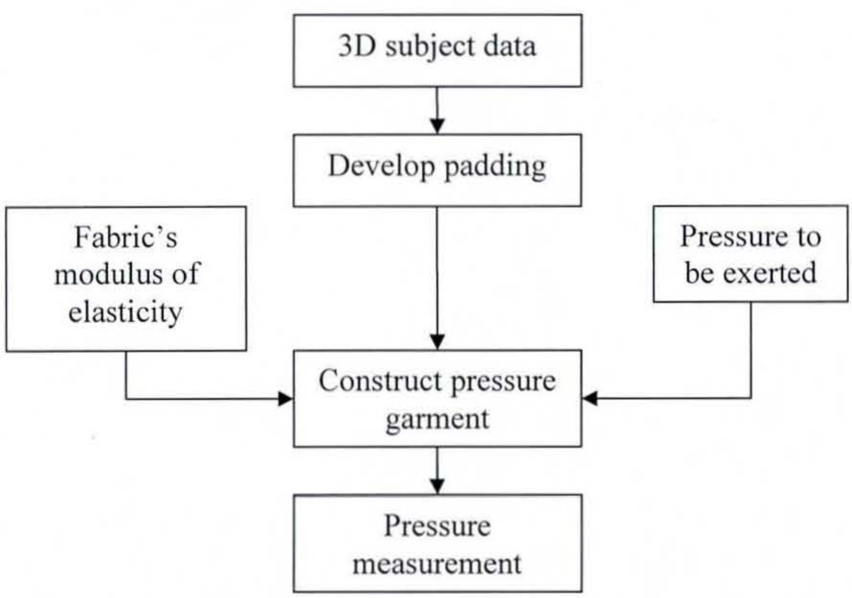

Figure 5.11 Flowchart for the methodology to validate the padding development

5.4.1 Scanning

The same 10 subjects used in the pressure garment development, reported in Chapter 4, have been used in this experiment.

5.4.2 Fabric's modulus of elasticity

Pressure garment fabrics used are the same as before, reported in Section 3.5.2.

5.4.3 Padding construction

First, the 2D patterns developed for the padding have been cut out from hard paper for the outer surface (part that will make contact with pressure garment fabric), and a soft paper for the inner surface (part that will make contact with human body). Both parts are attached together using sticky tape to create the padding profile. To make the padding to keep its shape and represent soft tissue when the pressure was applied, the volume enclosed by the padding was filled with plain flour which helps to uniformly distribute the pressure. The top and bottom of the padding has been covered to prevent the flour from seeping out. Figure 5.12 shows the complete padding. Flour is not intended to be used in the treatment of burn injuries.

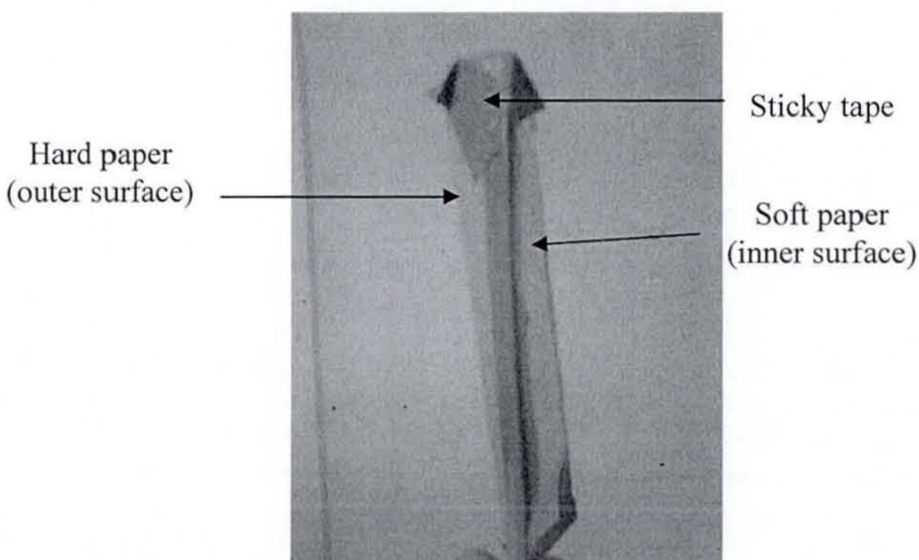

Figure 5.12 Complete padding

5.4.4 Measurement of the padding's volume

A programming system has been developed to calculate the volume of the padding. The process consisted of calculating the area of each layer, and multiplying it by its height, to obtain its volume. By adding each layer's volume, the total volume of the padding is determined.

As shown in Figure 5.13, the padding was constructed using two parts, an outer surface (green) and an inner surface (red).

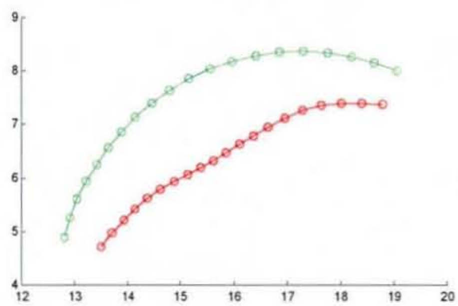

Figure 5.13 Outer surface and inner surface of the padding

If I and O are the data sets for the inner and outer surfaces of the padding, then

$$I = [xb_{i,j} \quad yb_{i,j} \quad zb_{i,j}]$$

$$O = [xc_{i,j} \quad yc_{i,j} \quad zc_{i,j}].$$

where i indicates the layer's number and j shows the point's position in the layer.

The centre of the layer's circle (*xpm, ypm*), as explained previously in Section 5.1.1, is added at the end of each layer of the padding for each part. So, if there are two layers for an area, the set I (refer to Figure 5.14) is changed to:

$$I = \begin{bmatrix} xb_{1,1} & yb_{1,1} & zb_{1,1} \\ \vdots & \vdots & \vdots \\ xpm_1 & ypm_1 & zpm_1 \\ xb_{2,1} & yb_{2,1} & zb_{2,1} \\ \vdots & \vdots & \vdots \\ xpm_2 & ypm_2 & zpm_2 \end{bmatrix}$$

and set O (refer Figure 5.15),

$$O = \begin{bmatrix} xc_{1,1} & yc_{1,1} & zc_{1,1} \\ \vdots & \vdots & \vdots \\ xpm_1 & ypm_1 & zpm_1 \\ xc_{2,1} & yc_{2,1} & zc_{2,1} \\ \vdots & \vdots & \vdots \\ xpm_2 & ypm_2 & zpm_2 \end{bmatrix}$$

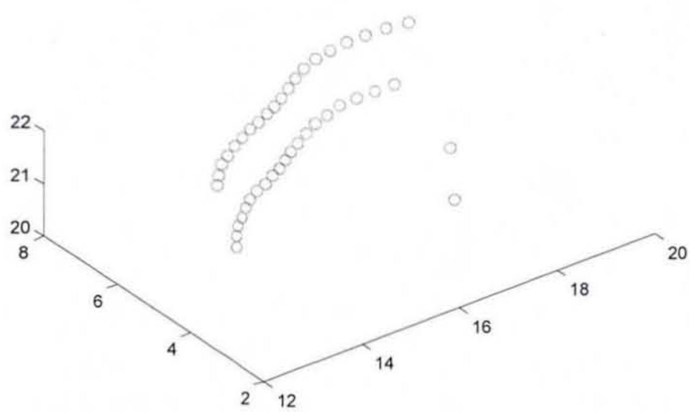

Figure 5.14 Data for the inner surface of the padding

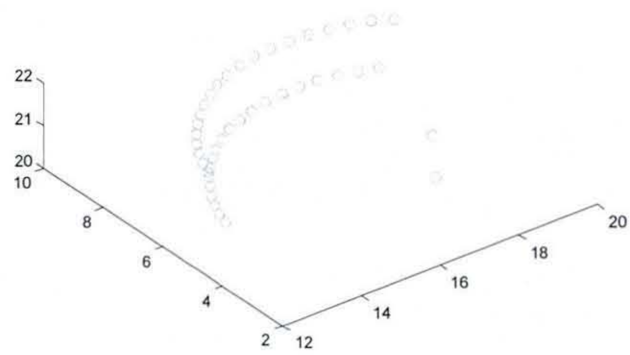

Figure 5.15 **Data for the outer surface of the padding**

First, each layer's area, both from the profile of the outer and inner surfaces of the padding, is calculated using their coordinates, starting from the bottom layer. For example, for the inner surface of the padding, the area of its first layer can be determined by using the following formula:

$$Area_l = \frac{1}{2}\left(\begin{vmatrix} xb_{1,1} & xb_{1,2} \\ yb_{1,1} & yb_{1,2} \end{vmatrix} + \begin{vmatrix} xb_{1,2} & xb_{1,3} \\ yb_{1,2} & yb_{1,3} \end{vmatrix} + \ldots + \begin{vmatrix} xb_{1,n} & xpm_1 \\ yb_{1,n} & ypm_1 \end{vmatrix} + \begin{vmatrix} xpm_1 & xb_{1,1} \\ ypm_1 & yb_{1,1} \end{vmatrix}\right),$$

The area is then multiplied by its height (obtained by calculating the difference between the z-coordinate of the layer and that of the next layer) to obtain its volume. The process continued with the next layer until all the volumes of each layer is calculated. By adding the volume of each layer, the total volume is determined. The next step is to subtract the inner volume from the outer volume to obtain the total volume for the padding.

5.4.5 Construction of the pressure garment for padding the body

The size and shape of the pressure garment to be used in conjunction with the padding is now different than the pressure garment used for the same body part without the padding due to increased size. For the new pressure garment, the circles that envelope the body cross sectioned shape and the padding is used for each layer.

This closely represents the circumference of the body shape plus the padding. Pressure to be exerted on the padding is 2666 Pa, and similar fabric with previous research is used to develop the garment.

The method used to transform the 3D model into the pattern is the same as the one explained previously in Section 3.4.

5.4.6 Sensor calibration

The same sensor calibration method to the method described in Section 3.5.4 is used to calibrate the sensor.

The experiment was conducted over two days, so there are two sensor calibrations. Figure 5.16 shows the results for the sensor calibrations.

5.4.7 Measurement of the padding's pressure

First, the pressure garments for the body that have been developed earlier without the padding, as shown in Figure 4.18, has been used. Pressure has been measured at a location where the padding was supposed to be inserted. Then, the pressure garment has been replaced with the newly developed pressure garment for the body and the padding. The padding was located in place. A sensor was inserted at the previously measured location between the padding and the body and its pressure was measured. The result was then compared with the previous result when no padding was used.

Day	Sensor calibration
1	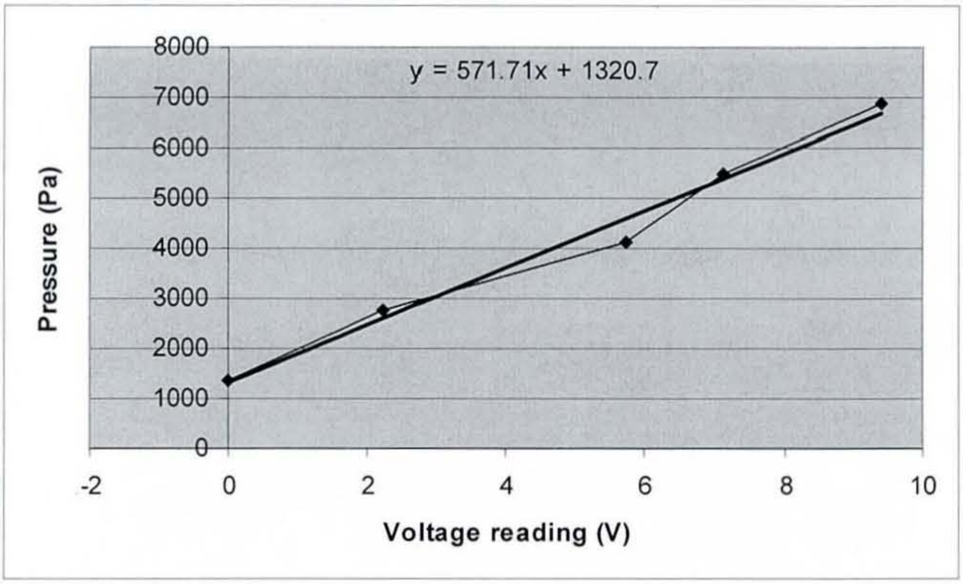
2	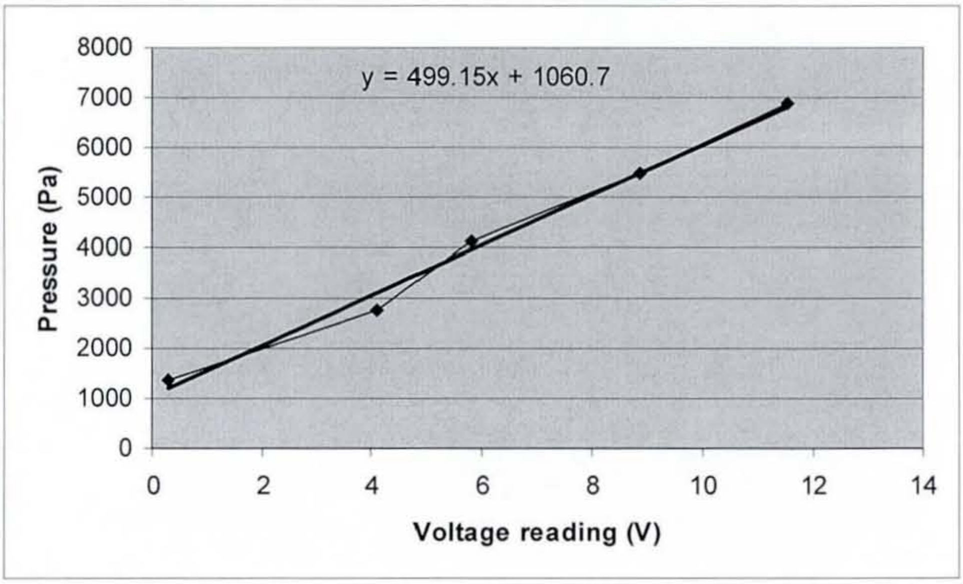

Figure 5.16 Sensor calibrations for the experiment

5.5 Results of the experiment

The experiment conducted to verify the padding developed using the padding model.

Two days were allocated for pressure measurement under the padding. On the first day, six subjects were measured while on the second day four people were measured. The results of the third experiment are presented in Figure 5.17.

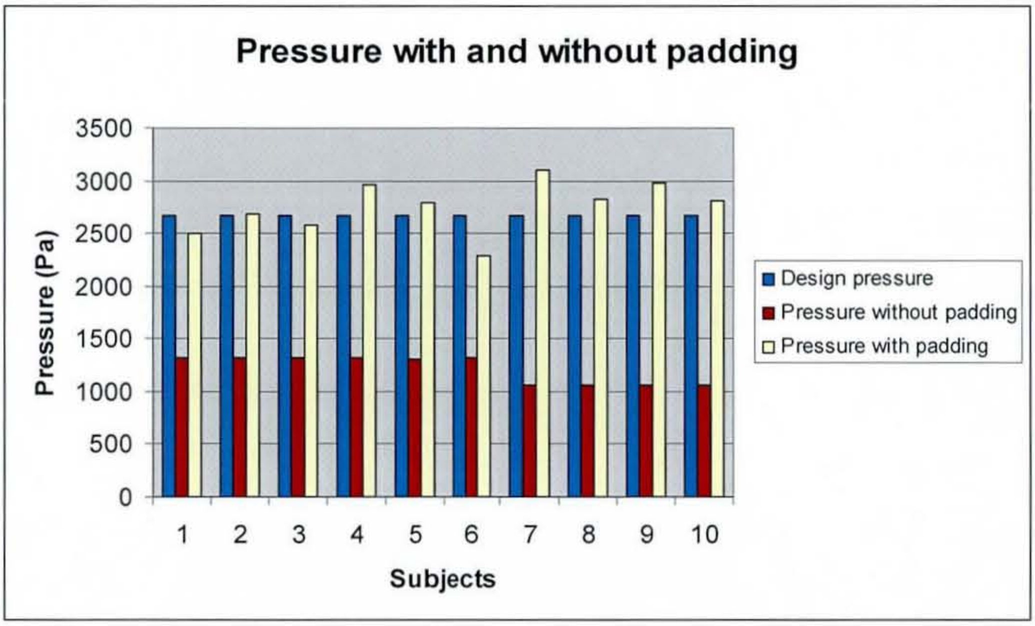

Figure 5.17 Results of pressure measurement

As shown in Figure 5.17, the developed pressure garment and the padding have successfully exerted the required additional pressure to the area with low level of pressure. Figure 5.17 shows pressure that it exerts is quite close to the intended pressure.

5.6 Discussion

The objective of developing padding is to increase the pressure at an area that would not experience the required pressure without the padding due to flatness and/or a concave surface. First, a process has been developed to identify the locations with low pressure on the wounded area. Then, a model has been developed to construct the padding and a pressure garment has been developed to be used in conjunction with the padding to apply a specific pressure to the area.

The developed procedure has been successful in determining the locations that have low garment/body pressures as shown in Figure 5.6 and Table 5.1 (second column). Figure 5.4 shows that the locations identified for padding have been either at concave areas (subjects 1, 3, 8 and 10) or flat areas (subjects 2, 4, 5, 6, 7 and 9).

The padding developed, when used in conjunction with the specifically generated pressure garment, can exert the specific design pressure on the location. As shown in Figure 5.17, the pressure that the padding and pressure garment applied together is close to the intended pressure.

However, there is an issue that the research has faced in developing the padding. This concerns a body with dual padding.

There are certain cases where body injuries need two padding pieces. Figure 5.18 shows an example of this type of case. If the method mentioned above is used to develop the padding, then two padding pieces will need to be created. In this case, a different approach is needed, first to separate both padding pieces and second to develop them separately.

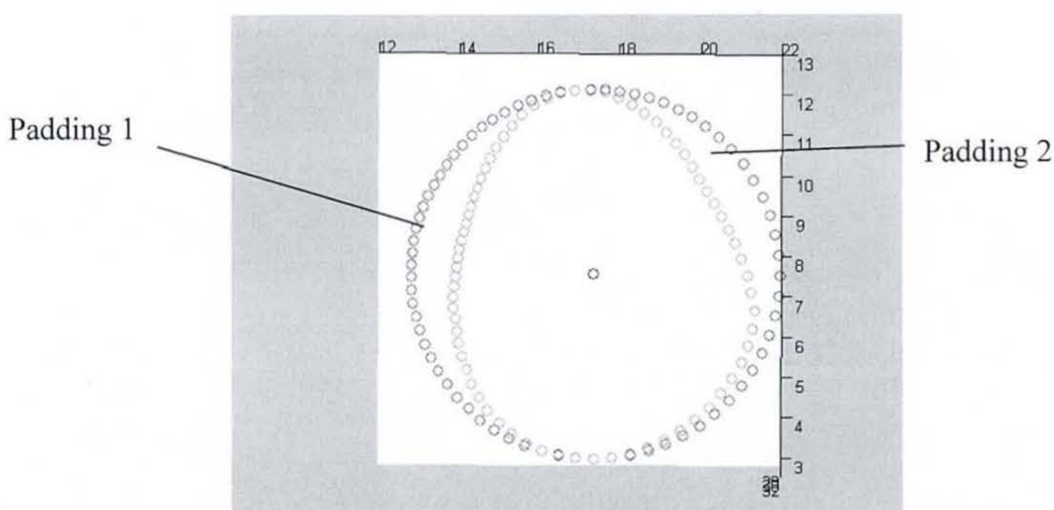

Figure 5.18 Area with two paddings

To separate the two padding pieces, the distance between two neighbouring points, d_i, in the same layer is calculated where;

$$d_i = \sqrt{(x_i - x_{i-1})^2 + (y_i - y_{i-1})^2}$$

After that, the average of these distances, d_{ave}, was determined using following formula;

$$d_{ave} = \frac{\sum_{i=1}^{n} d_i}{n}$$

The average distance was compared with the distance of each point from the points before and after. For example, for point n, the distances calculated were the distance between the point n-1 and point n (d_{n-1}), and distance between point n and point n+1 (d_n). If either one of these distances is bigger than the average of distance, it will be assumed to be the edge of the padding at the layer (refer Figure 5.19).

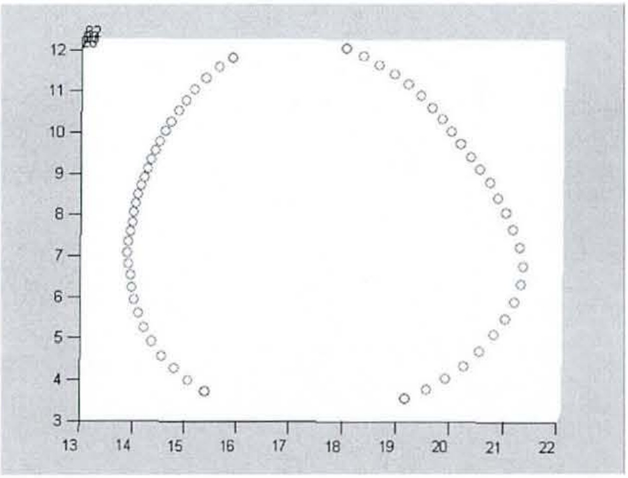

Figure 5.19 Edge points at each layer (represents by blue points)

When all the edges of the padding at each layer are known, they were used as guidance to separate the two padding pieces. If the area needs two padding pieces, there will be four edge points at each layer; two for padding 1 and another two for padding 2 (refer Figure 5.19). By using either points 1 and 3 or points 2 and 4, a straight line with the equation of y=mx+c was constructed. For example, as shown in Figure 5.20, point 2 and point 4 are used to separate the two paddings. A straight line was drawn from point 2 to point 4 and this line divided the padding into two.

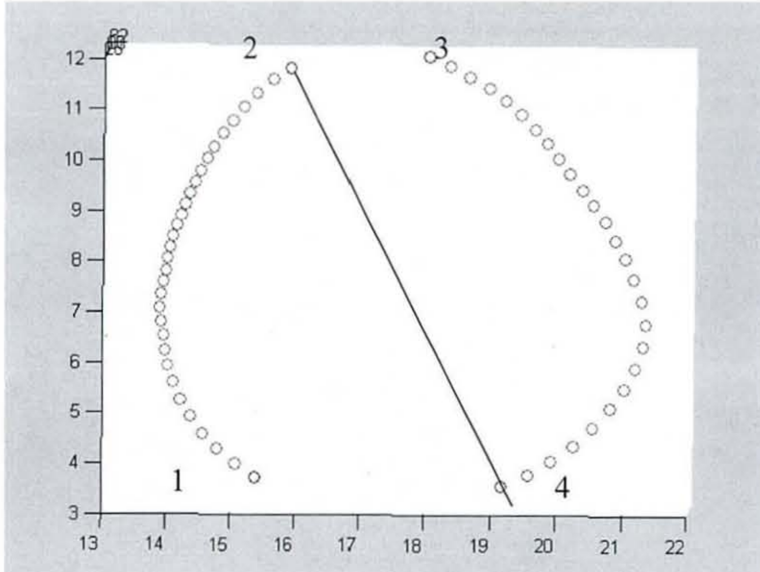

Figure 5.20 **Straight lines across edge points 2 and 4**

y value of the linear equation (y_{le}) was calculated by substituting x of the linear equation with coordinate x from the padding's points (x_{pad}).

$$y_{le} = mx_{pad} + c$$

If the value of y_{le} is smaller than value of coordinate y from the padding's points (y_{pad}), then the padding's points belong to Padding 1. However if y_{pad} is greater than y_{le}, then the points belongs to Padding 2. The process is repeated to the next layer until all of the points were separated into two entities (refer Figures 5.21 and 5.22). After that, the next step is to construct the 3D padding model for each of them. The method used was detailed in Section 5.2.

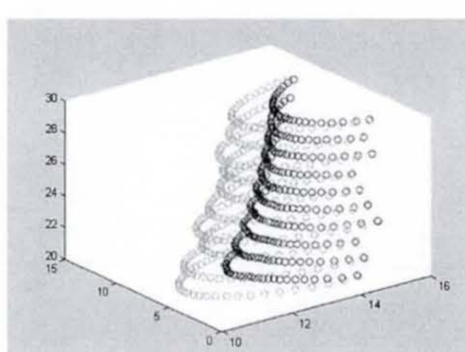

Figure 5.21 **Padding 1**

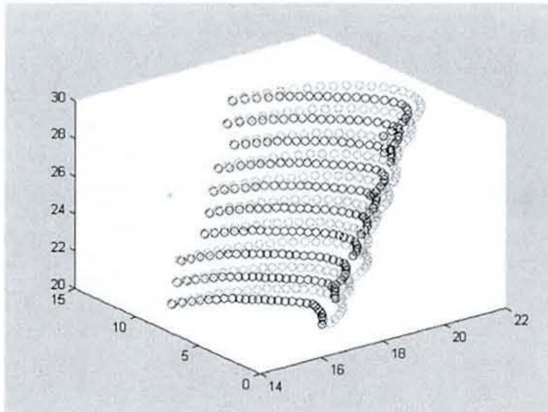

Figure 5.22 **Padding 2**

5.7 Summary

This chapter has discussed the method proposed to develop padding for low pressure areas. Padding is important in pressure treatment of a burn injury because it can increase the pressure at an area where the pressure garment is incapable of applying pressure because of a flat or concave surface under the section of the garment. This research has been conducted to create padding with the correct shape to exert a specific pressure on the target area.

This research has developed a method to determine the low pressure location, by using a circle that envelopes the body. Since the body itself is almost circular in shape, then the area which is not being covered closely by the circle can be assumed to be a low-pressure area requiring padding.

In developing the padding model, data from the body and the circle represent the inner and outer parts of the padding. The parts are flattened to produce a 2D pattern. The patterns are then combined together to generate the padding.

In order to develop the pressure garment for the padding and body, data for the enveloping circle are used. The data is triangulated to form the 3D pressure garment and transformed into the 2D pattern design.

To verify the computer program, a set of experiments has been conducted. Pressure has been measured from the volunteer subjects of the previous experiment, both with and without padding. Results show that the padding can deliver a pressure close to that specified at the outset. However, the developed padding for this experiment was only intended to show the effect of using padding with pressure garment on low-pressure area. In real life, it is suggested that different material to be used because the use of the developed padding on real burns injuries will reduce breathability of the wounded area. Furthermore, it also will cause discomfort for patients since the padding will limit their mobility due to their weight. Breathability and comfort is also crucial for wound treatment.

Chapter 6 Discussion

In this research, a system that can design pressure garments for the treatment of burn injuries has been developed. The process includes the following;

- Use of a 3D digital image of human body
- Development of a 3D pressure garment model
- Development of a pressure garment pattern
- Construction of the pressure garment and testing
- Development of a pressure distribution prediction model
- Development of a padding model, and finally
- Construction of the pressure garment with padding and testing

First, the burn injury person was scanned to obtain their 3D body data using a body scanner. Then, the injured area on the body has been selected. A pressure garment model and its 2D pattern have been generated for the area based on the body data. The garment has been constructed and tested using human volunteers. A pressure distribution model has been developed and verified to estimate the pressure that the garment applies. A padding model for low pressure area on the body and its pressure garment pattern has also been developed and tested using volunteers.

The novelties of the research:

- Use of digital scanned body data

  The first novelty is using a body scanner to develop the pressure garment. The idea of using a body scanner to develop the pressure garment is not a new idea. It has been proposed by Dias *et al.* (2002). However, their work is more focused on developing a pressure garment by using a 3D sewing technique. This research has explored the possibility of generating a pressure garment pattern using the body scanner.

- 3D model of the pressure garment using body data and its 2D pattern and method to generate them

The second novelty is that this research has generated a pressure garment pattern design by directly flattening the 3D pressure garment model. The 3D model was developed based on 3D body data obtained through the body scanner. This flattening method is essential to ensure that the constructed pressure garment can be perfectly wrapped around the wounded area. The current practise used body measurement to predict the shape of the pressure garment pattern.

- Pressure garment model to simulate the pressure distribution

  This research has developed a pressure prediction model by using a new technique to calculate the radius. In the model, the radius of curvature is calculated by using data points from the 3D body model. This method will enable researchers to predict pressure not only on a cylinder, but also on more complex shapes. The radius of curvature calculated using this method can give more accurate results. Currently, some other researchers also used Laplace Law to predict the pressure exerted by the garment on the body, but they treated the human body as a circular shape in estimating the pressure. By making this assumption, they calculated the radius of the circle by using the measured circumferences of the human body. However, the Laplace Law states that the radius of curvature of a point is the radius of the osculating circle at that point and not the radius taken from the body's circumference.

- A method to develop pressure garment padding for low pressure areas.

  Since this research is a pioneer in padding design, methods proposed in this research to develop the padding is new knowledge. This method includes procedures to locate the area with low pressure and to design the padding's patterns and a method of padding creation.

6.1 The 3D pressure garment model and 2D pattern development

The current pressure garment design process still uses conventional methods which use manual body measurement to make the pressure garment. The only current commercial advancement in this area is the introduction of a system to develop the pressure garment pattern based on input of body measurement.

To overcome the above problems, this research proposes the use of a body scanner to create the pressure garment pattern. The objective of this research is to design the pressure garment pattern using the 3D body data obtained through the scanner. This research has succeeded in generating the pattern. First, a 3D pressure garment model was developed based on a reduction factor calculated at each of the body layers. The reduction factor was calculated using a formula developed by Ng and Hui (2001). The formula indicates that the reduction factor is affected by pressure to be exerted, fabric properties and body curvature. Then the 3D model was flattened into a 2D pattern. The pattern developed is suitable for pressure garment construction. The developed pattern was first shown to exert a specific design pressure when being applied to a cylindrical item. Then the method developed extended to pressure garment pattern development for wounded body parts and it was subsequently experimentally verified.

The proposed method has five advantages. The first advantage is that it has reduced time and effort for the body measurement process and increased the accuracy of the measurement. The current practise needs the customer to measure their body at certain locations as accurately as possible, and send the information to manufacturers. However, the body measurement processes were not only time consuming, but also a hard effort for the customer, especially for burn injury patients. Thus, the new method offers a new way to measure their body faster and without any direct contact to their wounded area. Furthermore, data obtained by the new method contain more detailed information about the body, such as body curvature, which is impossible to be provided by manual measurement. The information is important for the pressure garment pattern designing process and pressure prediction.

The second advantage is that the method will enable customer involvement at an early stage of the design because the developed pressure garment model can be visualized first before manufacturing (refer Figure 6.1). Patients can decide which colour of pressure garment they prefer and can view it beforehand whether it will suit their taste, increasing the customer choice and satisfaction. This eventually will increase customer satisfaction in using the product, and decrease the number of rejections.

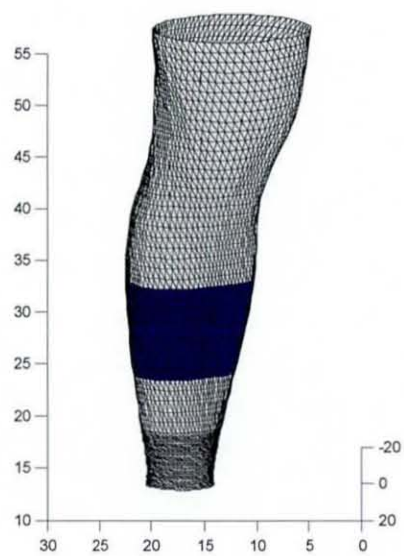

Figure 6.1 **3D body model with padding for customer view**

The third advantage is the developed pressure garment was constructed using a reduction factor that takes into consideration the body size at small vertical interval layer of 1 cm. The smaller interval means that the developed 3D pressure garment model closely resembles the body shape. Thus, the pressure garment can be designed to provide a better customised fit to the patient, and the garment can exert specific pressure to the wounded area. The current manufacturing process uses a standard reduction factor for all the people, regardless of their size.

The fourth advantage is that the pressure garment pattern can be generated directly by flattening the 3D pressure garment model. Currently, manufacturers use a system that develops patterns based on limited body measurement data. Even though the manufacturers claim that their pressure garment is customized, the way they estimate the shape of body cannot be considered as customized, because each body has its own characteristics. The method that has been developed in this research enables the manufacturer to develop a precise pattern to cater for different bodies. Instead of using a trial and error approach, the proposed method could help manufacturers to make pressure garments much more accurately, first time.

The final advantage is that the developed system is very flexible. By changing a design parameter, for example the pressure to be exerted of the fabric's modulus of elasticity, the shape of the pressure garment pattern can easily be recalculated . The flexibility can give the manufacturers the opportunity to adapt to their customer request more rapidly.

However, there are some limitations of this method. The first limitation is the developed pattern is not suitable to be used for the head and foot area. For these areas, a different flattening method must be employed. The reason is the developed pattern can exert pressure from the horizontal side of body only, and not from the vertical side. However, for the foot area, the pressure must be from vertical side as well to enable the healing process, thus the developed flattening method cannot be used. For the head area, the pattern is difficult to be generated here because the effect of some parts like ears, nose and eyes, is very difficult.

The other limitation is the developed pattern does not take variations in soft tissue stiffness into account. The tissue stiffness is very important because if it is low, then the tissue will contract under pressure, thus make the body became smaller in size under the pressure garment. This eventually will lead to adecrease in pressure exerted from the garment.

6.2 The development of pressure distribution model

Beside pressure garment pattern design process, another area which needs attention is the pressure measurement. Currently, most of researchers used direct measurement that usually involves the use of a sensor, to measure the pressure exerted by the pressure garment. However, the drawback of the direct measurement is it can only measure the pressure at a limited number of places. Moreover, for large injured surfaces, it is difficult for the sensor to access a remote area due to the limited length. The method of direct measurement on the human body is considered to be time-consuming and uneconomical. The main reason for the associated time and cost is that the pressure garment needs to be constructed first to enable direct pressure measurement. Furthermore, it is also intrusive for the patient causing discomfort.

This research has proposed a non contact pressure simulation method to predict the pressure distribution exerted by the pressure garment. The prediction model was calculated using the radius of curvature of the body and the material properties of the fabric. The results from the prediction model compared well to the experimental data. The pressure distribution model provides an alternative to the actual pressure measurements.

There are three advantages of the developed prediction model. The first advantage is the model enables a manufacturer to make early assessment of their pressure garment whether it can deliver the intended pressure. This reduces the cost and time because the problems are now identified before any manufacturing process. These abilities also reduce the number of defective pressure garments that are sent back by the customer due to fitting problems because the level of pressure can be assessed earlier.

The second advantage of using the prediction model is that a complete pressure map of the wounded area is given instead of several point pressures that are measured by a pressure sensor. The pressure at a difficult to access areas using direct measurement can be predicted by the model. This enables the manufacturers or therapists to gain better advice the customer and to alter the pattern design if necessary. The model also can be used by therapists to identify the locations with flat or concave area which will not receive adequate pressure and will need padding.

Another advantage of the developed method is that it will provide a non contact measurement to patients who naturally do not like their body being intruded. Patients may consider body pressure measurement as intrusion to their privacy. This method can give alternative pressure estimation to such people.

The limitation for the developed method in this research is that it does not take into consideration the influence of body contraction under the pressure garment. Thus, it will affect the prediction results because the prediction model uses the radius of curvature, which depends upon the measured shape of the body under no pressure, to predict the pressure. Since the shape of the scanned body is under no pressure, it will be different from the shape of body under pressure exerted by the pressure garment. The matter has been raised and discussed by Ng and Hui (2001) and used in developing their formula. They even included in their formulae a parameter called compression factor to overcome the issue. However in this research, the compression factor was not included since it is considered to be irrelevant because it was different from one location to another although still considered on the same layer. Furthermore, the compression factor will make the pressure garment smaller because a body under contraction will become smaller, thus will increase its tension and pressure.

6.3 The padding development

In a human body, there are certain areas/ parts that need extra pressure because the pressure level at the areas is lower than the design pressure exerted by the garment. According to the literature survey, there is no research related to padding development. However, there is evidence that the use of padding can help in preventing the formation of scar tissue due to burn injury. Hence this research has suggested a method to design and construct customised padding with the correct shape to exert a specific pressure on the target area.

This research has succeeded in developing a model that can locate areas with a low level of pressure and a procedure to design padding to provide extra pressure to the area. The constructed padding along with its pressure garment, have been shown to exert the intended specific pressure to the area (Chapter 5).

The advantage of the developed method is that it can model and construct padding for an area with low pressure. Currently, based on an internet survey on pressure garment manufacturers, no manufacturers offer the padding as one of their medical items for burn injury. Thus, this research on padding construction offers an extra advantage for pressure garment manufacturers to offer and an improved service to their clients.

However, the method used during this research to construct the padding is far from being perfect. There are some issues that need to be addressed, such as to develop a big padding, before the proposed method can be used for the whole body. Although padding developed in this research is able to deliver the intended pressure to an area that would without the padding experience a low level of pressure, its construction method is difficult and time consuming. This aspect would require further attention.

Chapter 7 Conclusions and suggestion for further work

7.1 Conclusions

This research has achieved the following objectives.

vi. Developed a 3D pressure garment design procedure using data obtained by a body scanner,

vii. Generated a pressure garment pattern from the 3D design obtained from the body scanner,

viii. Developed a model to simulate the pressure that is exerted by the pressure garment and verified it experimentally

ix. Developed padding modelling procedure for a low-pressure area and verified experimentally.

To achieve the stated objectives, this research has created an algorithm that used 3D body data, obtained by using a body scanner, along with the fabric properties to develop a 3D pressure garment model. Then the 3D garment model is flattened to generate a 2D pressure garment pattern design. Actual pressure garment has been constructed based on the pattern design, and tested on a cylindrical item to verify whether it can deliver the specific pressure that it was designed for. The research also develops a pressure distribution prediction model based on body curvature and fabric properties to simulate the pressure exerted by the pressure garment to the human body. Experiments have been conducted to verify the model on volunteers. The final task in this research was to develop a procedure to design and construct padding for areas with a low level of pressure. The pressure garment for the padding and body has been constructed and applied to volunteers to verify the padding.

The experimental results demonstrated that the pressure garment made following the garment design and pattern development process proposed can deliver the specific designed pressure to cylindrical items.

The pressure distribution prediction model was shown to be in reasonable agreement with the experimental results. The predicted pressure could be closer to the experimental result if the soft tissue compression of the human body can be taken into account. The tissue tends to contract under pressure, thus make the radius of curvature change from the 3D body. This leads to considerable local variations between predicted and experimental results. However, in general, the model can predict the pressure applied to the body part and be used as a tool to estimate the pressure of a custom-made pressure garment on the body part without necessitating physical measurements.

Finally the procedure to design and create padding for areas with low level of pressure has proven to successfully apply extra pressure to these areas. Experiments demonstrated that the developed pressure garment with padding can exert the specific designed pressure more uniformly to the affected body part.

The main novelties of this research, therefore are;

i) A method to develop 3D pressure garment model using 3D body data and its corresponding 2D pattern design.
ii) A pressure distribution prediction model using radius of curvature calculated using 3D body data and fabric properties to predict the applied pressure by the pressure garment.
iii) A method to locate low pressure area on the body in order to design and construct a customized padding for the identified low pressure area.

7.2 Suggestion for further work

There is significantly more research which needs to be carried out to enable the commercial development of the pressure garment designed using the methods defined in this research.

This research used 3D body scanner to obtain the data. However, the cost of the body scanner is high, thus it is impossible for each hospital to have it. The best solution may be to allocate the body scanner to big hospital only. But the solution will cost patients their time and effort to go to the hospital that may be far away. Thus, the first suggestion for future research is to develop a technology that can obtain accurate 3D body data from picture or video. The technology will enable patients to just provide their image, which can be send by email, to pressure garment manufacturer for body measurement. The manufacturer can extract 3D body data from the image using the technology for pressure garment development. Currently, the technology of obtaining 3D body data from image is available, but its accuracy is questionable.

The method to design pressure garments which is proposed in this research is applicable to the upper and lower limbs and torso only. Thus, the second suggestion for future study is to develop a new method to design the pressure garment pattern for all parts of human body including small areas like foot and hand, and areas with many curvatures, such as head. The research is important because patterns for these areas are very complex and difficult to develop. It is also important to note that method to design pressure garment pattern for head area is different from the rest of body. The reason is, the pattern at the area must have space for eyes, mouth and nose. These properties will influence the elasticity of the fabric. The accuracy of the developed pattern is also important to ensure that the pattern can fit patients comfortably. Thus, the developed method must be able to estimating the difference between the actual circumference and the calculated circumference so that the predicted pressure can be more accurately calculated.

The third suggestion for future study is to develop a method of predicting the effect of soft tissue on the pressure and pressure measurement. The research will involve study of the relationship between pressure and body contraction. The relationship varies from individual to individual and depends upon gender, lifestyle and age. There are a few studies done on this topic, but it is not comprehensive and subject matter not fully understood. This research is important not only to develop pressure garment, but also in order to develop a more accurate pressure prediction model.

The fourth suggestion is to study a method to develop a pattern that has several properties in it. The new pattern will enable the pressure garment to exert uniform pressure to the wounded area. The pattern can be constructed by using two methods.

The first method is by assembles different fabrics to make the pattern. The second method is by construct the pattern using a single fabric, but with different knitting process for each location depends on the pressure that it intends to exert.

This research has developed a model to predict pressure distribution under pressure garment. However, the model is capable to predict pressure at a static position. However, patients need to move around. Thus, for future research, it is suggested that a prediction model that can predict pressure distribution when a person is moving should be developed. The capabilities will enable a manufacturer to construct a more practical pressure garment that can cater for all conditions. The idea for the research is to prepare a model for a garment where the body is changing at every movement. Since the pressure predicted by this model depends on the shape of body, thus by measuring radius of curvature at each point of the body at every movement, the pressure distribution can be predicted.

Another area that needs further study is padding. Even though padding developed by this research is low cost to create, it is difficult to construct and time consuming. Also the shape and size of the padding for a given injured part requires further attention for a more accurate padding development.

Material for the padding is suggested to be silicon gel because it can keep it shape under pressure, has similar properties to the soft tissue and make contact with the wounded area which helps the healing process. Currently, the silicon gel is used in scar treatment and act as a padding. Method to construct the customized silicon gel padding is by using casting process. Padding constructed by this research can act as a mould. However, instead of flour used in the experiments reported here, a more suitable material which is breathable and provides comfort to the patient should be used, such as the nonwoven fabrics developed for this purpose (Anand, 2009).

References

ANAND, S. (2009) Private communication, Loughborough.

AZARIADIS, P. N. & ASPRAGATHOS, N. A. (1997) Design of plane developments of doubly curved surfaces. *Computer-Aided Design,* 29, 675-685.

AZARIADIS, P. N. & ASPRAGATHOS, N. A. (2001) Geodesic curvature preservation in surface flattening through constrained global optimization. *Computer-Aided Design,* 33, 581-591.

BAULAIN, U. (1997) Magnetic resonan imaging for the in vivo determination of body composition in animal science. *Computers and Electronics in Agriculture,* 17, 189-203.

BOMBARO, K. M., ENGRAV, L. H., CARROUGHER, G. J., WIECHMAN, S. A., FAUCHER, L., COSTA, B. A., HEIMBACH, D. M., RIVARA, F. P. & HONARI, S. (2003) What is the prevalence of hypertropic scarring following burns? *Burns,* 29, 299-302.

CHAN, A. P., FAN, J. & YU, W. M. (2005) Prediction of men's shirt pattern based on 3D body measurements. *International Journal of Clothing Science and Technology,* 17, 100-108.

CHIRICOTA, Y. (2003) Three-dimensional garment modelling using attribute mapping. *International Journal of Clothing Science and Technology,* 15, 346-358.

CHIRICOTA, Y., COCHAUX, O. & PROVOST, A. (2001) Geometrical modelling of garments. *International Journal of Clothing Science and Technology,* 13, 38-52.

CHO, Y., OKADA, N., PARK, H., TAKATERA, M., INUI, S. & SHIMIZU, Y. (2005) An interactive body model for individual pattern making. *International Journal of Clothing Science and Technology,* 17, 91-99.

CHO, Y. S., KOMATSU, T., TAKATERA, M. & PARK, H. (2006) Posture and depth adjustable 3D body model for individual pattern making. *International Journal of Clothing Science and Technology,* 18, 96-107.

CORDIER, F., SEO, H. & MAGNENAT-THALMANN, N. (2003) Made-to-measure technologies for an online clothing store. *IEEE Computer Graphics and Application,* 23, 38-48.

DAANEN, H. A. M. & VAN DE WATER, G. J. (1998) Whole body scanners. *Displays,* 19, 111-120.

DEASON, V. A. (1997) Anthropometry: the human dimension. *Optics and Lasers in Engineering,* 28, 83-88.

DIAS, T., COOKE, W., FERNANDO, A., JAYAWARNA, D. & CHAUDHURY, N. H. (2002) Pressure garment.

DURKIN, J. L., DOWLING, J. J. & ANDREWS, D. M. (2002) The measurement of body segment inertial parameters using dual energy X-ray absorptiometry. *Journal of Biomechanics,* 35, 1575-1580.

ECKERT, C. M. & BEZ, H. E. (2000) A garment design system using constrained Bezier curves. *International Journal of Clothing Science and Technology,* 12, 134-143.

FAN, J. & CHAN, A. P. (2005) Prediction of girdle's pressure on human body from the pressure measurement on a dummy. *International Journal of Clothing Science and Technology,* 17, 6-12.

FANG, J. J. (2003) 3D collar design creation. *International Journal of Clothing Science and Technology,* 15, 88-106.

FANG, J. J. & LIAO, C. K. (2005a) 3D apparel creation based on computer mannequin model - Part 1: system kernel and formulas. *International Journal of Clothing Science and Technology,* 17, 292-306.

FANG, J. J. & LIAO, C. K. (2005b) 3D apparel creation based on computer mannequin model: Part II: implementations. *International Journal of Clothing Science and Technology,* 17, 307-319.

FERGUSON-PELL, M., HASIGAWA, S. & BAIN, D. (2000) Evaluation of a sensor for low interface pressure applications. *Medical Engineering and Physics,* 22, 657-663.

FONOV, S., GOSS, L. P., JONES, E. G., CRAFTON, J., FONOV, V. & OL, M. (2005) New method for surface pressure measurements. *43rd AIAA Aerospace Science Meeting.*

FONOV, V., FONOV, S., JONES, S. & CRAFTON, J. (2004) Image prosessing technique for shear-stress optical measurement. *11th International Symposium on Flow Visualization.*

FONTANA, M., RIZZI, C. & CUGINI, U. (2005) 3D virtual apparel design for industrial applications. *Computer-Aided Design,* 37, 609-622.

GAIED, I., DRAPIER, S., & LUN, B. (2006) Experimental assessment and analytical 2D predictions of the stocking pressures induced on a model leg by Medical Compressive Stockings. *Journal of Biomechanics*, 39, 3017-3025.

GIELE, H. P., LIDDIARD, K., CURRIE, K. & WOOD, F. M. (1997) Direct measurement of cutaneous pressures generated by pressure garment. *Burns,* 23, 137-141.

HARDAKER, C. H. M. & FOZZARD, G. J. W. (1997) Towards the virtual garment: three-dimensional computer environments gor garment design. *International Journal of Clothing Science and Technology,* 10, 114-127.

HARRIES, C. A. & PEGG, S. P. (1989) Measuring pressure under burns pressure garments using the Oxford Pressure Monitor. *Burns,* 15, 187-189.

HILTON, A., BERESFORD, D., GENTILS, T., SMITH, R., SUN, W. & ILLINGWORTH, J. (2000) Whole-body modelling of people from multiview images to populate virtual worlds. *The Visual Computer,* 16, 411-436.

HINDS, B. K. & MCCARTNEY, J. (1990) Interactive garment design. *Visual Computer,* 6, 53-61.

HINDS, B. K., MCCARTNEY, J. & WOODS, G. (1991) Pattern development for 3D surfaces. *Computer-Aided Design,* 23, 583-592.

HOBDEN, J. (1998) If it can be seen it can be measured. *Aircraft Engineering and Aerospace Technology,* 70, 117-119.

HUI, C. L. & NG, S. F. (2003) Theoretical analysis of tension and pressure decay of a tubular elastic fabric. *Textile Research Journal,* 73, 268-272.

HUNSTON, M. (2002) Innovative thin-film pressure mapping sensors. *Sensor review,* 22, 319-321.

ISTOOK, C. L. & HWANG, S. J. (2001) 3D body scanning systems with application to the apparel industry. *Journal of Fashion Marketing and Management,* 5, 120-132.

JONES, P. R. M., BROOKE-WAVELL, K. & WEST, G. M. (1995) Format for human body modelling from 3D body scanning. *International Journal of Clothing Science and Technology,* 7, 7-16.

JONES, P. R. M. & RIOUX, M. (1997) Three-dimensional surface anthropometry: application to the human body. *Optics and Lasers in Engineering,* 28, 89-117.

KANG, T. J. & KIM, S. M. (2000a) Development of three-dimensional apparel CAD system; Part 1: flat garment pattern drafting system. *International Journal of Clothing Science and Technology,* 12, 26-38.

KANG, T. J. & KIM, S. M. (2000b) Development of three-dimensional apparel CAD system; Part II: prediction of garment drape shape. *International Journal of Clothing Science and Technology,* 12, 39-49.

KANG, T. J. & KIM, S. M. (2000c) Optimized garment pattern generation based on three dimensional anthropometric measurement. *International Journal of Clothing Science and Technology,* 12, 240-254.

KIM, S. M. & KANG, T. J. (2002) Garment pattern generation from body scan data. *Computer-Aided Design,* 35, 611-618.

LINNEY, A. D., CAMPOS, J. & RICHARDS, R. (1997) Non-contact anthropometry using projected laser line distortion: Three-dimensional graphic visualisation and applications. *Optics and Lasers in Engineering,* 28, 137-155.

LUO, Z. G. & YUEN, M. M. F. (2005) Reactive 2D/3D garment pattern design modification. *Computer-Aided Design,* 37, 623-630.

LUO, X. & Luo, H. (2006) A computing model of pressure distribution from tight underwear. *Journal of Computational and Applied Mathematics,* 195, 106-112.

MACINTYRE, L. & BAIRD, M. (2005) Pressure garments for use in the treatment of hypertrophic scars - an evaluation of current construction techniques in NHS hospitals. *Burns,* 31, 11-14.

MACINTYRE, L. & BAIRD, M. (2006) Pressure garments for use in the treatment of hypertropic scars- a review of the problems associated with their use. *Burns,* 32, 10-15.

MACINTYRE, L., BAIRD, M. & WEEDALL, P. (2004) The study of pressure delivery for hypertropic scar treatment. *International Journal of Clothing Science and Technology,* 16, 173-183.

MACINTYRE, L. (2007) Designing pressure garments capable of exerting specific pressures on limbs. *Burns,* 33, 579-586.

MAGNENAT-THALMANN, N. & VOLINO, P. (2005) From early draping to haute couture models: 20 years of research. *Visual Computer,* 21, 506-519.

MAKLEWSKA, E., NAWROCKI, A., LEDWON, J., KOWALSKI, K., (2006) Modelling and Designing of Knitted Products Used in Compressive Therapy. *FIBRES &TEXTILES in Eastern Europe,* 15, 111-113.

MANN, R., YEONG, E. K., MOORE, M. L. & ENGRAV, L. H. (1997) A new tool to measure pressure under burn garments. *Journal Burn Care Rehabilitation,* 18, 160-163.

MAY-PLUMBEE, T., EISCHEN, J., BRUNER, D., KENKARE, N., PANDURANGAN, P., BAE, J. H. & POWELL, B. (2005) 3D virtual draping with fabric mechanics and body scan data. *National Textile Center Annual Report: November 2005.*

MCCARTNEY, J., HINDS, B. K. & CHONG, K. W. (2005) Pattern flattening for orthotropic materials. *Computer-Aided Design,* 37, 631-644.

MCCARTNEY, J., HINDS, B. K. & SEOW, B. L. (1999) The flattening of triangulated surfaces incorporating darts and gussets. *Computer-Aided Design,* 31, 249-260.

MCCARTNEY, J., HINDS, B. K., SEOW, B. L. & GONG, D. (2000a) Dedicated 3D CAD for garment modelling. *Journal of Material Processing Technology,* 107, 31-36.

MEUNIER, P. & YIN, S. (2000) Performance of a 2D image-based anthropometric measurement and clothing sizing system. *Applied Ergonomics,* 31, 445-451.

NG-YIP, F. S. F. (1993) Medical clothing- a tutorial paper on pressure garment. *International Journal of Clothing Science and Technology,* 5, 17-24.

NG, S. F. & HUI, C. L. (2001) Pressure model of elastic fabric for producing pressure garments. *Textile Research Journal,* 71, 275-279.

NG, S. F. F. (1994) Medical clothing- The stress relaxation and shrinkage of pressure garments. *International Journal of Clothing Science and Technology,* 6, 17-27.

NG, S. F. F. & HUI, C. L. P. (1999) Effect of hem edges on the interface pressure of pressure garments. *International Journal of Clothing Science and Technology,* 11, 251-261.

OKABE, H., IMOKA, H., TOMIHA, T. & H, N. (1992) Three dimensional apparel CAD system. *Computer Graphics,* 26, 105-110.

PARGAS, R. P., STAPLES, N. J. & DAVIS, J. S. (1997) Automatic measurement extraction for apparel from a three-dimensional body scan. *Optics and Lasers in Engineering,* 28, 157-172.

PETRAK, S. & ROGALE, D. (2001) Methods of automatic computerised cutting pattern construction. *International Journal of Clothing Science and Technology,* 13, 228-239.

PRATT, J. & WEST, G. (1995) *Pressure garment- A manual on their design and fabrication,* Oxford, Butterworth Heinemann.

REDA, D. C., WILDER, M. C., MEHTA, R. D. & ZILLIAC, G. (1998) Measurement of continuous pressure and shear distributions using coating and imaging techniques. *AIAA Journal,* 36, 895-899.

RIOUX, M. (1997) Colour 3D electronic imaging of the surface of the human body. *Optics and Lasers in Engineering,* 28, 119-135.

ROBB, R. A. (2000) Virtual endoscopy: development and evaluation using the Visible Human Datasets. *Computerized Medical Imaging and Graphics,* 24, 133-151.

RODEL, H., SCHENK, A., HERZBERG, C. & KRZYWINSKI, S. (2001) Links between design, pattern development and fabric behaviours for clothes and technical textiles. *International Journal of Clothing Science and Technology,* 13, 217-227.

SIEBERT, J. P. & MARSHALL, S. J. (2000) Human body 3D imaging by speckle texture projection photogrammetry. *Sensor Review,* 20, 218-226.

SIMMONS, K. P. & ISTOOK, C. L. (2003) Body measurement techniques: Comparing 3D body scanning and anthropometric methods for apparel applications. *Journal of Fashion Marketing and Management,* 7, 306-332.

SPENCER, D. J., (1983) *Knitting Technology*, Oxford, Pergamon Press

STYLIOS, G. K., HAN, K. & R, W. T. (2001) A remote, on-line 3D human measurement and reconstruction approach for virtual wearer trials in global retailing. *International Journal of Clothing Science and Technology,* 13, 65-75.

SUL, I. H. & KANG, T. J. (2004) Improvement of drape simulation speed using constrainedfabric collision. *International Journal of Clothing Science and Technology,* 16, 43-50.

SUL, I. H. & KANG, T. J. (2006) Interactive garment pattern design using scissoring method. *International Journal of Clothing Science and Technology,* 18, 31-42.

TARAKANOV, A. & ADAMATZKY, A. (2002) Virtual clothing in hybrid cellular automata. *Kybernetes,* 31, 1059-1072.

THOMAS, S. (2003) The use of the Laplace equation in the calculation of sub-bandage pressure. *EWMA Journal,* 3, 21-23.

TURNER, J. P. (1994) Development of a commercial made-to-measure garment pattern system. *International Journal of Clothing Science and Technology,* 6, 28-33.

VAN DEN KERCKHOVE, E., STAPPAERTS, K., FIEUWS, S., LAPERRE, J., MASSAGE, P., FLOUR, M. & BOECKX, W. (2005) The assessment of erythema and thickness on burns related scars during pressure garment therapy as a preventive measure for hypertropic scarring. *Burns,* 31, 696-702.

WANG, C. C. L., SMITH, S. S. F. & YUEN, M. M. F. (2002b) Surface flattening based on energy model. *Computer-Aided Design,* 34, 823-833.

WANG, C. C. L., WANG, Y., CHANG, T. K. K. & YUEN, M. M. F. (2003) Virtual human modeling from photographs for garment industry. *Computer-Aided Design,* 35, 577-589.

WANG, C. C. L., WANG, Y. & YUEN, M. M. F. (2002a) Feature based 3D garment design through 2D sketches. *Computer-Aided Design,* 35, 659-672.

WANG, C. C. L. & YUEN, M. M. F. (2005) Editorial: CAD methods in garment design. *Computer-Aided Design,* 37, 583-584.

WILLIAMS, S., KNAPP, D. & WALLEN, M. (1998) Comparison of the characteristics and features of pressure garments used in the management of burn scars. *Burns,* 24, 329-335.

WONG, A. S. W., LI, Y., & ZHANG, X. (2004) Influence of Fabric Mechanical Property on Clothing Dynamic Pressure Distribution and Pressure Comfort on Tight-Fit Sportswear. *Sen'i Gakkaishi*, 60, 293-299.

XU, B., HUANG, Y. & CHEN, T. (2002) Body scanning and modeling for custom fit garments. *Journal of Textile and Apparel Technology and Management,* 2, 1-11.

YANG, Y. & MAGNENAT-THALMANN, N. (1992) 3D garment design and animation: A new design tool for the garment industry. *Computer in Industry,* 19, 185-191.

YILDIZ, N. (2006) A novel technique to determine pressure in pressure garments for hypertrophic burn scars and comfort properties. *Burns*, 33, 59-64.

YIP, C., MEHMOOD, Z., & SHAH, M. (2008) Letter to the Editor: Lego® as a customisable pressure garment insert. *Burns*, 34, 430-431.

YU, W., FAN, J., QIAN, X. & TAO, X. (2004) A soft mannequin for the evaluation of pressure garments on human body. *Sen.i gakkaishi,* 60, 57-64.

ZAMENHOF, R., REDMOND, E., SOLARES, G., KATZ, D., RILEY, K., KIGER, S. & HARLING, O. (1996) Monte carlo-based treatment planning for boron capture therapy using custom designed models automatically generated from CT data. *International Journal of Radiation Oncology Biology Physics,* 35, 383-397.

ZHANG, X., YEUNG, K. W. & Y, L. (2002) Numerical simulation of 3D dynamic garment pressure. *Textile Research Journal,* 72, 245-252.

ZHONG, Y. & XU, B. (2006) Automatic segmenting and measurement on scanned human body. *International Journal of Clothing Science and Technology,* 18, 19-30.

Appendix A Body data

(Note: The 5 decimal places result from the body scanner software. This does not imply sub μm resolution)

(cm)	(cm)
x- y- z-	x- y- z-
-16.48037 2.88036 -22.36875,	-17.8784 -7.13251 -22.36875,
-16.07838 2.679731 -22.36875,	-18.33465 -7.009604 -22.36875,
-15.71151 2.445401 -22.36875,	-18.77682 -6.839762 -22.36875,
-15.37223 2.220623 -22.36875,	-19.20037 -6.626203 -22.36875,
-15.0481 2.020118 -22.36875,	-19.60681 -6.380033 -22.36875,
-14.74179 1.813386 -22.36875,	-19.99395 -6.102341 -22.36875,
-14.4473 1.606367 -22.36875,	-20.35423 -5.788882 -22.36875,
-14.134 1.435937 -22.36875,	-20.68419 -5.442445 -22.36875,
-13.80835 1.269363 -22.36875,	-20.97437 -5.061753 -22.36875,
-13.4855 1.079844 -22.36875,	-21.21287 -4.647332 -22.36875,
-13.16045 0.8707174 -22.36875,	-21.40093 -4.209517 -22.36875,
-12.83074 0.6404783 -22.36875,	-21.54749 -3.759302 -22.36875,
-12.5233 0.3695901 -22.36875,	-21.66219 -3.303489 -22.36875,
-12.25837 5.372574e-002 -22.36875,	-21.74834 -2.843909 -22.36875,
-12.03201 -0.2959548 -22.36875,	-21.82611 -2.382716 -22.36875,
-11.84393 -0.6726941 -22.36875,	-21.90499 -1.915022 -22.36875,
-11.68966 -1.070294 -22.36875,	-21.95944 -1.435666 -22.36875,
-11.5745 -1.485817 -22.36875,	-21.96196 -0.9484701 -22.36875,
-11.51883 -1.915025 -22.36875,	-21.91333 -0.4592651 -22.36875,
-11.52392 -2.348659 -22.36875,	-21.81204 2.554681e-002 -22.36875,
-11.58361 -2.778458 -22.36875,	-21.66724 0.5036539 -22.36875,
-11.67452 -3.20275 -22.36875,	-21.47134 0.9665152 -22.36875,
-11.79203 -3.621443 -22.36875,	-21.23145 1.41172 -22.36875,
-11.94605 -4.029417 -22.36875,	-20.947 1.832923 -22.36875,
-12.13826 -4.421948 -22.36875,	-20.61423 2.218831 -22.36875,
-12.36571 -4.796144 -22.36875,	-20.22436 2.54689 -22.36875,
-12.61479 -5.15863 -22.36875,	-19.78682 2.807072 -22.36875,
-12.8861 -5.509304 -22.36875,	-19.3196 3.002668 -22.36875,
-13.19227 -5.833638 -22.36875,	-18.83208 3.12823 -22.36875,
-13.5269 -6.133029 -22.36875,	-18.33359 3.176664 -22.36875,
-13.89037 -6.401037 -22.36875,	-17.84057 3.161287 -22.36875,
-14.28211 -6.62922 -22.36875,	-17.36544 3.104464 -22.36875,
-14.69608 -6.81733 -22.36875,	-16.91052 3.001579 -22.36875,
-15.12536 -6.972019 -22.36875,	-16.41422 2.957283 -23.36875,
-15.56645 -7.098144 -22.36875,	-16.00606 2.737924 -23.36875,
-16.01925 -7.185661 -22.36875,	-15.63147 2.511878 -23.36875,
-16.48037 -7.231948 -22.36875,	-15.28258 2.295992 -23.36875,
-16.94605 -7.23777 -22.36875,	-14.95511 2.08154 -23.36875,
-17.41327 -7.205715 -22.36875,	-14.64182 1.873583 -23.36875,

Appendix B SUBJECTS LEG FIGURE

<table>
<tr><th>Subject</th><th>Leg</th></tr>
<tr><td>1</td><td>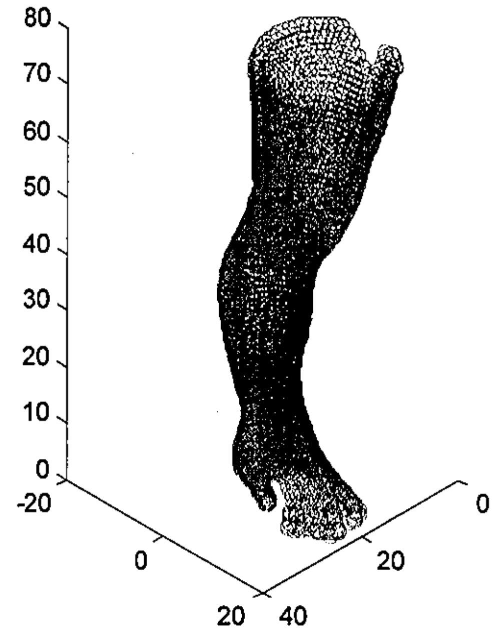
</td></tr>
<tr><td>2</td><td>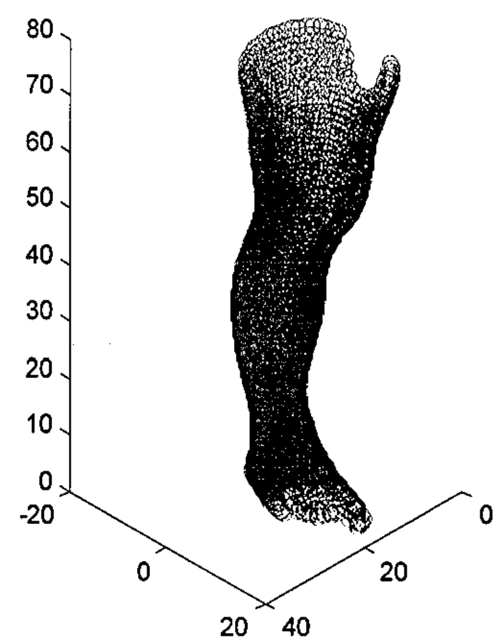
</td></tr>
</table>

3

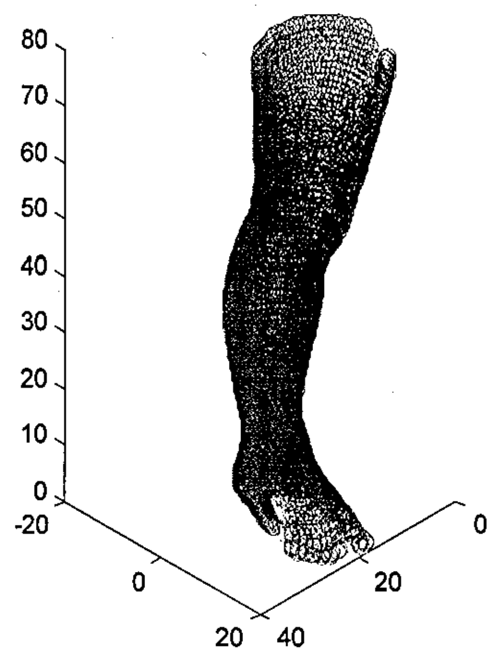

4

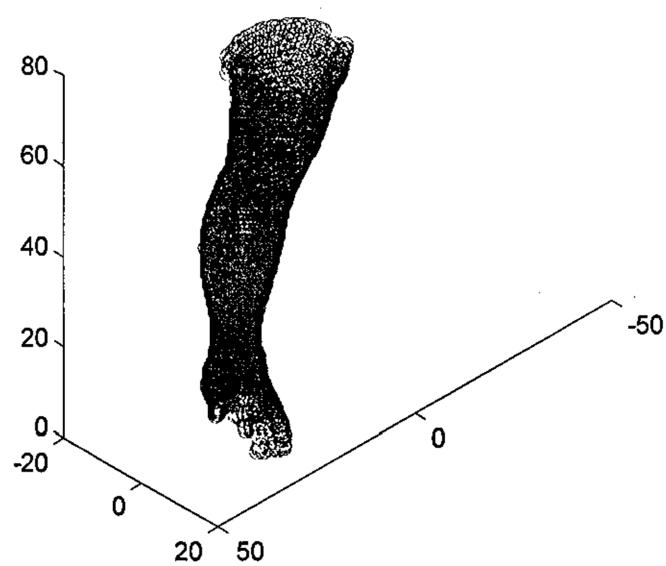

5	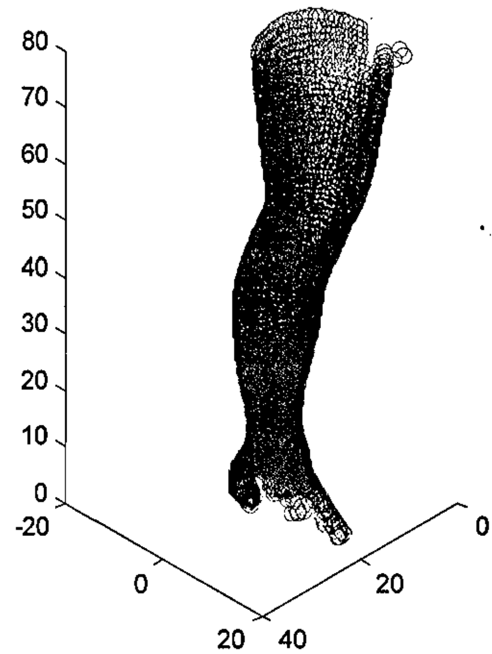 80 70 60 50 40 30 20 10 0 -20 0 20 40 20 0
6	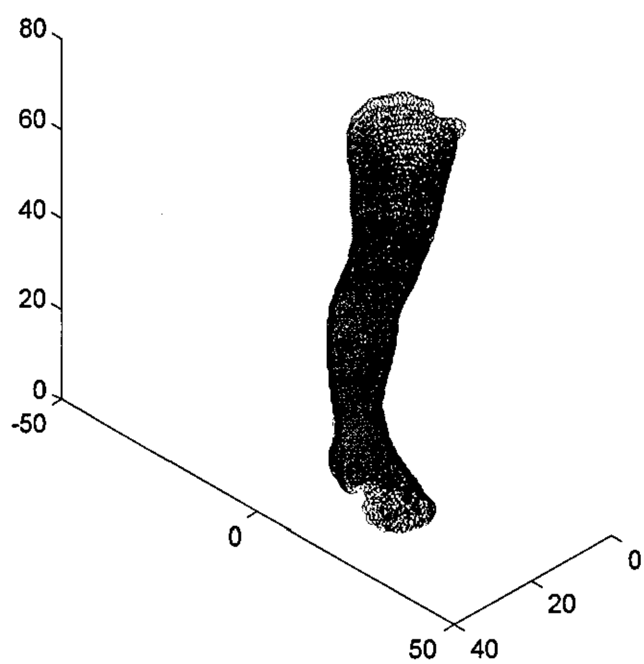 80 60 40 20 0 -50 0 50 40 20 0

7	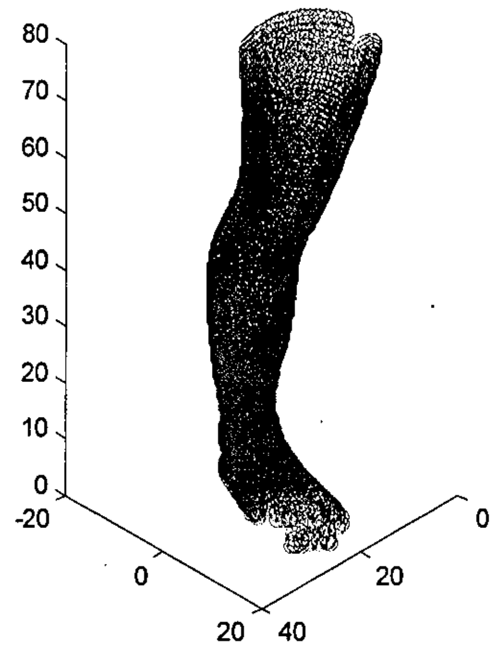80 70 60 50 40 30 20 10 0 -20 0 20 40 20 0
8	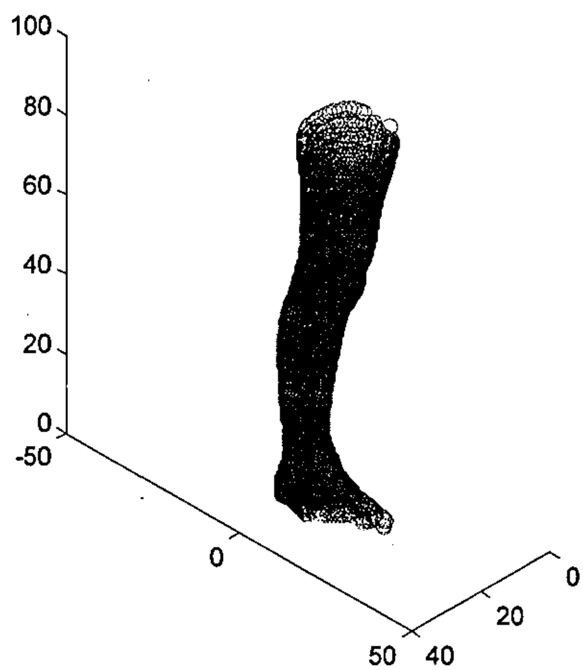100 80 60 40 20 0 -50 0 50 40 20 0

9	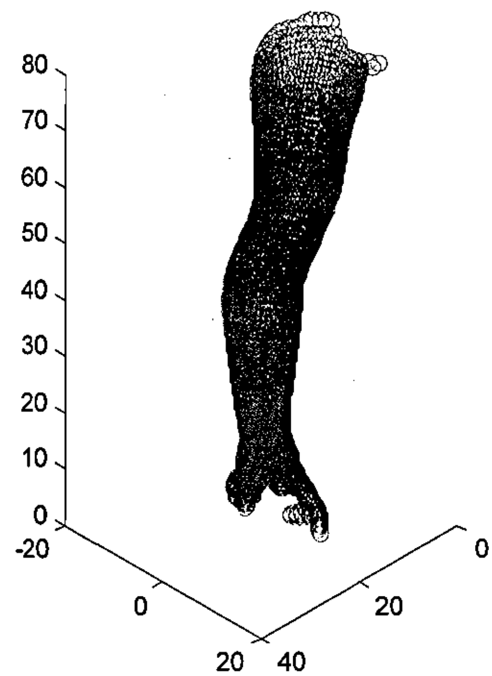 80 70 60 50 40 30 20 10 0 -20 0 20 40 20 0
10	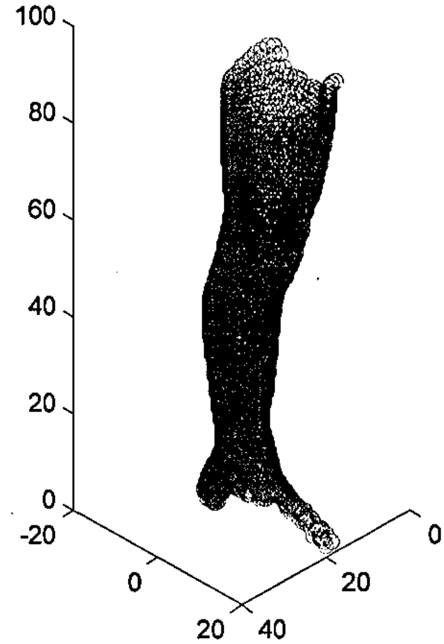 100 80 60 40 20 0 -20 0 20 40 20 0

Appendix C A NEW METHOD TO DEVELOP AND ASSESS PRESSURE GARMENTS

Proceedings of the second Ambience conference, Boras, Sweden (2008).

A New Method to Develop and Assess Pressure Garments

M. N. Salleh, M. Acar and N. D. Burns
Wolfson School of Mechanical and Manufacturing Engineering,
Loughborough University, Leicestershire, LE11 3TU, UK
M.N.Salleh@lboro.ac.uk, M.Acar@lboro.ac.uk, N.D.Burns@lboro.ac.uk

ABSTRACT
This paper concerns the development of pressure garment modeling, pattern generation and making up to exert a specific pressure on a wounded area. First, raw data of a body part was extracted using a body scanner to develop a 3D body model. Then, a 3D pressure garment was generated using a novel modeling approach taking into account the properties of the fabric and the curvature of body parts. The 3D pressure garment was then flattened into a 2D pressure garment pattern design. Finally a computer simulation and pressure measurements were used to validate the method.

Author Keywords
Pressure garment, 3D body data, pressure distribution, pattern.

INTRODUCTION

Around 2.4 million injuries related to burns are reported each year in the United States (1), approximately one million people suffer substantial or permanent disabilities resulting from their injuries. One of the treatments for burn injuries is the use of pressure garments. Pressure garments are tight fitting elastic garments which apply pressure to the wounded area of the human body for treatment. They prevent and control the formation of hypertrophic scars by applying counter pressure to the burn wounded area. The garments are usually made either by the occupational therapists (OTs) or the commercial companies. However, resulting from the present approach to producing the garment, there are some problems related to the fitting, cost, delivery time and customer satisfaction.

There is relatively little research literature on the pressure garment making process except for the notable work of Pratt and West (2) and Macintyre and Baird (3). They stated that the method used by various different pressure garment manufacturers is very similar. First, patients' wounded area is manually measured as accurately as possible. By using a reduction factor, the dimensions of the garment are calculated to ensure that the correct pressure is applied to the wounded area. Then, patterns are developed based on the calculated dimensions, cut and sewn together, and other features like zips are added to complete the garment. The pressure garment is then sent to the hospital where it is fitted to the patient. If the pressure garment does not fit well, then the product is sent back to the company with details for improvement. This is a time consuming process.

The major problem in the process is the 'fit' of the garment (4,5) because the garment is normally developed based on the information provided by the client. Patients complete a detailed measurement form in order to enable the companies to develop the pressure garment accurately. Even though this information is detailed, without accurate measurements of the wounded area, it does not always lead to the creation of accurate pressure garments that provide a good fit and the right pressure.

There are further problems due to the garment losing its properties (6) over the long period of time that it should be worn, typically between 4 months to 3 years (5). The garment must therefore be constructed again from time to time to effectively treat the wounded area. Also in the case of weight gain or loss, the garment must be re-ordered.

METHODOLOGY

Dimensional measurements of body parts with soft tissue is considered to be a difficult task (7,8). To overcome this problem, this research explores the possibility of using a novel 3D design and modeling approach to create a pressure garment that can exert the appropriate pressure on the wounded part of the body. The method utilises a body scanner to generate a three dimensional image used to determine the required dimensions of the wounded area, a 3D pressure garment model using the scanned data and fabric properties, conversion of the 3D data to a 2D garment pattern, making the pressure garment and verification of the garment by simulation and in situ pressure measurements.

The system can also act as a communication tool between the client and manufacturer, enabling the latter to obtain more detailed and accurate information on the wounded area, for example its exact location and size. It also enables the manufacturer to carry out an initial evaluation and assessment of the garment using the simulation of the pressure that the garment applies.

There are a number of steps in the proposed pressure garment generation method. Figure 1 shows the flowchart of the methodology proposed.

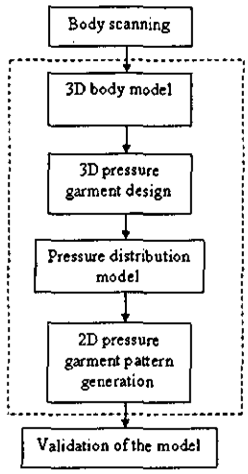

Figure 1. Flowchart of methodology

3D data acquisition

For this research, [TC]^2 NX12 (9), a 3D horizontal type body scanner is used to extract 3D (x, y, z coordinates) raw data of the subject body. The object is scanned in layers in the horizontal plane. The x and y coordinates of each 'layer' are measured, z being the vertical axis, which is incremented by 1 cm until the whole object is scanned. The coordinates of the data can be obtained by converting the (.wrl) files into text files (.txt) (10). The data are then exported to Matlab, and the 3D data are transformed again to create 3D point cloud to form 3D human body model.

3D pressure garment design

The design process begins with the identification of the wounded area by using both the lower and upper limits of the location of the wounded area. In this research, an area between 20-30 cm heights of the left leg of a mannequin is used as the wounded area. All data between the limits of the wounded area are transformed to create a 3D body image.

The flowchart of developing a 3D pressure garment model is shown in Figure 2.

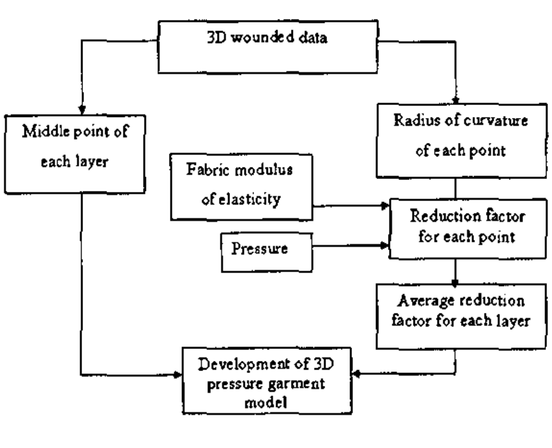

Figure 2. Flowchart to develop 3D pressure garment model

Centroid

The coordinates of the centroid of the layer can be calculated as follows:

$$MP_j = \left(\frac{\sum_{i=1}^{n} x_i}{n}, \frac{\sum_{i=1}^{n} y_i}{n} \right) \qquad (1)$$

Radius of curvature

Current pressure garment models assume a circular cross-section to calculate the radius. However, body segments are rarely circular and therefore the radius of curvature of a curve at a given point should be used. The radius of curvature is the radius of the osculating circle at that point. This research therefore proposes the three-point-method to estimate the radius of curvature. (Figure 3).

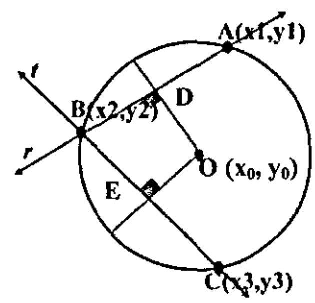

Figure 3. Radius of curvature

The center of the circle lies on the perpendicular bisectors of any two chords, such as AB and BC. Lines that are perpendicular to each other have negative reciprocal slopes. Hence, if slopes between AB and BC are m_{AB} and m_{BC} respectively, then the slope for DO and EO are $-\frac{1}{m_{AB}}$ and $-\frac{1}{m_{BC}}$, where D and E are the centres of AB and BC respectively, and O is the centre of the circle.

The equation of lines DO and EO can be found by substituting the slope DO and EO into the general equation of a straight line

$$y = mx + c$$

where m is the slope, c is the y-intercept of the line determined from the equation of lines AB and BC, where

$$y_{DO} = -\frac{1}{m_{AB}} x_{DO} + \left(\frac{y_1 + y_2}{2} + \frac{1}{m_{AB}} \left(\frac{x_1 + x_2}{2} \right) \right) \qquad (2a)$$

and

$$y_{EO} = -\frac{1}{m_{BC}} x_{EO} + \left(\frac{y_3 + y_2}{2} + \frac{1}{m_{BC}} \left(\frac{x_3 + x_2}{2} \right) \right) \qquad (2b)$$

These two lines will intersect at the centre of the circle where $y_{AB} = y_{BC} = y_0$ and $x_{AB} = x_{BC} = x_0$. By using both equations,

$$x_0 = \frac{m_{AB}m_{BC}(y_3 - y_1) + m_{AB}(x_2 + x_3) - m_{BC}(x_2 + x_1)}{2(m_{AB} - m_{BC})}, \tag{3}$$

By substituting x0 into equation 2, the y_0 value can be calculated. The radius can be found by using the distance formula from the centre to any of the three points, A, B or C. By using this method, the radius of curvature at each point on the body model in a given layer can be determined by using the point and its two neighboring points. A good approximation of the radius of curvature can be obtained this way. The exact result can be achieved if the distance between the neighboring points is close to zero.

Reduction Factor

The reduction factor is the factor that is used to reduce the original body measurement to obtain the size of the pressure garment in order to apply the required pressure. Thus, if C_0 is the original circumference of the wounded area, then the pressure garment circumference C_1 should be;

$$C_1 = (1 - \text{Re})C_0 \tag{4}$$

where Re is the reduction factor. According to Laplace Law, tension (T), radius of curvature (ρ) and the pressure (P) that is to be exerted on the wounded area have a definite relationship which is given by the formula

$$P = \frac{T}{\rho}$$

The surface tension of the pressure garment can be calculated using Hooke's Law.

$$T = EI\frac{(C_0 - C_1)}{C_1} \tag{5}$$

where EI is the flexural rigidity of the fabric (11). By combining the above formulae, the reduction factor (Re) is given by

$$\text{Re} = \frac{1}{1 + \dfrac{EI}{P\rho}} \tag{6}$$

EI can be determined by calculating the tangent of the load-elongation curve.

The radius of curvature for each point in a given layer is calculated first; then a corresponding reduction factor is determined. Finally, the average of these is found to represent the reduction factor for that layer.

By combining both the reduction factor and the centroid, 3D pressure garment can be developed as shown in Figure 4.

If it is assumed that G_j is the centroid of layer j with coordinates of x_{mp} and y_{mp}, A_i is one of a series of points that form the layer of the body and Re is the reduction factor for the layer, the location of the pressure garment's points, A' (x_i', y_i') can be determined by using the following formulae:

$$\begin{aligned} x_i' &= x_{mp} + \cos\theta.GA' \\ y_i' &= y_{mp} + \sin\theta.GA' \\ \theta &= \arctan\left(\frac{y_i - y_{mp}}{x_i - x_{mp}}\right) \\ GA' &= (1 - \text{Re})\sqrt{(x_i - x_{mp})^2 + (y_i - y_{mp})^2} \end{aligned} \tag{7}$$

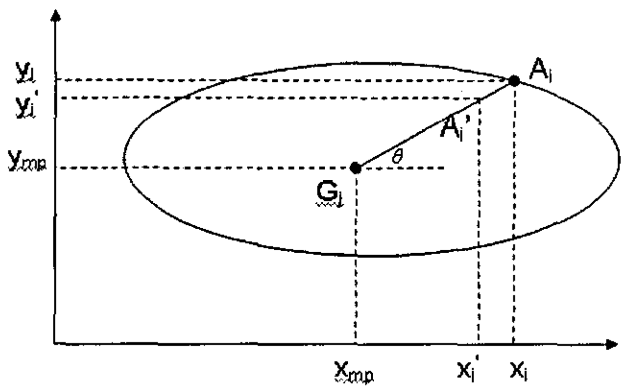

Figure 4. 3D pressure garment plotting

Pressure distribution model

Since it is almost impossible to calculate the exact pressure, a model is required to predict the pressure distribution. The model is essential since it provides an initial estimation of the pressure that the garment is expected to apply. The flowchart for the model is shown in Figure 5.

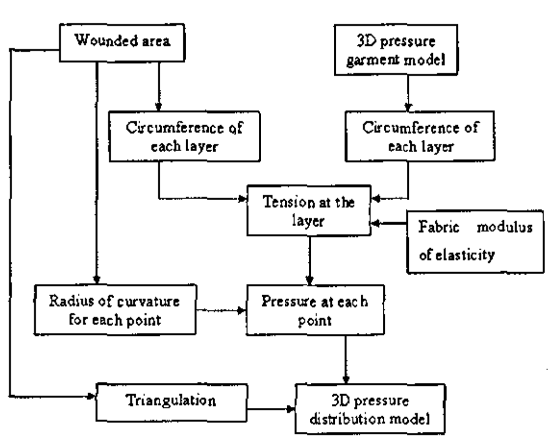

Figure 5. 3D pressure distribution model flowchart

Tension

The tension exerted by the fabric on the body can be calculated using Hooke's Law. It is assumed that the body contour and size will not change under the fabric pressure.

Thus, if P_n (x_n, y_n) indicates the coordinates of the n^{th} point in one layer, the circumference of the body layer j is given by;

$$C_j = \sum_{i=1}^{n} \sqrt{(x_i - x_{i-1})^2 + (y_i - y_{i-1})^2} \tag{8}$$

The number of points in each layer depends on the size of the cross section. For example, for the leg section scanned here, n is 72. The circumferences of the pressure garment at each layer, each layer separated by 1 cm, can similarly be calculated. Then the 3D pressure garment surface is flattened into 2D pattern.

Experiments

Two experiments have been conducted. The first experiment was to validate the developed pressure garment pattern. In the validation, a cylinder with circumference of 31.5 cm and height of 20 cm was used. Pressure garments to exert 2666 Pa (20 mmHg) pressure to the cylinder have been developed using two different fabrics (fabric A and fabric B) with different moduli of elasticity of 504 N/m and 407.1 N/m respectively. According to the model, reduction factors for the fabrics should be 21% and 25% respectively. Exerted pressure has been measured using Tekscan's Flexiforce A201-1 sensor (12). Three sensors are inserted at different location on the cylinder, and average pressure was used for each fabric.

The second experiment was to validate the pressure distribution along the circumference of the model. In this experiment, two pressure garment patterns using fabric A have been developed to apply 2666 Pa and 5000 Pa pressure. A mannequin left leg was used as a leg specimen. The leg was scanned and two pressure garment patterns and pressure distribution models were developed for the segment of the leg between 20-30 cm height. The pattern was sewn together and applied to the mannequin's leg. Pressure was measured at eight locations around the leg at a given layer, and the results were compared with the predictions by the model. All measurements were taken again after 10 minutes to reduce drift effect.

RESULTS

Computer simulation

Figure 6 shows the result of the body scanning and wounded area position. The red points represent wounded area while the green points indicate the location of the pressure garment points after computation (Figure 7). Figure 8 shows the pressure garment's pattern for the area.

Figures 9 and 10 show the results of the pressure distribution model. Figure 9 shows the pressure distribution on the body part. Figure 10 shows the variation of pressure along the circumference of the body part for a given layer. With the aid of these plots it is possible to locate the areas which are subject to low or high pressure.

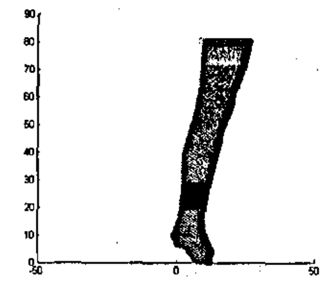

Figure 6. 3D body model with the wounded area (blue)

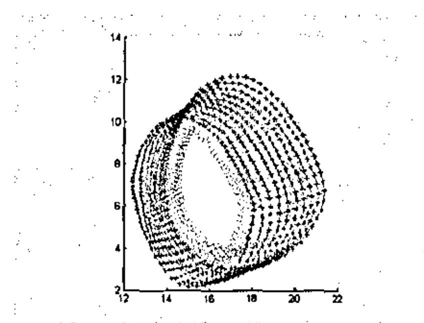

Figure 7. 3D pressure garment model (green)

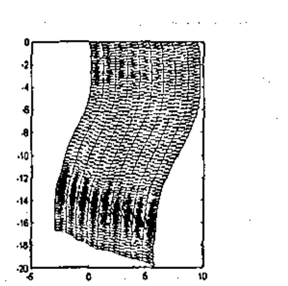

Figure 8. Pressure garment pattern

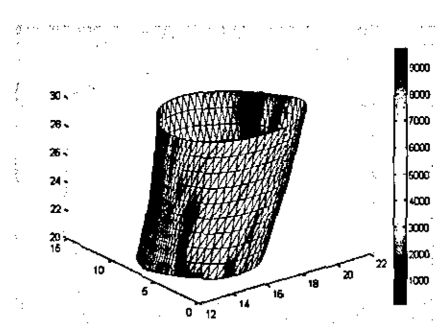

Figure 9. Pressure distribution on the leg

Experiment

The result of the first experiment for pressure validation is shown in Table 1. For experiment 2, the results of pressure distribution are shown in Figure 11 (for the designed pressure of 2666 Pa) and in Figure 12 (for the design pressure of 5000 Pa). The predicted pressure for experiment 2 is calculated by taking the average pressure at three points near the location of the experimentally measured pressure.

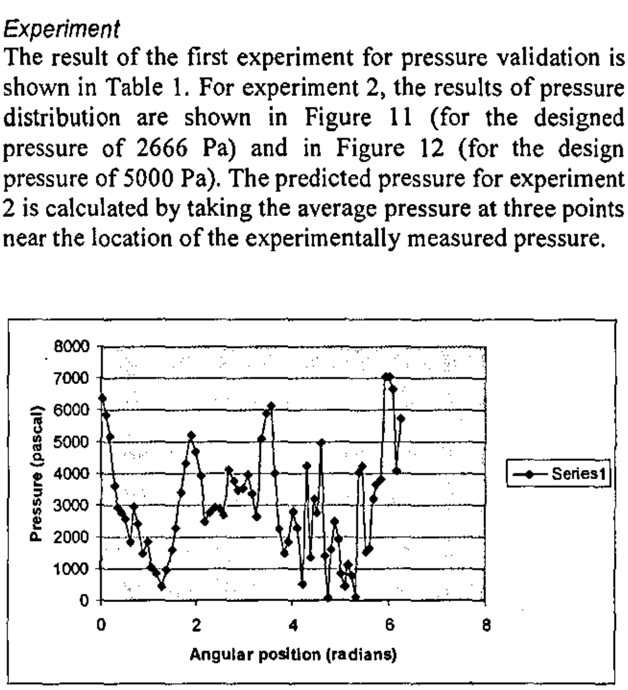

Figure 10. Circumferential pressure variation

Table 1. Pressures from Experiment 1

	Sensor 1 Pa (mmHg)	Sensor 2 Pa (mmHg)	Sensor 3 Pa (mmHg)	Average Pa (mmHg)
Fabric 1	2633 (19.75)	2614 (19.61)	2601 (19.51)	2616 (19.62)
Fabric 2	2628 (19.71)	2657 (19.93)	2871 (21.54)	2718 (20.39)

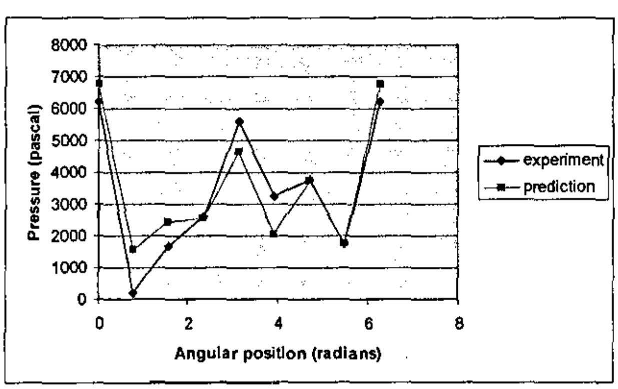

Figure 11. Comparison of the results of predicted and experimental pressure distribution (intended pressure = 2666 Pa)

DISCUSSION

The results show that the proposed method can be used successfully to create the required pressure garment. For a cylinder, the method can develop a pressure garment that can exert intended pressure uniformly around the surface as shown in Table 1. However, since the human body is not a perfect cylinder, the pressure that the garment applies on the leg segment varies around the circumference depending on the radius of curvature. Unlike previous methods which assume a circular cross-section to develop the garment for a body part, the proposed method uses all radius of curvatures to develop the pressure garment. Furthermore, the proposed pressure distribution model can be used to estimate the pressure that the garment should apply. Figure 11 and 12 shows comparison between the predicted pressures with the actual measurements. Both figures show that the model can be used to predict pressure exerted by the garment to a reasonable accuracy. The reason for the differences is believed to be caused by the inaccuracy of the sensor. As stated by Ferguson-Pell et al [12], the sensor can be affected by the curvature effect if the radius of curvature is less than 32 mm.

65

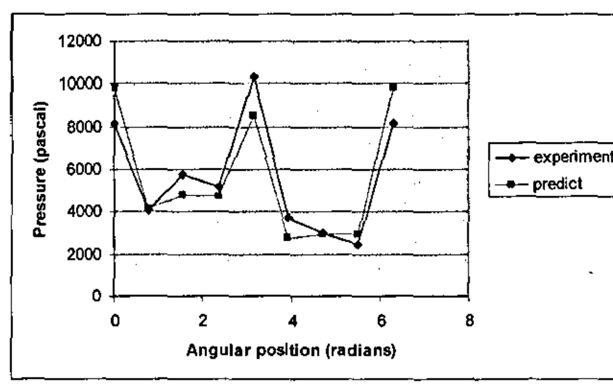

Figure 12. Comparison of the results of predicted and experimental pressure distribution (intended pressure = 5000 Pa)

CONCLUSIONS

This paper proposes a new method to produce a pressure garment. Unlike current conventional methods, it explores the possibility of using a 3D body model, based on 3D scanned body data, to determine the shape of the pressure garment pattern. This method uses a much more accurate scanned measurement of the body part for pressure garment production. Then, it uses the local radius of curvature, instead of the radius calculated from the circumference of body that assumes a circular cross-section to determine the reduction factor. Hence the manufactured garment provides a more accurate fit.

The proposed method also calculates the pressure exerted by the garment using the radius of curvature at each data point on the body. This enables an estimation of the pressure that should be exerted by the garment on the body before manufacturing the garment. This could be useful in estimating the pressure on the wounded area, especially on the parts of the body that cannot be possible to measure using the current pressure measurement devices.

The proposed method should also make the communication with the manufacturer more efficient and the production cycle much faster.

REFERENCES

1. http://www.burnsurvivor.com
2. Pratt, J. and West, G. *Pressure garment- A manual on their design and fabrication,* Oxford, Butterworth Heinemann, 1995.
3. Macintyre, L. & Baird, M. Pressure garments for use in the treatment of hypertropic scars- a review of the problems associated with their use. *Burns,* 32 (2006), 10-15
4. Macintyre, L. & Baird, M. Pressure garments for use in the treatment of hypertrophic scars - an evaluation of current construction techniques in NHS hospitals. *Burns,* 31 (2005), 11-14
5. Williams, S., Knapp, D. & Wallen, M. Comparison of the characteristics and features of pressure garments used in the management of burn scars. *Burns,* 24 (1998) 329-335
6. Ng, S. F. F. Medical clothing- The stress relaxation and shrinkage of pressure garments. *International Journal of Clothing Science and Technology,* 6 (1994), 17-27
7. Istook, C. L. & Hwang, S. J. 3D body scanning systems with application to the apparel industry. *Journal of Fashion Marketing and Management,* 5 (2001), 120-132
8. Simmons, K. P. & Istook, C. L. Body measurement techniques: Comparing 3D body scanning and anthropometric methods for apparel applications. *Journal of Fashion Marketing and Management,* 7 (2003), 306-332
9. http://www.tc2.com
10. Tekscan user's manual. F-Scan Pressure Assessment System. Version 5. (2001)
11. Ng, S. F. & Hui, C. L. Pressure model of elastic fabric for producing pressure garments. *Textile Research Journal,* 71 (2001), 275-279
12. Ferguson-Pell, M., Hagisawa, S. & Bain, D. Evaluation of a sensor for low interface pressure applications. Medical Engineering and Physics, 22 (2000), 657-663